INVESTIGATION ON SIX-PHASE SELF-EXCITED INDUCTION GENERATOR

Ph. D. THESIS

by

KIRAN SINGH

**DEPARTMENT OF ELECTRICAL ENGINEERING
INDIAN INSTITUTE OF TECHNOLOGY ROORKEE
ROORKEE- 247 667 (INDIA)
June, 2018**

INVESTIGATION ON SIX-PHASE SELF-EXCITED INDUCTION GENERATOR

A THESIS

*Submitted in partial fulfilment of the
requirements for the award of the degree
of*

DOCTOR OF PHILOSOPHY

in

ELECTRICAL ENGINEERING

by

KIRAN SINGH

**DEPARTMENT OF ELECTRICAL ENGINEERING
INDIAN INSTITUTE OF TECHNOLOGY ROORKEE
ROORKEE- 247 667 (INDIA)
JUNE, 2018**

INDIAN INSTITUTE OF TECHNOLOGY ROORKEE
ROORKEE

<u>CANDIDATE'S DECLARATION</u>

I hereby certify that the work which is being presented in the thesis entitled "**INVESTIGATION ON SIX-PHASE SELF-EXCITED INDUCTION GENERATOR"** in partial fulfilment of the requirements for the award of the Degree of Doctor of Philosophy and submitted in the Department of Electrical Engineering of the Indian Institute of Technology Roorkee, Roorkee is an authentic record of my own work carried out during a period from July, 2010 to June, 2018 under the supervision of Dr. G.K. Singh, Professor, Department of Electrical Engineering, Indian Institute of Technology Roorkee, Roorkee.

The matter presented in the thesis has not been submitted by me for the award of any other degree of this or any other Institute.

(**KIRAN SINGH**)

This is to certify that the above statement made by the candidate is correct to the best of my knowledge.

(G. K. Singh)
Supervisor

Dated: _____

ABSTRACT

Multi-phase /high phase number (more than 3Φ) systems are potential alternative to their three phase counterpart systems in respect of various beneficial advantages for high power electric applications. The affectionate utilization of renewable /non-conventional energy resources in fuel redemption had a need of low cost and appropriate generating systems in enlivening the small /large scale industrial applications and variety of future energy demands. Stand-alone /isolated induction generators are attractive substitutes having numerous relative advantages over the well-known synchronous generators in electric power generation in conjunction with non-conventional energy resources. The cost effective utilization of advantageous features during isolated mode in induction generator technology had opportunity to supplement the electric power from different site resources to underprivileged far-flung and remote areas. So, investigation on six-phase self-excited induction generator (SP-SEIG) has taken place during past decades for exploiting the propitious features of multi-phase machines conjointly stand-alone self-excited induction generators (SEIG) in the area of non-conventional energy generation for being a viable alternative over other generating systems.

Apart from literature, which interpret correlations among the machine parameters and variety of variables in multi-phase (six-phase) isolated mode of SEIG, further, efforts are made to draw special attention to highlight other potential issues related to the use of SP-SEIG (when both 3-Φ sets are designed with 30° displacement and their neutrals are isolated) in aspect of present and future development. As compared to existing new methodology, conventional techniques used during last several decades focus on modelling and analysis of SP-SEIG to analyze the steady state and dynamic performance of simple and compensated SP-SEIG during balanced /unbalanced conditions. Steady-state study is needed for ensuring good quality power and assessing the suitability of different configurations of SEIG. Transient behaviour during dynamic analysis provides the knowledge about the suitability of capacitor ratings, machine winding, and its insulation level for protection purpose. Small signal stability analysis is requisite to deliberate the stability of proposed system when each machine variable goes through small disturbances from its reference value by using popular techniques. An appropriate controller design and analysis is also carried out on simple SP-SEIG during consumer load variations for ensuring good quality power delivery in small reasonable generating system by a new technique.

In steady state analysis, a simple technique along with machine data is contemplated to predict the saturated magnetizing reactance 'X_m' and per-unit frequency 'F'. The steady state performance deals with a mathematical matrix model of simple and compensated six-phase self-excited (isolated) induction generator (SP-SEIG) using loop impedance method, based on graph theory from its per unit representation of per-phase generalized equivalent circuit, to

study the comparative steady-state behaviour of different configurations. The machine voltage regulation are enhanced by employing supplementary series capacitors within short-shunt and long-shunt configurations in self-excited induction generator 'SEIG'. The resultant matrix model is simple and flexible for various future modifications. The optimization of 'Xm' and 'F' variables of generalized matrix model are performed by using Newton-Raphson 'NR' routine based analytical technique for a variety of loading conditions and in different operating modes of fundamental configurations. Further, the computation of optimized 'X_m' and 'F' value participates in the estimation of various machine performance parameters. Steady state study is also needed for initializing the dynamic and transient simulation.

During dynamic analysis, a popular two axis (dq0) model of a saturated simple and compensated multi-phase (six-phase) self-excited induction generator (SP-SEIG) is constructed by park's transformation using mixed (stator current and magnetizing flux) state variables. The model is characterized with very simple system matrix in which only four elements could be dependent on saturation, when considered. Mixed stator current and air-gap flux state space model possesses the advantage of having variable speed operation under variable magnetizing flux level in the machine. Under variable speed operating conditions, flux level in the machine needs to be modelled accordingly that accounts for the main flux saturation. This mixed stator current and air-gap flux as a state-space variables model preserves the information about both stator and rotor parameters. On the other perspective, considerably simpler than d-q axis winding current model and has simple matrix. This saturated machine model is mostly applied in air-gap flux field oriented vector control strategy.

In transient behaviour analysis, performance equations in dynamic model utilize the steady state magnetizing inductance 'L_m' along with dynamic inductance 'L' rather than saturated magnetizing inductance 'L_m' and its derivative. During analysis, the effects of common mutual leakage inductance between two three-phase winding sets and cross saturation coupling between d- and q- axis of stator have not been considered. Differential equations has been computed with an explicit MATLAB algorithm for the implementation of 4th order Runge-Kutta 'RK4' subroutine. Proper values of shunt capacitor avoid the excessive voltage at the terminals of SP-SEIG under loading condition. A careful value selection of the combination, i.e. shunt and series capacitors also eliminates the enormous terminal voltage when switching the load, and can maintain the no-load voltage because of extra reactive power supplied by the series capacitors. The involvement of series capacitors satisfy the requirement of voltage regulation when load is suddenly switched on after few second and retains the no-load terminal voltage as per self-regulating nature.

The stability investigation in this thesis reveals that the eigenvalues are dependent upon the machine parameters and variables. The most critical parameter is the variation in

magnetizing inductance 'L_m', which focuses on stabilization of SP-SEIG. Firstly, Taylor series is applied to linearize the nonlinear equations of the machine; secondly, Eigenvalue basic criterion is used to find out the machine eigenvalues about small deviation using a group of higher order equations from the linearized SP-SEIG model during balanced operating condition. Lastly, the nature and magnitude of eigenvalues are correlated with the machine parameters and variables under no load and different loading conditions which provide a ground in the study of machine stability. So, the eigenvalue behaviour of a six-phase self-excited induction generator is varied in accordance with small deviations of machine parameters and variables for determining its small signal stability analysis. Further, two transfer functions between the mechanical input torque and small changes in active power and reactive power have also been established to identify the machine stability by graphical means.

Generator terminal voltage and frequency are also markedly affected by the excitation capacitor, connected load and rotor speed at renewable energy plants in remote sites or developing countries. On faults due to abrupt reduction in torque during short circuits, machine speed may accelerate and tends towards terminal voltage collapse with the immediate increase in reactive power of self-excited induction generator. So, there is need of control in extreme values of generator terminal voltage and frequency during variations in machine load characteristics or prime mover speed, and also need of speed control during faults in system. For enhancement in voltage and frequency regulation of SEIG, there are others different power electronics aid controllers. Power electronics aid controller are efficient, fast and up-to-date which facilitates a new birth and growth in to previous terminal voltage and generated frequency 'Voltage and Frequency' control schemes of self-excited induction generator during various operating conditions and /or in variable speed applications of SEIG when there is no governor control in small energy generating plants. Before, voltage and frequency control of 3-phase isolated induction generator was in consideration for researcher, here attempt is control of voltage and frequency of 6-phase isolated induction generator i.e. SP-SEIG.

Various isolated /capacitor-excited induction generator control techniques are in practice today. The most simple and popular control technique is by generating variable frequency supply which has constant voltage to frequency ratio. The constant 'voltage to frequency ratio' technique is popularly known as V/F control scheme, in which voltage is proportional to system frequency for keeping flux remains constant in control process. Similarly, a constant 'voltage and frequency' or 'V and F' or 'volt and hertz' new strategy controller and its scheme should be designed and formulated, respectively, for the sake of maintaining desired power quality, in spite of variations in consumer loads. Simplified and moderate Simulink model for voltage and frequency control of isolated six-phase induction generator can keep the terminal voltage and generated frequency remain constant so that generator output power remains constant.

Complete Simulink model has SP-SEIG, controller and its control scheme, and static load arrangement which retains the voltage and frequency almost fixed with marginal drop in machine speed during variations in consumer energy demands.

A new control strategy in voltage and frequency controller of SP-SEIG supplying static load is described with two closed control loops. V and F (volts and Hz) controller consists of current controlled voltage source inverter (CC-VSI) and a high frequency DC chopper. Both keeps the generated voltage and frequency constant against changes in load characteristics. Simulation outputs depict the constant generated voltage and frequency with change in load characteristics. In this way, proposed controller behaves as frequency and voltage regulator. Simplified Simulink model possess control scheme which generates gate drive signals to IGBTs switches of VSI and chopper switches. Simulink model of voltage fed controller 'VFC' has two PI controllers, first is to regulate AC terminal voltage (V_t) and second is for regulating DC bus voltage of VSI. First, a mathematical model of SP-SEIG supplying static load is derived under transient and dynamic conditions. Then, model of D.C. side of inverter along with current controlled voltage source inverter is developed for the control purpose of SP-SEIG. Having two PI controllers in Simulink model, it has complex functionality which is overlooked by its reliable and goal accomplished output performance.

An Outlook on whole research work involves change of variables approach revolutionized by R.H.Park in late 1920s. Park's theory has served as the advantageous theoretical foundations for the equations of transformation in arbitrary reference frame (proposed reference frame is stationary) in the analysis of SP-SEIG. Steady-state modelling using loop impedance and graph network theory; Steady-state analysis using NR numerical technique; Dynamic modelling using mixed variable approach; Transient analysis using conventional RK4 algorithm; Stability analysis by using an eigenvalue criterion in addition to standard (Root-locus) graphical tool, and, V and F control of SP-SEIG is carried out by using a new strategy. Although, NR numerical technique and RK4 algorithm are not seeding well in the computational analysis, yet not obsoleted being simple, fast and effective if initial guesses are perfectly chosen. Thesis task presents an opportunity to focus on following performances of SP-SEIG under balanced or unbalanced and resistive 'R' or resistive-inductive 'R-L' static loads to analyze the performance parameters of simple-shunt and compensated SP-SEIG.

> ➢ The steady state analytical machine performance results obtained by the proposed schemes are compared. Steady state initial values of few machine variables have been used for dynamic and transient analysis.

- Analytical dynamic and transient performance results are found for the R and RL loading on the machine system. In both the cases (R and R-L loading), the voltage drops are unequal and marked when variation from no load to full load.

- Stability is also an important factor being considered to investigate the effect of given values of excitation capacitance, speed and loads. Root-locus graphical tool create an opportunity to observe the behaviour of characteristic roots (or eigenvalues or latent roots) in the s-plane.

- Besides the assistance of isolated /capacitor excited induction generator, it has two crucial deficiencies for need of extra reactive power during faults and loss of excitation during abrupt change in machine load or prime mover speed. Capacitor excitation survives when there is almost constant system load or prime mover speed. So, a new controller scheme is employed for constant 'volt and hertz' or rotor speed for only one particular R loading to demonstrate an introspective spotlight on new strategy being applied in to the Matlab Simulink model of voltage and frequency controller of SP-SEIG.

Journals

[1] **Kiran Singh and Girish Kumar Singh**, "Modelling and analysis of six-phase self-excited induction generator using mixed stator current and magnetizing flux as state-space variables," Electric Power Components and Systems, Taylor & Francis Group, vol. 43, no. 20, pp. 2288–2296, Oct 2015.

[2] **Kiran Singh and Girish Kumar Singh**, " Stability assessment of isolated six-phase induction generator feeding static loads," Turk J Electrical Engineering & Computer Sciences, Vol. 24, No.5, pp. 4218-4230, 2016.

ACKNOWLEDGEMENTS

x

CONTENTS

LIST OF FIGURES

LIST OF TABLES

LIST OF ACRONYMS

3Φ	3phase
IG	Induction generator
AC	Alternating current
DC	Direct current
UHV	Ultra high voltage
MPT	Multi-phase transmission
SEIG	Self-excited induction generator
SP-SEIG	Six-phase self-excited induction generator
MP-SEIG	Multi-phase self-excited induction generator
H.P.O.	High phase order
VAR	Reactive volt ampere
V /F	Voltage and frequency ratio
PWM	Pulse width modulation
CC-VSI	Current controlled voltage source inverter
IGBT	Insulated gate bipolar transistor
PI	Proportional-integral
NR	Newton Rapshon
RK4	4th order Runge - Kutta

LIST OF SYMBOLS

r_1, r_2	Per phase stator resistance of 3Φ stator winding sets *abc* and *xyz*.
r_r	Per phase rotor resistance referred to stator.
X_1, X_2	Per phase stator leakage reactance of 3Φ stator winding sets *abc* and *xyz*.
X_m	Magnetizing reactance at rated frequency.
X_{lm}	Common mutual leakage reactance between the 3Φ stator winding sets.
X_r	Per phase rotor leakage reactance referred to stator.
X_{cp1}, X_{cp2}	Capacitive reactance due to C_{p1} and C_{p2} at rated frequency of winding sets *abc* and *xyz*.
X_{css1}, X_{css2}	Short shunt series capacitive reactance for self-regulating series compensation.
X_{cls1}, X_{cls2}	Long shunt series capacitive reactance for self-regulating series compensation.
V_g	Air gap voltage
F, u	Self-excited electrical frequency (p.u.) and rotor speed (p.u.), respectively
V_{t1}, V_{t2}	Per phase terminal voltages of 3phase winding sets *abc* and *xyz*.
I_{s1}, I_{s2}	Per phase stator current of 3phase winding sets *abc* and *xyz*.
I_r	Per phase rotor current referred to stator.
I_{l1}, I_{l2}	Per phase load current of 3phase winding sets *abc* and *xyz*.
P_{out1}, P_{out2}	Output power of three-phase winding sets *abc* and *xyz*.
VAR_1, VAR_2	Reactive power of 3phase winding sets *abc* and *xyz*.
R_{L1}, R_{L2}	Per phase pure resistive load of 3phase stator winding sets *abc* and *xyz*.
X_{L1}, X_{L2}	Per phase inductive reactance of 3phase stator winding sets *abc* and *xyz*.
V_{d1}, V_{q1}	d-q axis voltage of winding set I.
V_{d2}, V_{q2}	d-q axis voltage of winding set II.
V_{dr}, V_{qr}	d-q axis rotor voltage referred to stator.
ψ_{d1}, ψ_{q1}	d-q axis flux linkage per second of winding set I.
ψ_{d2}, ψ_{q2}	d-q axis flux linkage per second of winding set II.
ψ_{dr}, ψ_{qr}	d-q axis rotor flux linkage per second referred to stator.
ψ_{dm}, ψ_{qm}	d-q axis magnetizing flux linkage per second.
i_{d1}, i_{q1}	d-q axis current of winding set I.
i_{d2}, i_{q2}	d-q axis current of winding set II.
i_{dr}, i_{qr}	d-q axis rotor current referred to stator.
T_e	Electromagnetic torque

T_m	Mechanical input torque
T_L	Load torque
P	Number of pole pairs
J	Moment of inertia of rotor (kg.m^2)
ω	Speed of the reference frame
ω_r	Rotor speed
ω_b	Base speed
θ_r	Electrical angular displacement of the rotor
$L_{\sigma 1}$	Stator leakage inductance per phase of set I
$L_{\sigma 2}$	Stator leakage inductance per phase of set II
$L_{\sigma r}$	Rotor leakage inductance per phase referred to stator.
L_m	Per phase steady-state saturated magnetizing inductance .
L	Per phase dynamic inductance.
L_{dq} / L_{ldq}	Cross-saturation coupling between the d-q axis of stator.
L_{lm}	Common mutual leakage inductance between the stator winding sets.
$1/L_{dd}, 1/L_{qq},$ $1/L_{dq}$	Saturation dependent coefficient of system matrix A.
$\cos\phi, \sin\phi$	The angular displacements of the magnetizing current space vector with respect to the d-axis of the common reference frame.
i_{d1c}, i_{q1c}	d-q axis current through shunt capacitor across winding set I.
i_{d2c}, i_{q2c}	d-q axis current through shunt capacitor across winding set II.
i_{d1L}, i_{q1L}	d-q axis current along resistive load across winding set I.
i_{d2L}, i_{q2L}	d-q axis current along resistive load across winding set II.
C_{p1}, C_{p2}	Shunt capacitor per phase along the stator set I, and II.
C_{se1}, C_{se2}	Short - shunt capacitors across the stator winding set I and II respectively.
C_{ls1}, C_{ls2}	Long - shunt capacitors across the stator winding set I and II
p , σ	Differentiation w. r. t. time, index for constant
V_a, V_b, V_c	3phase line voltages across winding set I.
V_x, V_y, V_z	3phase line voltages across winding set II.
i_a, i_b, i_c	3phase line currents through winding set I.
i_x, i_y, i_z	3phase line currents through winding set II.

Rest of symbols are defind in the text

This chapter describes introduction to the research work. It will start with some background on need of SP-SEIG from its inception.

1.1 Overview

The most outstanding challenges which are encountered by human beings since last several years are the definite resources of energy, water and food, environmental risks and rising political instabilities. These challenges and their interaction with the traditional energy resources have been given birth to a fourth industrial revolution of renewable energy. When the future of global energy markets is discussed, two main concerns feature regularly and giving rise to an attempt to draw lessons from past experiences with periods of industrialization and structural change, and the impact they had on energy demand. Indeed, despite the warnings of Hubbert, world economics are counting on traditional fossil fuels. However, conventional fossil fuels such as coal, oil and natural gas, which have been a key energy source since the industrial revolution, are not only facing depletion, but has also gradually, become a source for concern regarding its serious adverse effects on our environment. Hence, the quest to develop clean and renewable energy sources, such as solar, wind, hydro and solar hydrogen energy, is imperative and timely.

In the late 1920s design towards the double-winding generators emerged to improve efficiency and mitigate certain limitations of large generating units [1-4]. Since then, the accelerated growth in multi-phase was observed by a series of developments. Traditionally, the use of synchronous generators has their priorities in electric power generation for harnessing the renewable energy sources, but induction generators have made their rapid strides and further researched these days due to their relative advantageous features over the conventional synchronous generators.

The relative advantages of multi-phase induction generator over multi-phase synchronous generator [5] seed its operation in stand-alone mode, in conjunction with the synchronous generator and in grid-connected mode. The application of multi-phase generators has also been explored in electric power generation, transmission, and utilization. For these reasons, distributed power generation had received attention in the remote areas to reduce the cost of delivering power being hiked up due to the large investment and losses in a transmission line. With the increased demand of sophisticated design techniques and huge concern of economic, environmental and other issues, multi-phase (H.P.O) machine construction and power transmission are in consideration for the last several years. A multi-phase system has more than 3Φ on the same stator of machine system. It can be multiple or non-multiple of 3Φ, common or non-common neutral and phase shift between the phases depends on prime no. of coils in each phase group (integer no.) positioned with phase belt angle from each to next. If

no. of coils are equal to 2 in each phase group; phase displacement between both coils is 90° whereas if no. of coils are odd in each phase group; phase displacement between the each coils is equal to '360° /no. of coils'. In recent years, particularly multi-phase induction machine has fascination towards variable speed drive applications in relation to three-phase induction machine due to its inviting features [4-9].

Six-phase transmission system is also an interesting, attractive and most common multi-phase power system. The research on six-phase system is rivalling for many reasons. This is also rendering the future prospects of SP-SEIG. SP-SEIG comprises two sets of 3Φ (asymmetrical or symmetrical) windings unlike 3Φ-SEIG to supply inaccessible far-flung areas where it is not viable to establish and maintain electrification. In both winding distribution, asymmetrical six-phase (split-phase) induction machines [3] are practical case of multi-phase induction machine consisting of two identical 3Φ stator windings sharing the same magnetic circuit. This winding designs are built by splitting the phase belt of a conventional 3Φ machine into two subgroups (two sets), which are displaced from each other by 30° and giving rise to an asymmetrical structure considering the angular displacement between any two adjacent phases is not similar. The feasibility of self-excited (stand-alone) induction generator will expedite the electrification of semi-isolated and isolated, rural and remote locations with conventional as well as non-conventional energy sources.

The concept of an independent or isolated induction generator at predetermined voltage and frequency was emerged in 1935 [10]. An isolated mode of induction generator has incorporated all the foregoing advantages and overlooked the most of disadvantages by using external excitation capacitor. External excitation capacitors which are connected in shunt across the terminals of the machine is supplying the exciting or magnetizing current and has took place the role of synchronous machine which was connected previously in the system. However, in spite of having a number of advantages, it suffers from the frequency drop, poor voltage regulation and low power factor in most of the studied cases. In island operation, voltage regulation has to be different from the one used in a grid connected mode. When regulator has fast step response, problems with the stability may also appear to be studied. Therefore, the wide acceptance of these isolated capacitor-excited induction generator depends on the methodology to be adapted in omitting these unbalanced operations. For completeness, the aforementioned problems are briefly discussed below.

1.1.1 Voltage Regulation

As usual, the voltage regulation of SEIG /MP-SEIG must also have to maintain within the lower and upper acceptable limits. This requires choice of a distinct scheme and proper evaluation of stand-alone induction generator characteristics for constant voltage operations. Generally, Among the advantages may be listed, the SEIG (excited with fixed value capacitor)

has a poor voltage regulation due to the insufficient reactive current (increased gap between the VARs supplied by the shunt capacitors and the VARs demanded by the load and machine) with increasing load, which gives reason to drooping load characteristics. This inherent poor voltage regulation restricts the application of SEIG as an isolated or stand-alone unit and so, the requirement of VARs must be fulfilled with the loading for achieving good voltage regulation over the entire load range of the machine. As yet the practice of using induction generators has not been adapted to any appreciable extent. There are different voltages regulating schemes to maintain the constant or minimum voltage variations from no load to full load:

- Power electronic controller
- Magnetic amplifier (Saturable core reactor)
- Series capacitor schemes.

The voltage regulation issues can be improved by using additional series capacitors in each line of the SEIG system. Series capacitors are used in short-shunt or long-shunt operating configurations of SEIG system known as compensated SEIG which can feed static or dynamic loads. The behaviour of compensating SEIG includes all possible situations, in which its behaviour is considerably differs with the inductive loads on the account of its behaviour with the remaining static loads. These inductive loads are prone to causing voltage dip, inrush current, and varying power factor throughout the whole loading range. To compensate poor voltage regulation of compensating SEIG feeding inductive loads results in unbalanced operations. Some typical unbalanced operations in MP-SEIG, which may cause disturbances in machine systems, are summarized below:

- Excessive heating.
- Winding stress.
- Shaft vibrations due to the unequal phase currents and voltages.

All these disturbances may contribute to unbalanced operations for both utility and customers. Therefore, the choice and acceptance of this compensated MP-SEIG is dependent on the distinct methodology proposed to overcome the problems of its unbalanced performance during handling the dynamic loads, poor voltage and frequency regulation [5].

1.1.1.1 Series Capacitor Compensation Scheme

There were different proposed schemes to overcome the poor voltage regulation of SEIG over the past decades. But all were low reliable and complex due to the power electronic circuitry. Then, the addition of the series capacitor did play an attractive role of vital acceptance as compared to all other voltage regulating schemes. So, voltage regulation of

SEIG can be improved by using additional series capacitors either in short-shunt or long-shunt configurations.

- Short-shunt scheme
- Long-shunt scheme

There are three external elements, i.e. terminal capacitance; load impedance and speed that can take place in examining the voltage profile of SEIG. By varying one of these elements at a time the performance characteristics of SEIG can be drawn. For maintaining the adequate voltage and frequency within the acceptable limit during the connected load, the choice of suitable excitation and series capacitors widen the scope of the steady-state characteristics. There are various simple and proposed methods for getting the minimum and maximum values of terminal and series capacitors in both the above configuration. A generalized complete compensating scheme of SP-SEIG is presented in Figure 1.1.

1.1.1.2 Voltage and Frequency Controller

It may use one of the new proposed strategies for induction generator for rotor speed control purpose and inevitably maintains the constant V and F. An attempt for controlling V and F in SP-SEIG is very important and typical task. Basic building blocks of V and F controller-SP-SEIG system is shown in Figure 1.2. It includes additional control blocks across both 3Φ sets. As mentioned before, to stumbling handicaps in applications of capacitor excited induction generator, power electronics controllers are more appropriate scheme in industrial and large power generating units along with conventional and non-conventional energy sources as their prime movers [11 - 15].

1.1.2 Stability Study

The susceptibility of a system to develop a tendency to maintain the equilibrium during disturbances, either large or small is called stability. When six-phase IG is used to supply in an autonomous or grid connected mode, it has made concern of machine stability against its design parameters. Stability problem has two categories:

- steady state
- transient
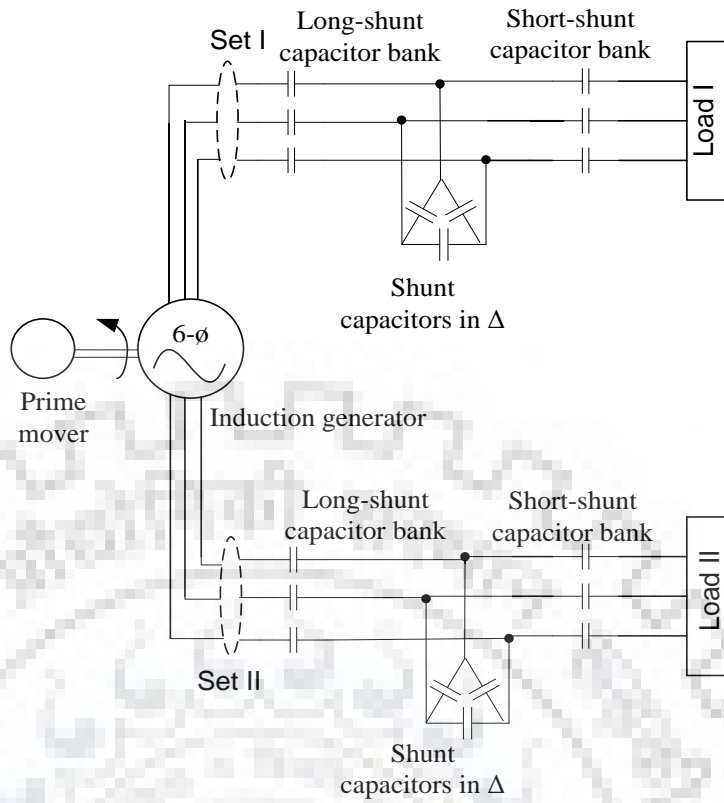
Figure 1.1: Schematic diagram of complete combined six-phase self-excited induction generator in simple and compensated scheme.
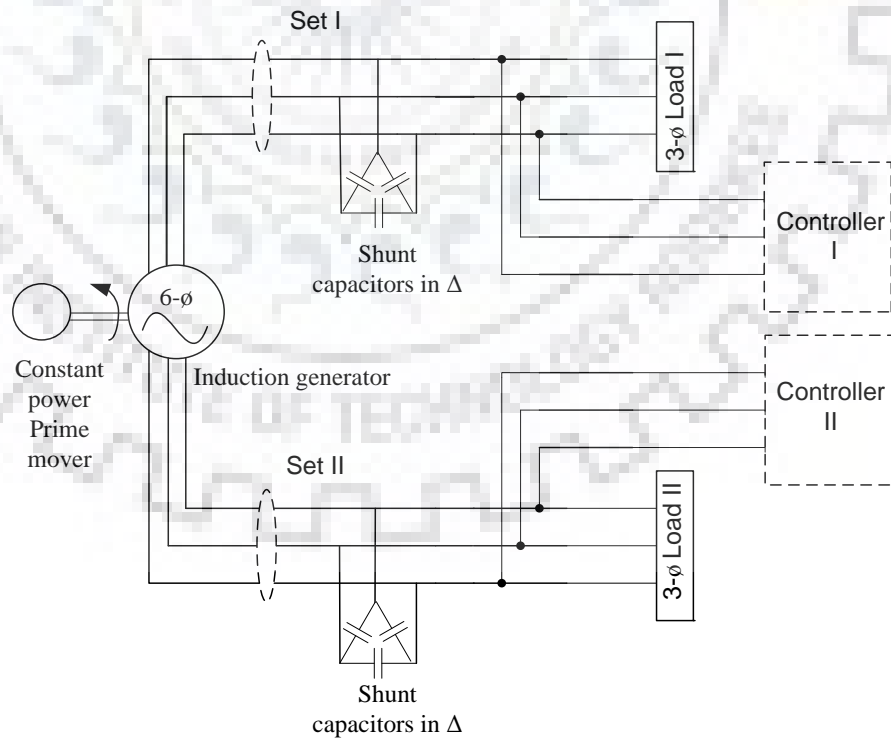
Figure 1.2: Schematic diagram of complete six-phase self-excited induction generator along with V and F controller.

5

Table 1.1 : Prime sources of instability

Sources of instability

Variable frequency power source	Improper selection of system parameters	Assumption made in neglecting various effects	Electrical and/or mechanical disturbances
At low speeds (low frequencies) particularly, and also over other range of frequencies.	Changes in machine parameters, filters parameters and rectifier commutating reactance. Small horse power rating machine contribute small inertia constant.	Saturation effect, Skin effect, Iron losses and Mechanical damping etc.	Gradual power changes, Automatic control device, Occurrence of a fault due to sudden application /removal of load and sudden disconnection of lines.

Steady state stability belongs to slow and small disturbances whereas transient stability tends to ensure that system hold out against the transient during major disturbance. Extension of steady state stability is dynamic stability, concerns with small and long lasting disturbances. Transient stability deals with sudden and large disturbances. Small signal (small disturbance) stability is an important study in among all [16 - 19].

The prime sources of instability in the machine and power system are given in Table 1.1 from [1, 20]. Six-phase to three–phase transformer is a major source of instability in grid connected mode. In isolated mode, induction generator requires special attention during faults due to abrupt variation in electrical torque. As a result, voltage collapse occurs in the generators due to increased reactive power.

1.2 Literature Review

First attempt in 1969 by Ward and Harer [21] have mentioned that torque pulsation amplitude can be decreased with increased number of stator phases during the prior survey on an inverter supplied 5Φ induction motor. Nelson and Krause [22] have realized computer simulation of inverter fed 6Φ motors. This study concluded that 6th harmonic torque pulsation was eliminated with increased peak stator currents by keeping 30° phase belts. Schouten et. al., Toliyat et. al. and Danzer [1] have achieved both simulation and experimental results for 5Φ motors. Five phases (5Φ) were chosen to reduce current magnitudes as per suitability of thyristors in inverter source, though it leads to excessive 3rd harmonic current. More than 3Φ were suggested for higher extent of reliability.

These past efforts to establish multi-phase induction motors demonstrate few attractive benefits. The most promising benefits are obtained from the 30° angular spacing between both 3Φ sets of a 6Φ motor. The consequences of 30° displacement angle are elimination of 6m±1 (m=1, 3, 5…) orders of all air-gap flux harmonics. Result of this, all rotor copper losses, and 6m (m=1, 3, 5…) orders of torque harmonics are also eliminated. Remaining fascinating advantages are lower current per phase without increase in per phase voltage, reduced iron loss, improved reliability and increased total output power rating of system being in same frame. Later, these advantageous features of multi-phase motors are also followed by multi-phase generators [1].

Similarly, researchers on multi-phase machines and drives [23] have reported specific application of asymmetrical six-phase machines with variable-speed drives. Advantages like reliability improvement, reduction in the spatial harmonic content of MMF, reduction in torque pulsation etc. Although research in multi-phase machine is not at an advanced stage in electric energy generation as compared to variable-speed drives. The generator schemes presented

in references of [3, 4] provide a general feasibility of multi-phase generating system. In last decade, advantageous features of the multi-phase motors were also followed by multi-phase generators in conjunction with renewable energy sources.

During the 1950s, researchers have fascinated towards physically simple, rugged and brushless appearance of the induction generator holding cage type rotor unit in electric power generation. The utilization of SEIG is recommended in both modes along with conventional as well as non-conventional energy sources over the limiting factors of synchronous generator and another machine [10, 24 - 26] in the area of small capacity power generation. For the sake of advantages over other generators and 3Φ system as briefly described in previous Sections and by [4], an isolated /capacitor excited induction generator and six-phase (multi-phase) technology, respectively, are elected in pursuing a further research task. The work carried out yet on isolated or capacitor excited 3Φ induction generator is so broad to explain, whereas, it is very limited [3 - 9] covering all aspects related to modelling, analysis, operation and control for isolated or capacitor excited multi-phase (6Φ) induction generator. Solely, a brief review is undertaken and followed.

First in 1939, Wagner was reported an approximate analytical method of SEIG. Barkle and Ferguson had also discussed approximate analysis of various aspects in induction generator for both modes. A significant investigation on induction generator took place around late seventies worldwide due to the global warming and other environmental crisis. Reference [10] was determined towards self-excitation phenomenon in induction machine. Although, efforts were genuine for bright future prospects, yet induction generators are cursed by their poor voltage regulation and need a proper voltage regulating scheme. By that time, scientists had also acknowledged enormous utilization of conventional sources is giving rise to depletion of its roots and must be rationalized by seeking other non-conventional resources. In this regard, wind was recognized as a potential renewable energy source and induction generator as efficient converters of the wind into electrical energy. The growth of wind energy systems using the induction generator and voltage regulator speeded up by using powerful devices (preferably SCRs). Voltage regulators which were controlled by thyristors [5, 25] had involved various types of demerits.

Around that time, the analysis of generator was based on approximations only and regardless of this, beneficial features of induction generator in small power generation have inspired the researchers for further exact analysis. In 1983, Elder et. al. did concentrate on various aspects of self-excitation in induction generator. During that time and later, various others literatures [10, 25, 27] were available for focusing on analysis, operation and design aspects of induction generator. In 1929, Park stated a dynamic analysis of synchronous generator. An improved

suggestion of dynamic analysis was also given by Krause in 1965. Other models were also arranged [5, 28]. The consistency of all models depends on appropriate inclusion of saturation. Inclusion of different types of saturation using various approaches has been considered [3 - 5, 7, 25, 28]. The d-q-0 reference frame transformation has long been used successfully in available literatures for the analysis and control of a 3Φ electric machine using single and mixed variable modelling [10]. Accurate analysis and VAR control of SEIG has been replaced synchronous generator in various applications using renewable energy systems.

A particular and serious aspect of SEIG is a poor voltage regulation was taken into account around 1935 by Basset et. al. [10], and further by Singh et.al [4, 5, 9] . In regard to this, an additional series capacitor is used in series with every phase of generator winding set for the purpose of voltage compensation. Compensation schemes in both configurations i.e. short-shunt and long-shunt act in the similar way of DC generator compounding and transmission line have been discussed [4, 10, 25]. Focus is also given on capacitance value selection for self-excitation and series compensation. Another important aspect also deserves special attention during faults is its dynamic behaviour [29]. When SEIG is employed as an isolated power source, the terminal voltage and frequency are severely influenced by rotor speed, excitation capacitors and connected loads in the field of low-head small hydroelectric and wind energy applications at the remote site. From all the cases discussed above, it become also necessary to incorporate analytical methods for stability analysis. A review has been brought out to highlight the various issues related to the current and future progress of SEIG [5].

The investigation on multi-phase machine is not stepping up rapidly as compared to multi-phase drives in the electric energy generation. The literature regarding multi-phase induction generator is nearly non-existence before 20th century and only three very important findings were drawing more attention. Research in this field is going on and numerous interesting developments have been reported in various available literatures. The first work and paper on multi-phase induction generator is appeared in 2005, followed by some more theoretical and practical works on SP-SEIG. Singh et. al. have been reported some beneficial research on SP-SEIG as a stand-alone generator in the field of renewable energy generation over the last decade. Single variable (flux) mathematical modelling for analyzing the detailed transient (dynamic) behaviour of simple-shunt and series compensated SP-SEIG has been presented. Saturated magnetizing inductance and its derivative are considered in whole analysis. It also discusses the behaviour of a SP-SEIG to operate as a stand-alone electric energy source in conjunction with a hydraulic turbine [4 - 9].

Reference [3] demonstrates an easy technique for finding out the appropriate values of shunt and series capacitances which are essential to initiate and maintain the self-excitation and self-regulation in a SP-SEIG. Steady-state behaviour along with the detailed performance

analysis of SP-SEIG have been presented using a nodal admittance based network analysis modelling [6] whereas [7] explains the advantages of using simple-shunt SP-SEIG and its practical feasibility by performing experimentation. The steady-state analysis of compensated SP-SEIG has been dealt by deploying the practical treatment along with hydro power plant [8]. In [9], performance evaluation of simple and compensated SP-SEIG is described in each topology of shunt capacitors by using a generalized and efficient modelling. A variety of transformations have also been proposed in past for the analysis of multiphase induction machines [3]. In which, symmetrical component and matrix theories have been served as the theoretical foundations for the d-q-0 reference frame transformation. The stability studies had carried out in detail for six-phase induction machine, but no more such study has been presented for multi-phase induction generator.

Stability and control analysis are also carried out by using the popular techniques [12, 13, 29]. Gorti et. al. discussed that besides the benefits of SEIG, the induction generator are having mainly two drawbacks; one is need of reactive power support and second is poor voltage regulation. The capacitor excitation is suitable only when there is almost constant load and prime mover speed, any change in load or speed may result in a loss of excitation. In past decades, some researchers have reported and attempted redesigning for improving hereditary underprivileged voltage regulation of SEIG by using different techniques and procedures on different design aspects of proposed machine. Several other researchers have made efforts by using compensation schemes in available literatures for ensuring better voltage regulation. Some followers of previous investigation have proposed new controllers for controlling different parameters of system by using appropriate novel schemes during constant power applications of SEIG. During, variable power applications of SEIGs i.e. when prime mover is renewable energy sources which are of variable magnitude in nature with irregular weather conditions, variety of different controllers are also designed and considered in past.

Among the various control strategy, authors have examined the transient performance of wind driven SEIG. In these control strategies, the use of fast switching solid-state devices i.e. MOSFET, IGBT and GTO has been reported in few literatures. Further, advancement in fast switching solid-state devices gives birth to compact compensators for the purpose of reactive power (VAR) controller of SEIG. Other literatures have reported and examined variety of static exciter or static VAR to provide reactive powers in IGs. Major emphasis has been given to develop the strategy for reactive power compensation and voltage regulation. In view of this, excitation and voltage regulator have been discussed [30]. Some have presented good modelling on voltage regulator of SEIG using solid state switches and others have designed SEIG controller by using voltage source PWM inverter

[4, 12, 13]. Mishra et. al. have presented new voltage regulator. Rest of work is related to feasibility of double stator winding of IGs for voltage regulation purpose. In 2004, Singh [5] has also been presented an appropriate review on voltage and frequency regulation of SEIG. In last decade, major research on V and F controller of 3Φ SEIG is reported [14, 31]. Some more valuable literatures are also available [15, 32] over the past five years.

As multi-phase /H.P.O. technologies are advantageous, so the purpose of meeting research gap, further, loop impedance method and mixed variable modelling for the steady-state and dynamic analysis are presented instead of nodal admittance method and single variable, respectively. Other additional analysis is stability using classical approach and 'V and F' control of SP-SEIG using new scheme.

1.3 Author's Contribution

Although, research report is purely literary works and has no practical evidence in the field of electric power generation but today's academic paper dream may become tomorrow's attractive future prospects. At present no grounds of any industrial intake of such machine system, still multi-phase AC generator could commence as a feasible remedy in wind and hydro power plants. Hopefully, all reviews of literatures in the studies of modelling, analysis, stability and control application will participate with full interest in the exploitation of beneficial features of SP-SEIG in the area of electric power generation using non-conventional energy sources. Works have been carried out for steady state performance of simple and compensated SP-SEIG; dynamic performance of simple and compensated SP-SEIG; stability analysis of SP-SEIG and 'V and F' control of SP-SEIG. Scope of all work is summarized below:

Steady-state performance of simple and compensated (short-shunt and long-shunt configurations) SP-SEIG supplying static loads has been studied for operational behaviour of machine under variety of operating conditions below the critical slip. A comparative study is established among the simple-shunt, short-shunt and long-shunt topologies of the studied machine for finding out the effectiveness of compounding schemes compared to its uncompounding schemes. For this, a generalized matrix model will help to understand the operation of simple and compensated SP-SEIG. Compensated or compounding schemes are utilized in cost compelling voltage regulation operation. Work related to the compounding of machine is considered for static loads, and in both modes of excitation shunt capacitor banks. Basically, two different types of compounding are in use for long time to investigate the voltage regulation i.e. short-shunt and long-shunt compensation schemes. Capacitor values have to be chosen throughout the range of machine loading for proper voltage regulation under fundamental pre-determined constraints.

The dynamic model is developed in d-q stationary reference frame by using mixed state variables, particularly, magnetizing flux and stator current. Modelling has been reported to investigate the machine dynamic performance during transient conditions. This incorporates main flux saturation in performance equations. Transient analysis of simple and compensated SP-SEIG is performed during balanced conditions using mixed state-space variables modelling. This analysis determines the onset of self-excited voltage build–up on no load. Transient performances are also related to sudden connection of electrical loads with different power factors (both resistive and inductive loads) at the machine external terminals. Use of mixed variables during dynamic or transient analysis of SP-SEIG has no dissimilarity in magnitude and pattern of output performance characteristics in corresponds to single variable analysis.

Stability investigation is an important factor and affected by the many design parameters of the machine during steady state operation. It will also help to determine, mainly, the influences of rotor speeds, system loads, shunt capacitors, and a variation of most critical parameter i.e. magnetizing inductance on the studied machine eigenvalues during isolated mode of induction generator in the field of non-conventional energy generation e.g. small wind and hydro power plants at the remote places in developing countries.

'V and F' control is also a serious and noticeable aspect during running conditions of SP-SEIG, when it is subjected to variable speed and variations in system loading. In stand-alone mode, and when induction generator is driven by a variable speed turbine coupled to renewable energy sources. It becomes also very necessary to choose appropriate and advanced control techniques to extract the almost constant voltage and frequency 'Volts and Hz'.

1.4 Organization of the Work

Whole research study embodies the detailed investigation on author's contributions as listed before. Organization has taken placed through six chapters. Contribution focuses on generalized per-phase equivalent circuit model, mixed stator current and magnetizing flux variable model, small signal linearized model and 'V and F' controller for steady state analysis, dynamic analysis, stability analysis, and constant voltage and frequency analysis of SP-SEIG, respectively.

The **Chapter-1** presents a general introduction of SP-SEIG taking in to account a concise study of 3Φ SEIG from its inception. It includes benefits of multiphase induction machine (6Φ-SEIG) over 3Φ induction machine (3Φ-SEIG) which gives reason for adopting SP-SEIG in future where it is applicable to harnessing non-conventional energy sources. Brief highlights of literatures review are also presented to give a focus on previous, current and future scopes of

selected work. Author contribution to the selected work is mentioned along with the orders of research work have been taken placed before.

The **Chapter-2** deals with a generalized model using graph theory to study the comparative steady-state behaviour of simple and compensated isolated SP-SEIG. The steady-state modelling is performed from the per-phase equivalent circuit of the machine by using loop impedance method based on graph theory. The resultant matrix model is convenient for computation, and flexible to various future modifications. Mathematical matrix model is solved by using the Newton-Raphson routine based analytical technique for the estimation of machine performance parameters. Analytical results obtained by the proposed schemes (loop impedance method and Newton-Raphson subroutine) are mutually compared, and verified by the previous competent literatures during the resistive loading at the terminals of SP-SEIG.

The **Chapter-3** concerns with a simple two axis (d-q) model of a saturated SP-SEIG using mixed stator current and magnetizing flux as state-space variables. This new set of orthogonal transformation (dq0) is characterized with a four saturation elements solely in-built system matrix. Selection of this model using proposed mixed variables is justified by its simplicity. Performance equations for the given machine use the steady state magnetizing inductance, and dynamic inductance. In view of simplifying the dynamic analysis, effects of common mutual leakage inductance and cross saturation coupling across the d-q axis of each stator have been pretermitted. The transient analysis of simple and compensated SP-SEIG supplying static loads throughout the machine full load capacity using 4th order Runge-Kutta subroutine is performed on two axis (d-q) developed mixed variable model of a saturated SP-SEIG aimed at a stand-alone renewable energy generation. Analytical results were also validated by previous literatures and were found to be in good agreement.

The **Chapter-4** presents the stability analysis of a SP-SEIG based on the eigenvalue stability criteria to its linearized model. This demonstrates the small signal stability behaviour during steady-state operating conditions. Eigenvalue approach also establishes an opportunity to correlate eigenvalues with machine parameters. This investigation reveals that the eigenvalues are dependent upon the machine parameters, and most critical parameter is a variation of magnetizing inductance. The eigenvalues are varied in accordance with the machine variables. Location of eigenvalues (poles) in the s - plane also gives an opportunity to know about absolute stability using Root-locus graphical tool from derived transfer functions.

The **Chapter-5** is a short introductory on voltage and frequency control of a SP-SEIG based on the new control strategy to its control model. This demonstrates the voltage and frequency behaviour during fluctuations in speed and load conditions. New control approach also establishes an opportunity to correlate terminal voltages with machine frequency or rotor

speed keeping generated power remains uninterrupted. This investigation reveals that the terminal voltage and frequency dependent upon the machine loading, and most critical factor is a variation of system speed. The speed of turbine /prime mover is varied in accordance with the energy sources i.e. renewable or conventional. A particular transient response during symmetrical resistive loads across both the 3Φ sets is simulated to validate the proposed analytical control scheme and gives focus about mechanism of 'V and F' controller in SP-SEIG.

The **Chapter-6** exposes the major conclusions and contributions of thesis task and states its future opportunity for additional research in this field.

1.5 Concluding Remarks

In this chapter, preliminaries on the research topic with brief literature survey have been discussed. Author contribution and thesis organization along with scope of research work have also been carried out. Discussion highlights the various specific issues in the literature review section towards growth and practical realization of six-phase (multi-phase) technology conjointly with capacitor excited (isolated) induction generator.

This chapter describes an analysis for better understanding about the behaviour of SP-SEIG from its design and operational point of view. Foremost, it will start with some background and need of presented analysis using capacitor excited per phase equivalent circuit of SP-SEIG during steady state. Then, a simple and unified solution to the mathematical formulation is discussed using a classical approach. Next, scopes of work along with author's contributions are explained.

2.1 Introduction

The steady state performance is an outstanding study for ensuring good quality power, assessing the suitability of different configurations of SEIG (simple shunt, short-shunt and long-shunt) for a particular application and as far as the normal and running conditions of machine are concerned. This analysis focuses on operational behaviour of a power generating system under its particular operating conditions. Both the terminal voltage and frequency are unknown and have to be computed for a given shaft speed, excitation capacitance, and load impedance. To investigate the various issues related to the use of SP-SEIG as a stand-alone system, Singh et. al. has reported some works in the last ten years. The first work appeared in 2005 followed by [3]. In all the previous works, authors have presented modelling and analysis, simple-shunt and series compensation schemes, practical feasibility along with performance evaluation of SP-SEIG. One of the induction generator's ability to generate power at varying speed facilitates its application in various modes. In isolated mode, i.e. capacitor self-excited mode, induction generator suffers from poor voltage regulation, which necessitates appropriate voltage regulating scheme [6-9]. In this regard, further, a comparative study of simple-shunt and compensated six-phase induction generator in different operating modes is employed for simplifying the complexity of the voltage regulators.

A large number of detailed articles are in the appearance for the popular techniques which have been used during steady state analysis, and in the operational study of simple and compensated SEIG feeding static loads. The act of compensation is needed for desired improvement in poor voltage regulation of SEIGs through either 'short-shunt' or 'long-shunt' scheme without any major effect in cost. Various analytical (and /or) numerical techniques are available for the analysis and calculation of steady-state performance and parameters of SEIGs, respectively. These seem, however, to fall into two main categories:

- Based on loop impedance model
- Based on nodal admittance model

Both modelling techniques are based on the per-phase modified capacitor excited equivalent circuit of simple and compensated SEIG can be expressed in per-unit or actual form. The p.u. representation simplifies the analysis of complex-system and gives more uniform values in comparison to its original representation. A per-phase capacitor excited

equivalent circuit of the simple and compensated SEIGs based on certain conjecture could also be used in finding out of irrefutable results [10].

Most of the previous techniques, either the nodal admittance or the loop impedance were used in determining the steady state performance of the generator from its modified per-phase equivalent circuit are very crucial tools. In both techniques, two nonlinear scalar equations are first derived from real and imaginary parts of the equivalent complex loop impedance or nodal admittance of the circuit. Then both partitioned equations are solved by two common approaches which are employed in solving of both techniques models.

- Optimizations
- Higher order polynomial functions

This chapter addresses loop impedance model technique for a brief comparative steady state study of simple and compensated six-phase isolated induction generator. Further, one of the suitable Newton-Raphson numerical analytical techniques has been proposed to solve non-linear complex loop impedance equations. Finally, these simultaneous nonlinear algebraic loop equations are used to determine the unknown variables 'Xm' and 'F' from real and imaginary parts of equivalent complex loop impedance, respectively, from per-phase per-unit modified equivalent circuit (normalized to self-excited base frequency) of SP-SEIG associated with resistive load.

2.2 Planning for Problem Formulation

The steady state performance evaluation of a simple and compensated SP-SEIG is accomplished from its per-phase per-unit equivalent circuit. Even though, the steady state analysis has been carried out in detail for 3Φ induction generators using the proposed methods (loop impedance model in conjunction with network graph theory, and Newton Raphson technique), this analysis with the proposed techniques still has no evidence for shunt and series compensated SP-SEIG on the basis of detailed literature review. In the present formulation, simplified mathematical loop equations matrix is solved by the Newton-Raphson technique to determine the values of unknown variables 'X_m' and 'F' of SP-SEIG under resistive load conditions. Primarily, equivalent circuit model is followed by the graph theoretic model used in formulation. Secondly, formulation addresses the loop impedance equations of SP-SEIG under different operating conditions from graph theoretic model. These steady state describing equations can also be used for the calculation of steady state initial values during dynamic simulation of machine model for the investigation of its output performance parameters. Finally, realized formulation is used in optimization and evaluation of performance parameters under resistive loads by using the Newton-Raphson numerical technique.

2.2.1 Steady State Modelling

The detailed mathematical modelling for steady state analysis in SP-SEIG requires its equivalent circuit representation. A per-phase generalized equivalent circuit referred to self-excited base frequency associated with resistive load is shown in Figure 2.1, when the SP-SEIG is driven by a d.c. motor drive, in which shaft speed 'u' is almost maintained fixed, but both 'X_m' and 'F' vary with the resistive loads and hence they must be taken as variables for a given load and excitation capacitance. Figure 2.1 shows generalized (mixed) equivalent circuit referred to self-excited base frequency [3] of a SP-SEIG under resistive load conditions in all the fundamental configurations.

In this mixed configuration, the shunt capacitive reactance for self-excitation, and the self-regulating series capacitive reactance for series compensation are connected across stator terminals, and in series with load impedance or placed between the generator terminal and shunt capacitance, respectively, short-shunt or long-shunt topologies, depends upon the application. In this mixed (generalized) configuration, only shunt capacitive reactance for the self-excitation is connected across the stator terminals in parallel manner. All branch impedance parameters of the equivalent circuit are given below.

$$Z_1 = \left(\left(r_r / (F\text{-}u) \right) + jX_r \right)$$

$$Z_2 = j2\pi F L_m$$

$$Z_3 = jX_{lm}$$

$$Z_4 = \left(\left(r_2/F + jX_2 \right) - jX_{cls2}/F^2 \right)$$

$$Z_5 = \left(\left(r_1/F + jX_1 \right) - jX_{cls1}/F^2 \right)$$

$$Z_6 = \left(-jX_{cp2}/F^2 \right)$$

$$Z_7 = \left(R_{L2}/F - (jX_{css2}/F^2) \right)$$

$$Z_8 = \left(-jX_{cp1}/F^2 \right)$$

$$Z_9 = \left(R_{L1}/F - (jX_{css1}/F^2) \right)$$
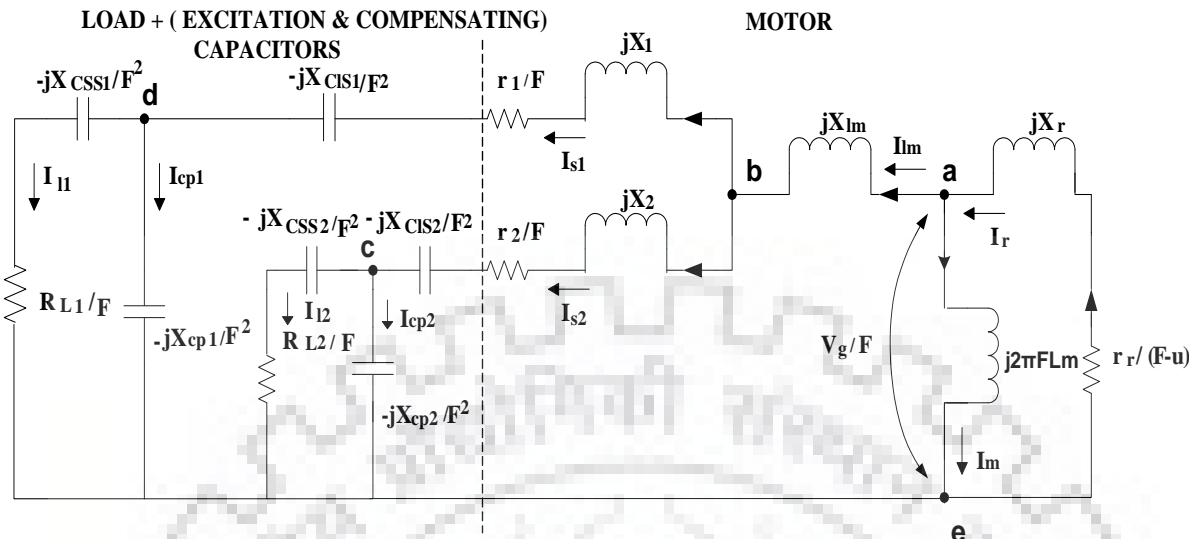
Figure 2.1: Per-phase generalized equivalent circuit of SP-SEIG in simple, short-shunt and long-shunt configurations under resistive load.
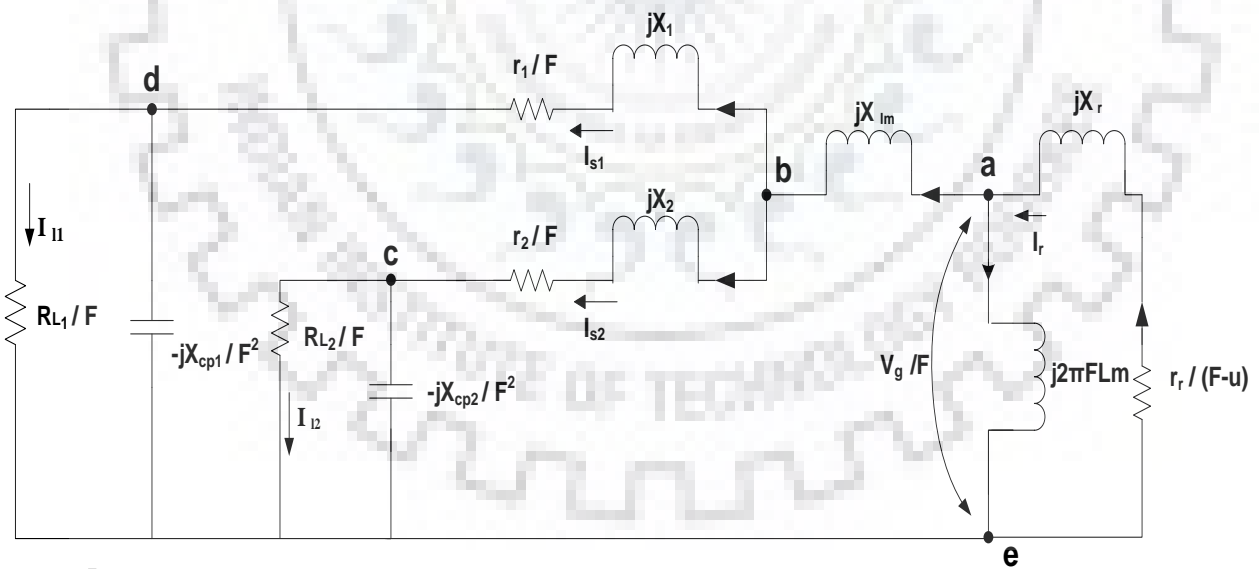
Figure 2.2: Per-phase equivalent circuit of SP-SEIG in simple-shunt configuration under resistive load.

2.2.1.1 Uncompensated Scheme

Figure 2.2 depicts a per-phase equivalent circuit of a proposed simple-shunt (Uncompensated) SP-SEIG referred to self-excited base frequency under the resistive load [3]. In this configuration, the shunt capacitive reactance for the self-excitation is only connected across the stator terminals and no other capacitive reactances are connected in series manner. All branch impedance parameters of the simple-shunt equivalent circuit are given below for resistive load.

$$Z_1 = \left(\left(r_r / (F-u) \right) + jX_r \right)$$

$$Z_2 = j2\pi F L_m$$

$$Z_3 = jX_{lm}$$

$$Z_4 = \left((r_2/F) + jX_2 \right)$$

$$Z_5 = \left((r_1/F) + jX_1 \right)$$

$$Z_6 = \left(-jX_{cp2}/F^2 \right)$$

$$Z_7 = \left(R_{L2}/F \right)$$

$$Z_8 = \left(-jX_{cp1}/F^2 \right)$$

$$Z_9 = \left(R_{L1}/F \right)$$

2.2.1.2 Compensated Scheme

Figure 2.3 shows the per-phase equivalent circuit of a short-shunt SP-SEIG under resistive load condition. In this configuration, the shunt capacitive reactance for self-excitation, and the short-shunt series capacitive reactance for series compensation or self-regulation are connected across stator terminals and in series with load impedance, respectively. All branch impedance parameters of the equivalent circuit are given below for resistive load.

$$Z_1 = \left(\left(r_r / (F-u) \right) + jX_r \right)$$

$$Z_2 = j2\pi F L_m$$

$$Z_3 = jX_{lm}$$

$$Z_4 = \left(r_2/F + jX_2 \right)$$

$$Z_5 = \left(r_1/F + jX_1 \right)$$
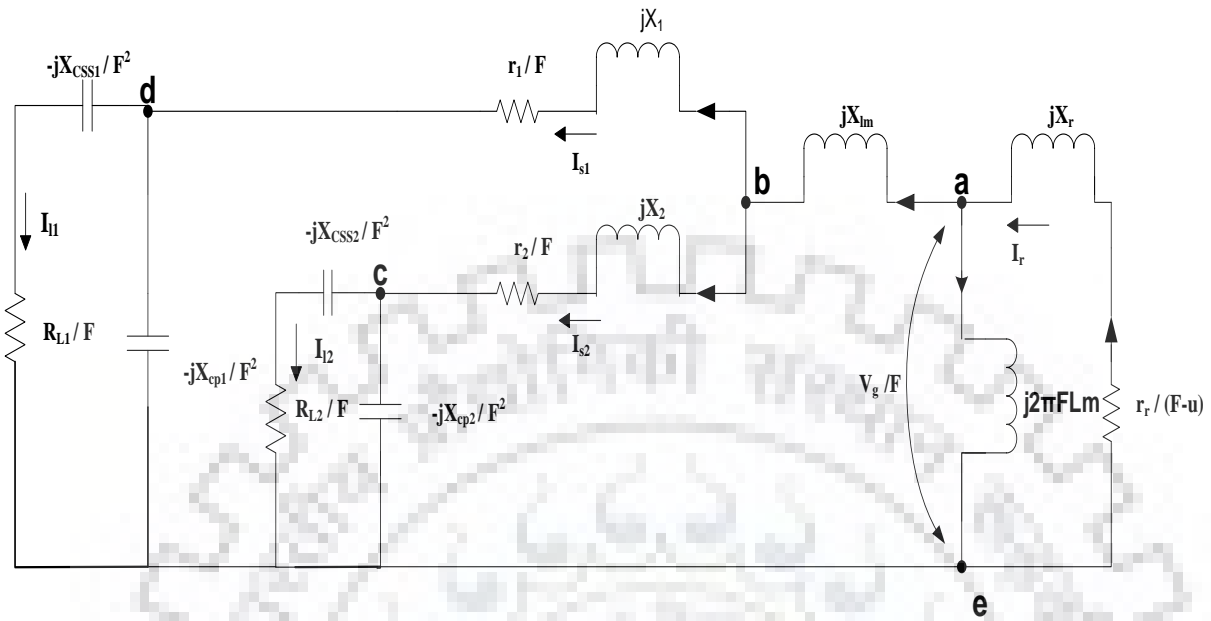
Figure 2.3: Per-phase equivalent circuit of SP-SEIG in short-shunt configuration under resistive load.
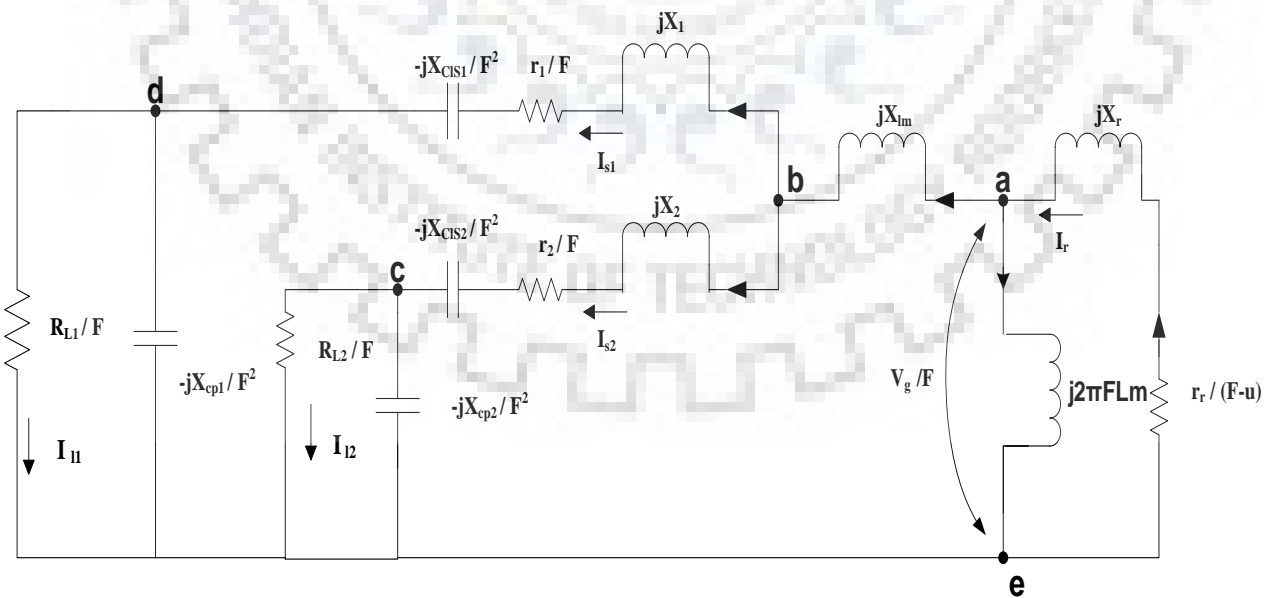
Figure 2.4: Per-phase equivalent circuit of SP-SEIG in long-shunt configuration under resistive load.

20

$$Z_6 = \left(-jX_{cp2}/F^2 \right)$$

$$Z_7 = \left(R_{L2}/F - (jX_{css2}/F^2) \right)$$

$$Z_8 = \left(-jX_{cp1}/F^2 \right)$$

$$Z_9 = \left(R_{L1}/F - (jX_{css1}/F^2) \right)$$

Figure 2.4 shows the per-phase equivalent circuit of a long-shunt SP-SEIG under resistive load condition. In this configuration, the shunt capacitive reactance for self-excitation and the long-shunt series capacitive reactance for series compensation /self-regulation are connected across stator terminals, and, placed between the generator terminal and the shunt capacitance, respectively. All branch impedance parameters of the equivalent circuit are given below for resistive load.

$$Z_1 = \left(\left(r_r/(F-u) \right) + jX_r \right)$$

$$Z_2 = j2\pi F L_m$$

$$Z_3 = jX_{lm}$$

$$Z_4 = \left(\left(r_2/F + jX_2 \right) - jX_{cls2}/F^2 \right)$$

$$Z_5 = \left(\left(r_1/F + jX_1 \right) - jX_{cls1}/F^2 \right)$$

$$Z_6 = \left(-jX_{cp2}/F^2 \right)$$

$$Z_7 = \left(R_{L2}/F \right)$$

$$Z_8 = \left(-jX_{cp1}/F^2 \right)$$

$$Z_9 = \left(R_{L1}/F \right)$$

2.2.2 Implementation of Applied Strategies

Foremost, graph theory is utilized for the purpose of mapping graph of a proposed network (per-phase generalized equivalent circuit of SP-SEIG) as in electrical engineering for the solution of network analysis problems. Secondly, the loop impedance technique is used for the formulation of proposed network equations from its resultant graph. Finally, the Newton-Raphson 'NR' technique is used for the optimization of the unknown variables 'X_m' and 'F' from the final realized loop impedance matrix of SP-SEIG.
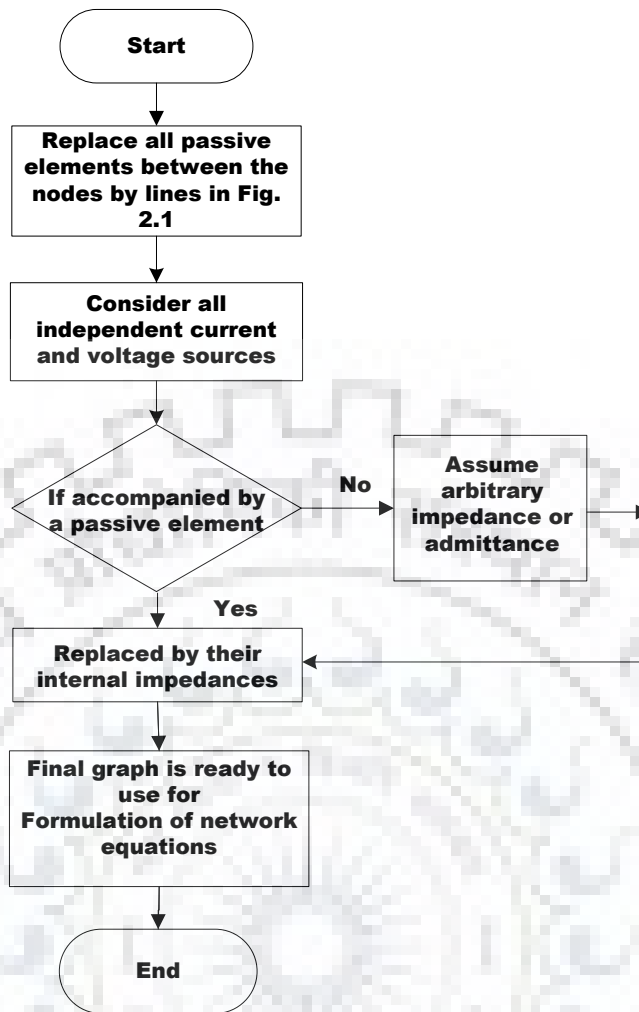
Figure 2.5: A flowchart of the steps used in drawing graph for per-phase equivalent circuit.

Tie-sets:[2,3,5,7,8]
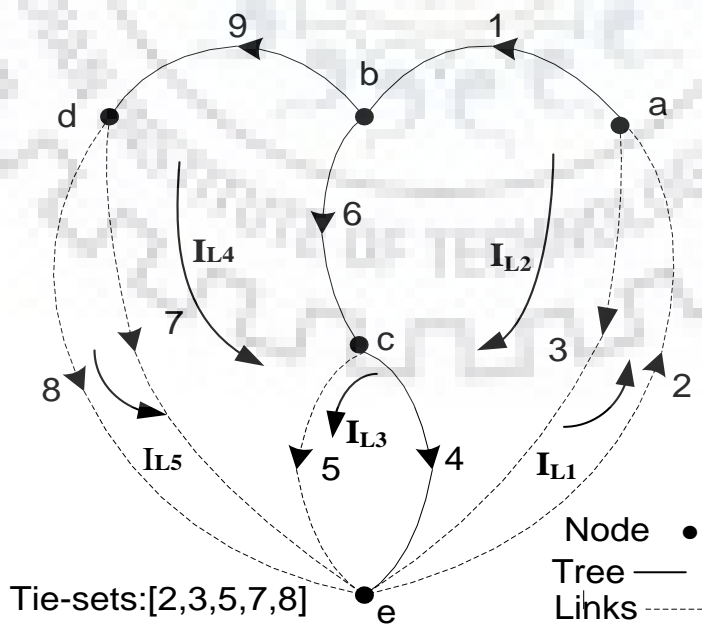
Figure 2.6: Tree with Links (Loops) and nodes in outlined graph.

2.2.2.1 Choice of Desired Graph

A linear graph (or simply a graph) is defined as a collection of points called nodes, and line segment called branches, the nodes being joined together by the branches. The steps which have been undertaken during the drawing of a graph from equivalent circuit are arranged chronologically in Figure 2.5. The graph with links, trees and tie-sets can be formed as shown in Figure 2.6. The number of branches, nodes, tree branches and links of the graph shown in Figure 2.6 is: Number of branches (b) = 9, Number of nodes (n) = 5, Number of tree branches $(n_t) = n - 1 = 4$, Number of links (L) = $b - n_t$ = 5.

2.2.2.2 Formulation of Network Equations

An algorithm has been undertaken during the formulation of network equations is also arranged in Figure 2.7 on loop impedance basis. In this flowchart, $Z_l = B_f Z_b B_f^T$ is the loop impedance matrix of the order of $(b-n+1)*(b-n+1)$. The above equation represents a set of $(b-n+1)$ number of equations, known as mesh or loop equations.

The equilibrium equation in matrix form on loop impedance basis can be expressed as

$$\left\{ [B_f][Z_b][B_f]^T \right\} [I_L] = [B_f] \left\{ [Z_b][I_s] - [V_s] \right\} \tag{2.1}$$

Where, $[B_f]$ is the tie-set matrix and implemented in Table 2.1, $[B_f]^T$ is the transposed matrix of $[B_f]$, $[Z_b]$ is the branch impedance matrix, $[I_L]$ is the independent link branch current column matrix, $[I_s]$ is the current-source column matrix and $[V_s]$ is the tree potential source column matrix. There are no current or voltage sources in Figure 2.1. Therefore, $[V_s] = [0]$ and $[I_s] = [0]$ in Equation (2.1). Hence, it is reduced to Equation (2.2).

$$\left\{ [B_f][Z_b][B_f]^T \right\} [I_L] = [0] \tag{2.2}$$

Where,

$$[B_f] = \begin{bmatrix} 1 & 1 & 0 & 1 & 0 & 1 & 0 & 0 & 0 \\ -1 & 0 & 1 & -1 & 0 & -1 & 0 & 0 & 0 \\ 0 & 0 & 0 & -1 & 1 & 0 & 0 & 0 & 0 \\ 0 & 0 & 0 & -1 & 0 & -1 & 1 & 0 & 1 \\ 0 & 0 & 0 & -1 & 0 & -1 & 0 & 1 & 1 \end{bmatrix}$$

$$[Z_b] = \text{diag}[Z_1, Z_2, Z_3, Z_4, Z_5, Z_6, Z_7, Z_8, Z_9]$$

$$[I_L] = [I_{L1} \quad I_{L2} \quad I_{L3} \quad I_{L4}]^T$$

By substituting, $[B_f]^T$, $[Z_b]$ and $[I_L]$ in the Equation (2.2), following matrix equation is obtained as:

$$\begin{bmatrix} Z1+Z2+Z4+Z6 & -Z2-Z4-Z6 & -Z4 & -(Z4+Z6) & -(Z4+Z6) \\ -Z1-Z4-Z6 & Z1+Z3+Z4+Z6 & Z4 & (Z4+Z6) & (Z4+Z6) \\ -Z4 & Z4 & Z4+Z5 & Z4 & Z4 \\ -(Z4+Z6) & (Z4+Z6) & Z4 & Z4+Z6+Z7+Z9 & Z4+Z6+Z9 \\ -(Z4+Z6) & (Z4+Z6) & Z4 & Z4+Z6+Z9 & Z4+Z6+Z8+Z9 \end{bmatrix} \times \begin{bmatrix} I_{L1} \\ I_{L2} \\ I_{L3} \\ I_{L4} \\ I_{L5} \end{bmatrix} = \begin{bmatrix} 0 \\ 0 \\ 0 \\ 0 \\ 0 \end{bmatrix} \quad (2.3)$$

Equation (2.3) can be rewritten as

$$[Z_l][I_L]=[0] \quad (2.4)$$

Where,
$$[Z_l]=\{[B_f][Z_b][B_f]^T\}$$

For successful voltage build-up $[I_L]\neq 0$ and therefore $[Z_l]$ should be a singular matrix i.e. $\det[Z_l]=0$ in Equation (2.4). So the absolute value of $\det[Z_l]$ should be zero i.e.

If,

$$\det[Z_l]=a+jb \quad (2.5)$$

Then,

$$\sqrt{a^2+b^2}=0$$

The matrix equations of $[Z_l]$ have been developed in Equation (2.5) by using the loop impedance technique and graph theory. Further, Equation (2.5) is used in Section 2.2.2.3 for the optimization purpose.

2.2.2.3 Formulation of Optimization

In numerical analysis, Newton's technique is also known as the Newton-Raphson 'NR' technique, is a method for finding successively better approximations to the roots of a real-valued function. This iterative procedure can be generalized by writing the following equation:

$$x_{i+1}=x_i-f(x_i)/f'(x_i)$$

Where i represent the iteration number. The program should check in whole iteration to see if the convergence condition, namely, $|f(x_{i+1})|<\varepsilon$ is satisfied. 'NR' technique is based on a taylor series development at an already known state. The 'NR' algorithm is the best known method of finding roots for a good reason: It is simple and fast. However, any 'NR' technique solution that takes more than 1000 iterations to converge is either ill-posed or contains a logical error. Debugging of the program will be called for at this point by changing the initial values provided to the program, or by checking the program's logic.

The matrix equations of $[Z_l]$ are developed by the loop impedance method using graph theory and $\det[Z_l]$ is solved by a 'NR' based computational technique prescribed in Figure 2.8. 'NR' computational technique is recorded chronologically to calculate the real and imagin-

24

```
                    ┌─────────────┐
                    │    Start    │
                    └─────────────┘
                           │
                           ▼
         ╱──────────────────────────────────────╲
        ╱   Take the directed graph from the      ╲
       ╱  Figure 2.6  by selecting the direction   ╲
      ╱      of current flow to coincide for        ╲
     ╱            current sources                    ╲
    ╱────────────────────────────────────────────────╲
                           │
                           ▼
         ┌──────────────────────────────────────┐
         │  Select  a tree from the directed graph │
         └──────────────────────────────────────┘
                           │
                           ▼
         ┌──────────────────────────────────────┐
         │  Place all voltage sources in the tree │
         │  and all current sources in the co-tree │
         └──────────────────────────────────────┘
                           │
                           ▼
    ┌──────────────────────────────────────────────────────┐
    │ If possible, place all control-voltage branches for   │
    │ voltage-controlled dependent sources in the tree and  │
    │ all control-current branches for current-controlled   │
    │ dependent sources in the co-tree                      │
    └──────────────────────────────────────────────────────┘
                           │
                           ▼
         ┌──────────────────────────────────────┐
         │  Write KVL for each fundamental loop (FL) untill │
         │  L=b-n+1 in the form of Bf * Vb =0    │
         └──────────────────────────────────────┘
                           │
                           ▼
         ┌──────────────────────────────────────┐
         │  Write KCL equations in the form of   │
         │  Ib=BfT*IL                            │
         └──────────────────────────────────────┘
                           │
                           ▼
         ┌──────────────────────────────────────┐
         │  Apply ohm's law V=RI for each        │
         │  branch                               │
         └──────────────────────────────────────┘
                           │
                           ▼
         ┌──────────────────────────────────────┐
         │  Finally, the equilibrium equations   │
         │  ZlIL=Bf [ZbIs-Vs]                    │
         └──────────────────────────────────────┘
                           │
                           ▼
                    ┌─────────────┐
                    │    stop     │
                    └─────────────┘
```

Start

Take the directed graph from the Figure 2.6 by selecting the direction of current flow to coincide for current sources

Select a tree from the directed graph

Place all voltage sources in the tree and all current sources in the co-tree

If possible, place all control-voltage branches for voltage-controlled dependent sources in the tree and all control-current branches for current-controlled dependent sources in the co-tree

Write KVL for each fundamental loop (FL) untill $L=b-n+1$ in the form of $B_f * V_b = 0$

Write KCL equations in the form of $I_b = B_f^T * I_L$

Apply ohm's law $V=RI$ for each branch

Finally, the equilibrium equations $Z_l I_L = B_f [Z_b I_s - V_S]$

stop

Figure 2.7: A flowchart of the algorithm used in the formulation of the network equations on loop impedance basis

25

Table 2.1 (TIE-SET MATRIX)

Link branchs (currents)	Circuit branchs								
	1	2	3	4	5	6	7	8	9
(I_{L1})	1	1	0	1	0	1	0	0	0
(I_{L2})	-1	0	1	-1	0	-1	0	0	0
(I_{L3})	0	0	0	-1	1	0	0	0	0
(I_{L4})	0	0	0	-1	0	-1	1	0	1
(I_{L5})	0	0	0	-1	0	-1	0	1	1

Table 2.2

When both winding sets (abc & xyz) are excited, and compensated along with equal resistive 'R' loading

S. No.	Z_{lo1} (p.u.)	Z_{lo2} (p.u.)	Simple-shunt configuration		Short-shunt configuration		Long-shunt configuration	
			F (p.u.)	X_m (p.u.)	F (p.u.)	X_m (p.u.)	F (p.u.)	X_m (p.u.)
1	13.10869	13.10869	0.9679	0.4896	0.9679	0.4887	0.9862	0.5391
2	10.0456	10.0456	0.9599	0.5032	0.9598	0.5012	0.9860	0.5506
3	5.6885	5.6885	0.9416	0.5389	0.9414	0.5318	0.9843	0.5798
4	4.2361	4.2361	0.9278	0.5711	0.9274	0.5570	0.9838	0.6050
5	3.8730	3.8730	0.9228	0.5839	0.9224	0.5664	0.9832	0.6148
6	3.5099	3.5099	0.9169	0.6003	0.9165	0.5779	0.9824	0.6271
7	3.1468	3.1468	0.9097	0.6217	0.9093	0.5923	0.9817	0.6428
8	2.7837	2.7837	0.9009	0.6510	0.9005	0.6106	0.9812	0.6636
9	2.4206	2.4206	0.8897	0.6936	0.8893	0.6345	0.9795	0.6927
10	2.0575	2.0575	0.8749	0.7608	0.8748	0.6669	0.9741	0.7360
11	1.6944	1.6944	0.8546	0.8826	0.8553	0.7120	0.9675	0.8070
12	1.3313	1.3313	0.8246	1.1693	0.8279	0.7740	0.9525	0.9442
13	0.9683	0.9683	0.7756	2.6161	0.7885	0.8388	0.9410	1.3139

Speed(u) =1.0 (p.u), $X_{cp1} = X_{cp2}$= 1.0007 (p.u.), $X_{css1} = X_{css2}$ =0.3567 (p.u.), $X_{cls1} = X_{cls2}$ = 0.1101(p.u.)

ary components from $\det[Z_1]=0$ and introduced in to the 'NR' controller separately components from $\det[Z_1]=0$ and introduced in to the 'NR' controller separately and recurrently. The controller generates corrections and updates of the unknown quantities 'X_m' and 'F' in the matrix $[Z_1]$, for the evaluation of $\det[Z_1]$ until $\det[Z_1]$ equal to the desired tolerance value ' ε '.

2.3 Design of Computer Based Matlab M-file Subroutine

Formulated mathematical model employing graph theory and loop impedance techniques has been directly used in the optimization process using 'NR' algorithm. Optimized unknown quantities 'X_m' and 'F' from the 'NR' controller of SP-SEIG are recurrently passed down in to the performance evaluation algorithm which presented in Figure 2.9 using MATLAB working environment.

2.4 Results and Discussion

In order to investigate and validate the comparative performances of the simple and compensated SP-SEIG using proposed analytical methods of Section 2.2.2, a 1.1 kW induction machine driven by DC motor, and its parameters are given in Appendix A. For this purpose, an algorithm is already constructed in Figure 2.9. Following two modes of excitation capacitor bank with the appropriate values are used in the whole analysis.

- Shunt capacitor connected to only one 3Φ winding set, and
- Shunt capacitor connected to both the 3Φ winding sets.

2.4.1 Appropriate Values of Simple and Series Capacitances

For detailed analysis of SP-SEIG, the appropriate values of shunt and series capacitances must be determined at different operating conditions for self-excitation and desired voltage regulation purposes, respectively. Other approximate values of capacitances were also considered for safe operation of the machine, but have violated in some other cases with the fundamental constraints given in [6]. Therefore, it becomes necessary to develop a methodology that will optimize the values of capacitances for satisfactory operation of the system including all constraints at desired operating condition. As a first approximate value of shunt capacitance is $C_{p1}=C_{p2}=38.5\mu F$ /phase when it was connected to both winding sets and $C_{p1}=C_{p2}=63.5\mu F$ /phase when it was connected to only single winding set. In the same way, the first approximate values of short-shunt and long-shunt capacitances are $C_{ss1}=C_{ss2}=108$ μF /phase and $C_{ls1}=C_{ls2}=350$ μF /phase, respectively, and were connected in series with each line of both winding sets. All values of capacitances are also experimentally verified and further, reconsidered during the theoretical analysis in Section 2.4.3 for verification purpose.

27

Start

Input $r_1, r_2, X_1, X_2, X_r, X_{lm}, r_r, u, F, R_{Lmin}, R_{Lmax}, \Delta R_L$
C_P , C_{ss} and C_{ls} (for simple -shunt , short - shunt and long
- shunt respectively).

Calculate $X_{CP1}, X_{CP2}, X_{css1}, X_{css2}, X_{cls1}, X_{cls2}$ **as per configuration used**

Specified the upper ranges of F and u
(u must be little more than F)

Iteration no. i = 1

Consider, X_m = unsaturated value
& F = u

Calculate $z_1, z_2, z_3, z_4, z_5, z_6, z_7, z_8, z_9$ **as per configuration used**

Calculate the real and imaginary parts of the det $[Z_1]$ **and then** $J_{11}, J_{12}, J_{21}, J_{22}$
for the selected configuration

if
Real $[Z_1]$
&
Imag $[Z_1] < \varepsilon$

no

yes

$i = i + 1$

Display X_m , F

$R_{L1} = R_{L1} + \Delta R_{L1}$
$R_{L2} = R_{L2} + \Delta R_{L2}$

Update X_m **& F using**
newton- rapshon technique

Result is deviated

no   **yes**

End

$R_{L1} < R_{Lmax}$ **&** $R_{L2} < R_{Lmax}$

no   **yes**

Figure 2.8: A flowchart of NR based computer algorithm for the optimization of X_m and F

Full discussion on the analytical optimization methods of different capacitances values are also explained in References [3, 6]. In order to have same no load voltage as in the case of the simple-shunt SP-SEIG, the equivalent capacitance 'C_{eq}' of the external circuit in long-shunt scheme should have the same approximate value as in the simple-shunt SP-SEIG and it is given by the relation i.e. $C_{eq} = C_{ls}C_p/(C_{ls}+C_p)$. Mostly the value of series capacitance is more than twice in long-shunt configuration in relation to short-shunt configuration.

2.4.2 Optimization of Magnetizing Reactance (X_m) and Frequency (F)

An optimization procedure of 'X_m' and 'F' is implemented by using a Newton-Raphson algorithm using two main constraints, when machine is in a region of saturation and slip is negative. All variations in 'X_m' and 'F' will take place accordingly with the changes in excitation capacitance, series capacitances, speed and load. All computed and optimized values of 'X_m' and 'F' in different operating modes of excitation and series capacitor banks for selected values under different resistive loading condition are not possible for depicting, only in the single operating mode of the machine are summarized in Table 2.2. Having identified the optimized variables values, it is also essential to estimate correctly the magnetizing characteristics and related air-gap voltages under different flux conditions, listed in Appendix A. Furthermore, optimized values of 'X_m' and 'F' are used in the overall comparative performance analysis of simple and series compensated SP-SEIG in Section 2.4.3 under different modes of machine operation.

2.4.3 Analytical Evaluation of Machine Variables

For the steady state analysis of 6 poles, SP-SEIG, machine parameters and its generalized block diagram for the six-phase connection are given in Appendix A for better understanding of machine operation. A 3Φ delta connected capacitor bank was connected to the terminals of each 3Φ star-connected winding sets of six-pole six-phase connection of machine when neutrals of both sets are isolated. One 3Φ star connected resistive bank was also used for loading purpose in each of the winding sets. Analytical results are addressed in Figures 2.10 through 2.26. Knowing the steady-state values of 'X_m' and 'F' at a given speed, load and capacitances (shunt and series) from Table 2.2, performance parameters are computed from the flowchart of Figure 2.9 in similar manner. In flowchart, when machine is on no load, then the values of X_{L1} and X_{L2} are equal to zero in the parameters Z_9 and Z_7 considering their limits as R_{L1} and R_{L2} tends to infinity in the equation $\det[Z_l]$ and then the equation is solved by 'NR' computational technique for the analysis of simple-shunt and compensated SP-SEIG at no load.
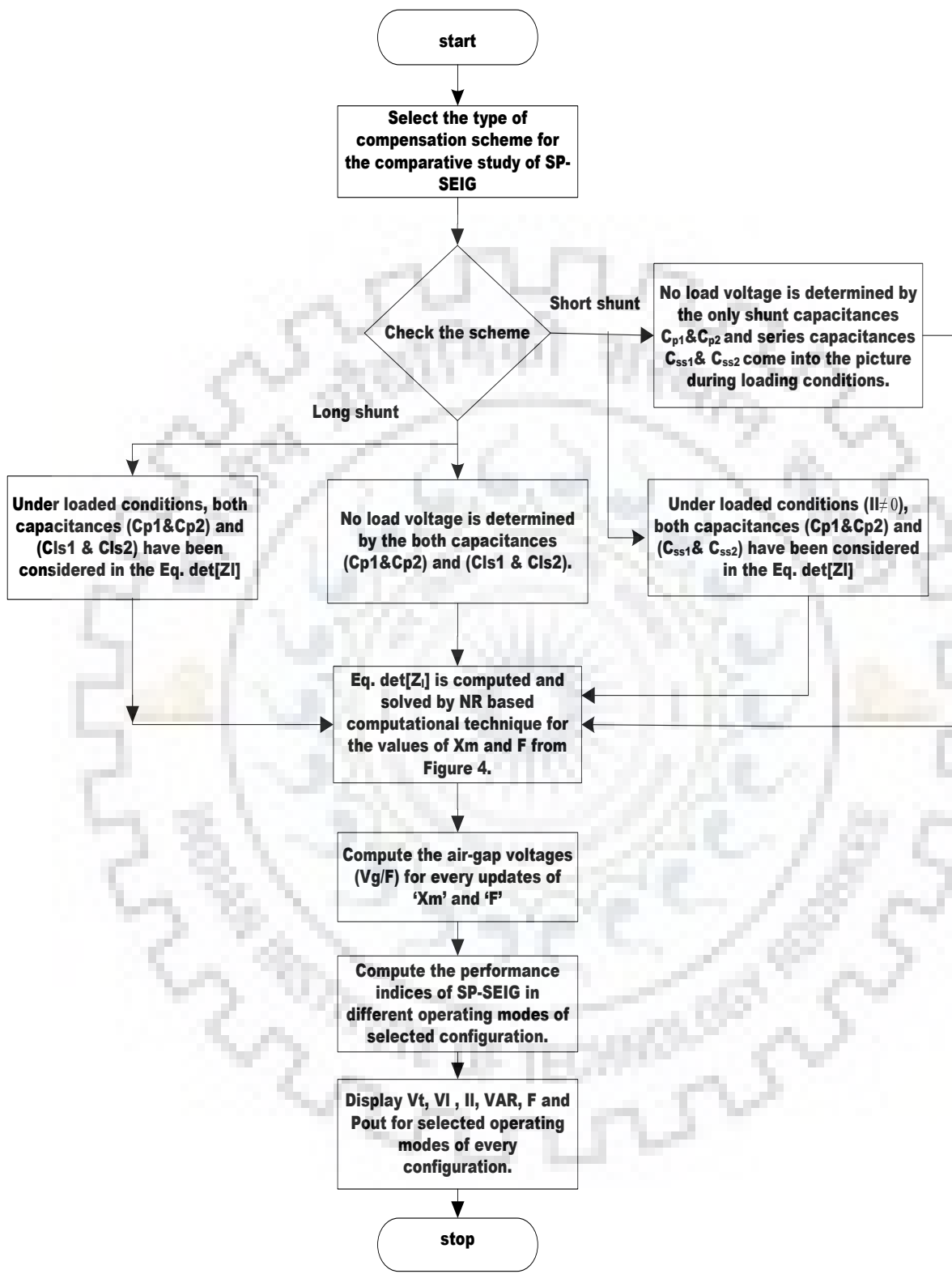
Figure 2.9: Flowchart for the steady state analysis of series compensated SP-SEIG

Various performance parameters namely terminal voltage, load voltage, load current, and frequency were determined w.r.t total output power under different loading conditions and in different mode of excitation and series capacitor banks. Comparative performance of the simple and compensated SP-SEIG are determined at no load, and loaded condition are summarized in Table 2.3. Computational results, which were carried out for the steady state performance analysis and parameter evaluation of SP-SEIG with simple and compensated configuration in different mode of operation for R loading are depicted and summarized in Figures 2.10 through 2.26, and Table 2.3, respectively, for verification purpose. Various performance parameters were studied w.r.t. total machine output power for different mode of excitation and series capacitor bank operation under different loading conditions. For the comparative configuration study, all different operating modes of all configurations (simple-shunt, short-shunt and long-shunt) are mentioned in Table 2.3.

2.4.3.1 Uncompensated SP-SEIG Operation

Simple-shunt or uncompensated configuration has following operating modes under particular resistive load conditions:

▪ Loading performance with simple-shunt connection at one 3Φ set of stator winding

Excitation capacitance (in the delta) C_{p1} = 63.5 µF is only connected across the 3Φ winding set *abc* when SP-SEIG operates at rated speed of 1.0 p.u. When separate R loading on each 3Φ set i.e. when resistive load on the *abc* winding set is gradually increased keeping the *xyz* winding set open '*operating mode I*' and when resistive load on the *xyz* winding set is gradually increased keeping the *abc* winding set is open '*operating mode II*' , respectively, are shown in Figures 2.10 and 2.11. When independent 'symmetrical' and 'asymmetrical' R loading on each 3Φ set which are correspond to '*operating mode III*' and '*operating mode IV*' are illustrated in Figures 2.12 and 2.13, respectively. In operating mode I, under no load condition, it is observed that the terminal voltage developed at excited 3Φ winding set is approximately 9 % more than the terminal voltage developed at unexcited 3Φ winding set.

▪ Loading performance with simple-shunt connection at both the 3Φ stator winding sets

Excitation capacitance (in the delta) $C_{p1}=C_{p2}$=38.5 µF are connected across the both winding sets when SP-SEIG operates at rated speed of 1.0 p.u. When separate R loading on each 3Φ set 'operating mode V', and When independent 'symmetrical' and 'asymmetrical' R loading on each 3Φ set corresponds to '*operating mode VI*' and '*operating mode VII*' are illustrated in Figures 2.14 through 2.16.

(a)

(b)

(c)

(d)
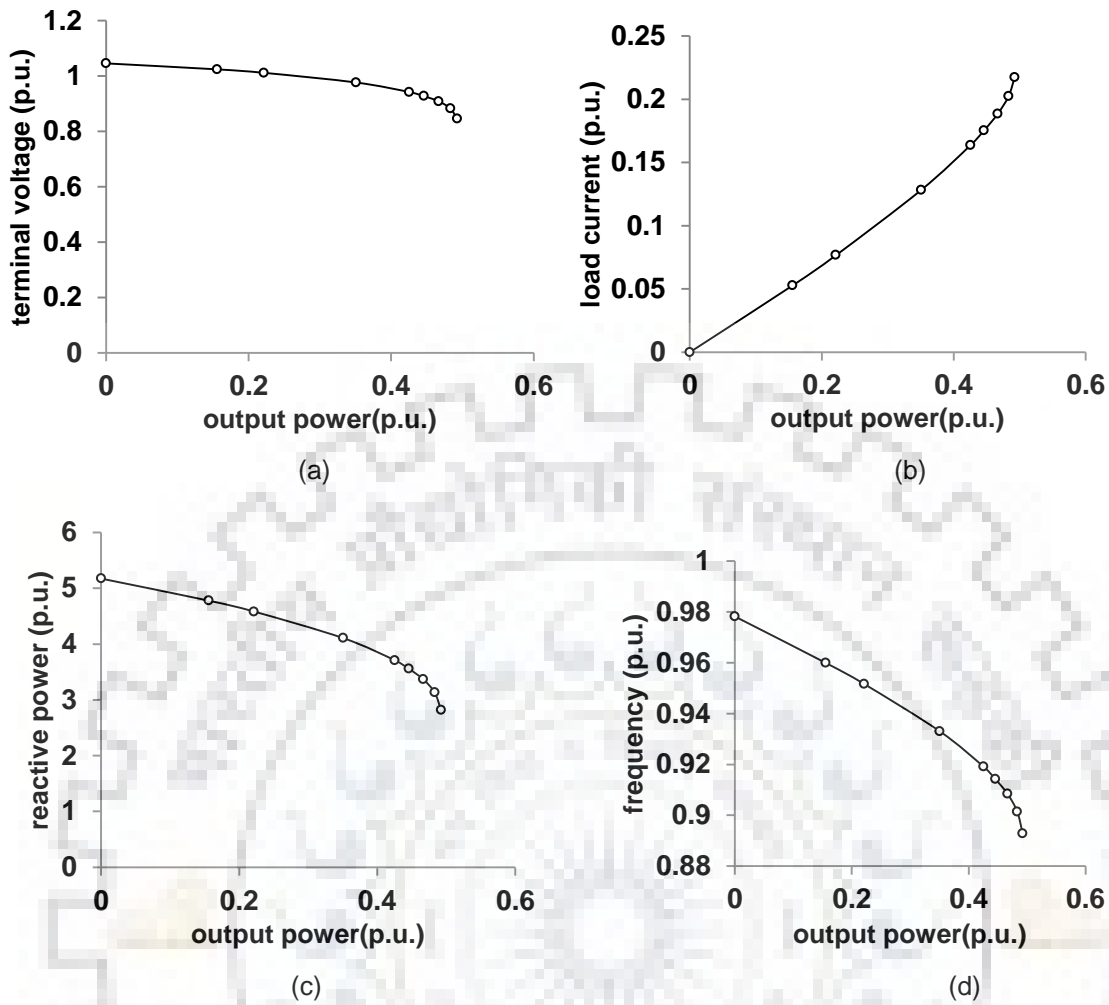
Figure 2.10: Variation of terminal voltage (a), load current (b), VAR (c) and frequency (d) of SP-SEIG as function of output power when R loading is switched on to excited set *abc* by keeping open the unexcited winding set *xyz*.

(a)

(b)
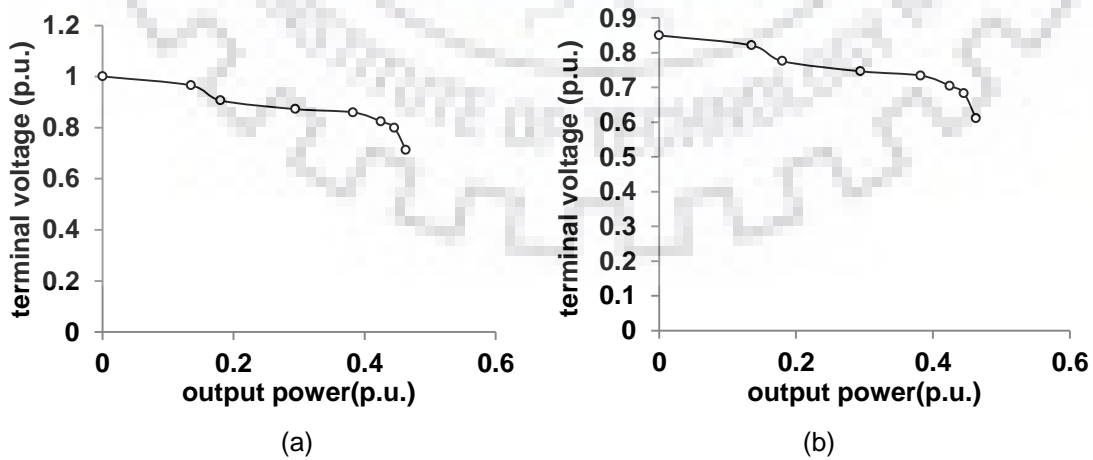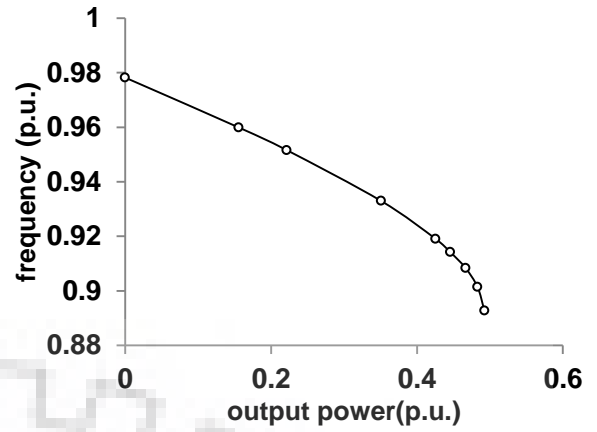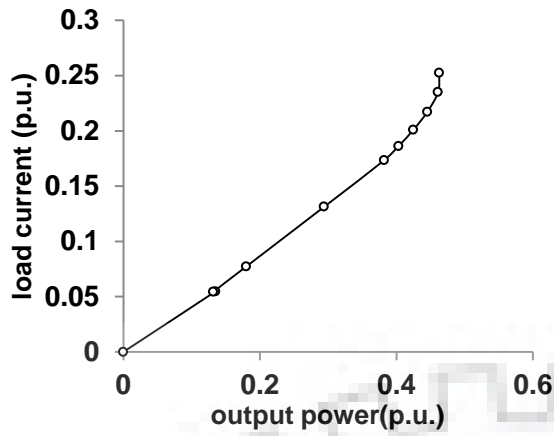
(c)

(d)

Figure 2.11: Variation of terminal voltage (a) (b), load current (c), and frequency (d) of SP-SEIG as a function of output power when R loading is switched on to unexcited set *xyz* by keeping open the excited winding set *abc*.
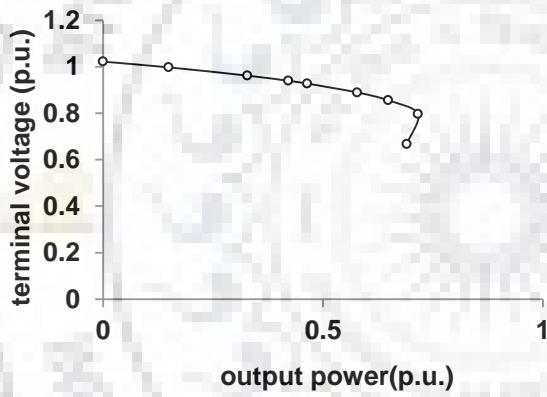
(a)

(b)
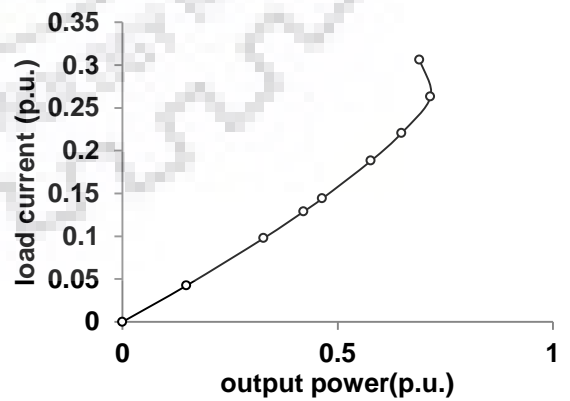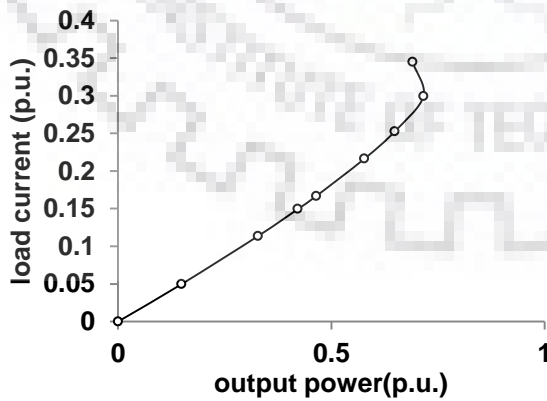
(c)

(d)
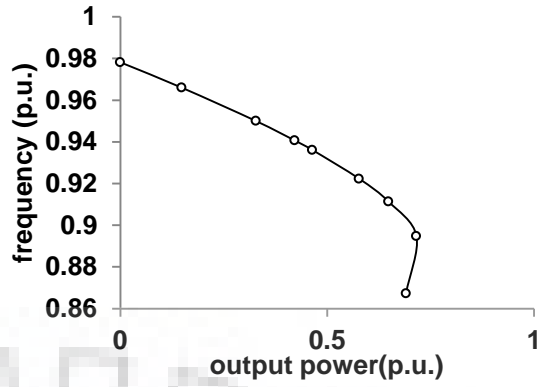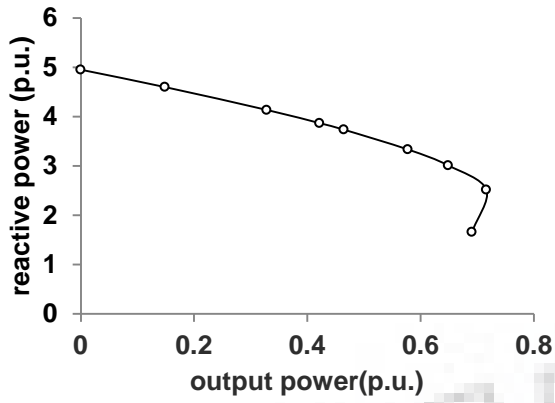
(e)

(f)

Figure 2.12: Variation of terminal voltage (a) (b), load current (c) (d), VAR (e) and frequency (f) of SP-SEIG as a function of output power when symmetrical R loading is switched on to the both sets (*abc* and *xyz)* and only winding set *abc* is excited.

(a)

(b)

(c)

(d)
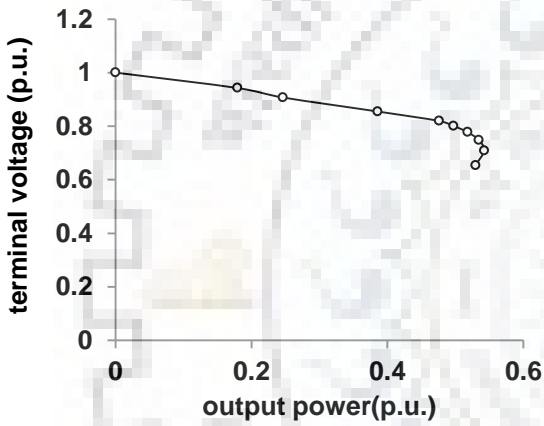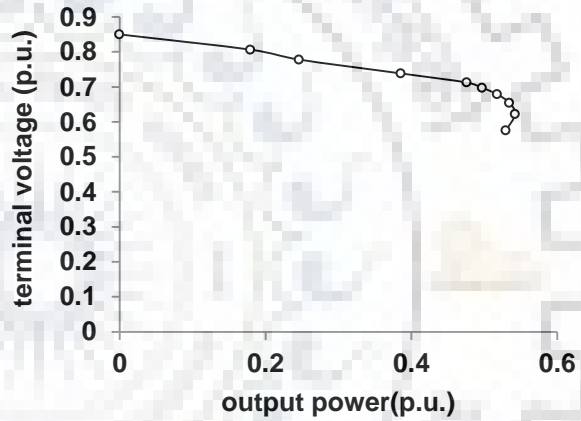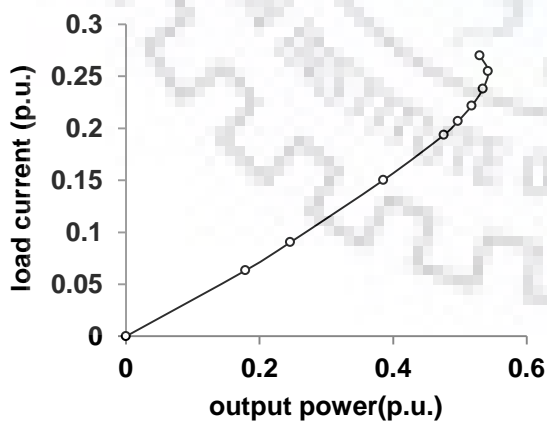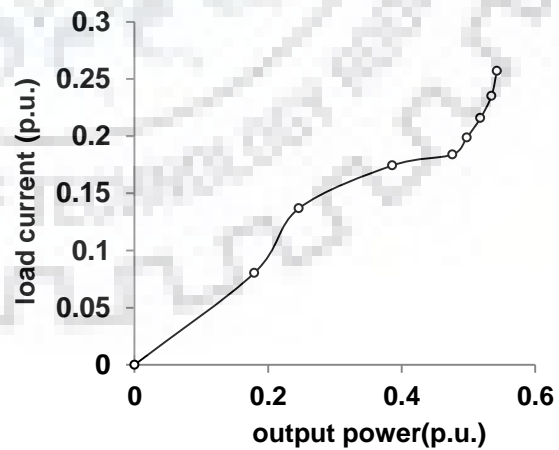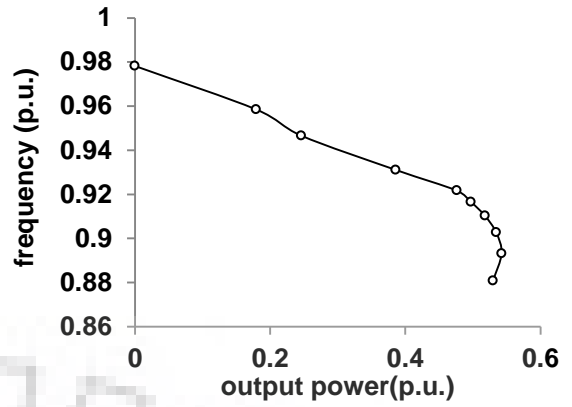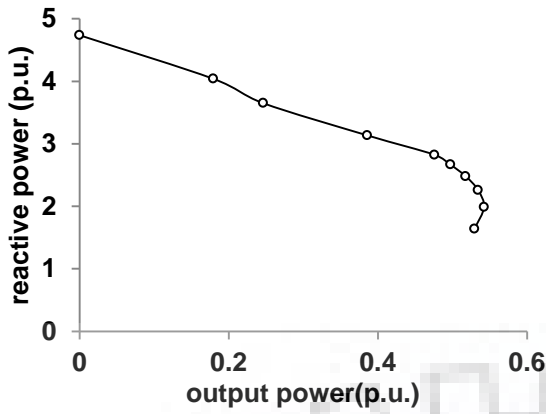
Figure 2.13: Variation of terminal voltage (a) (b), load current (c) (d), VAR (e) and frequency (f) of SP-SEIG as a function of output power when asymmetrical R loading is switched on to the both sets *abc* and *xyz* and only winding set *abc* is excited.
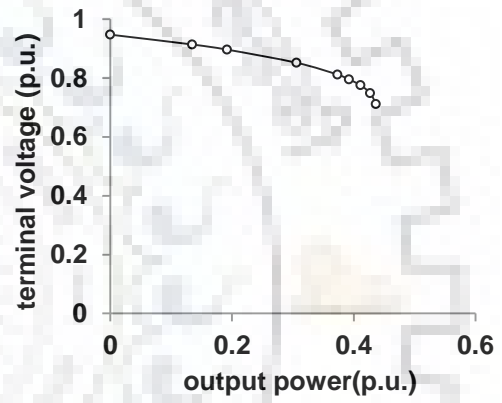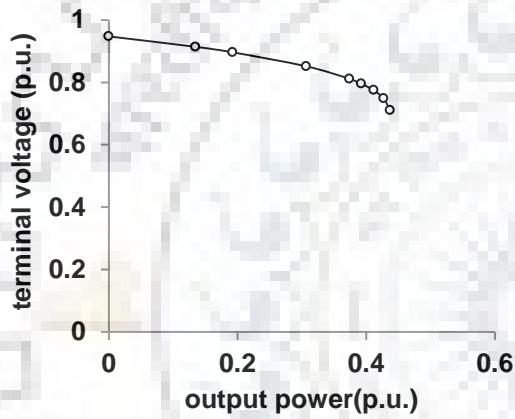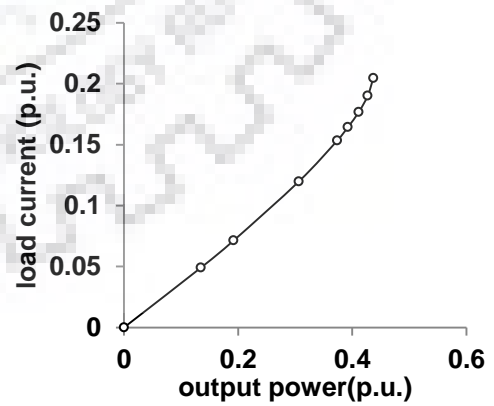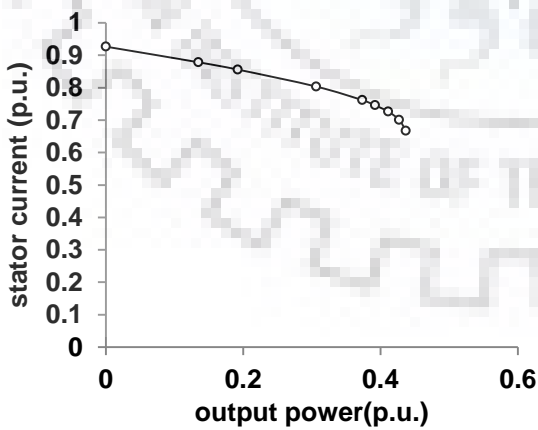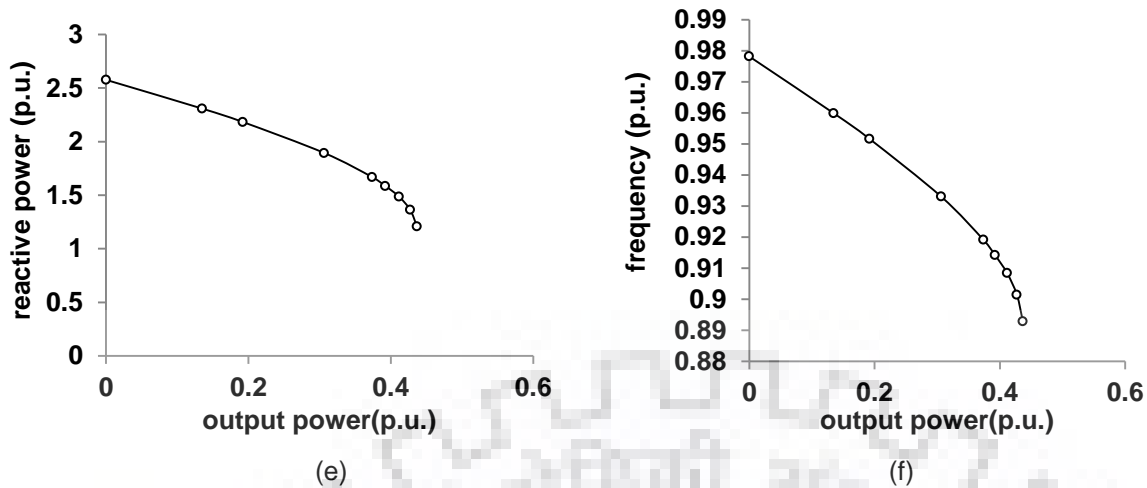
Figure 2.14: Variation of terminal voltage (a) (b), stator current (c), load current (d), VAR (e) and frequency (f) of SP-SEIG as a function of output power when both winding sets were excited and R loading is switched on to the winding set *abc* only.

(e)
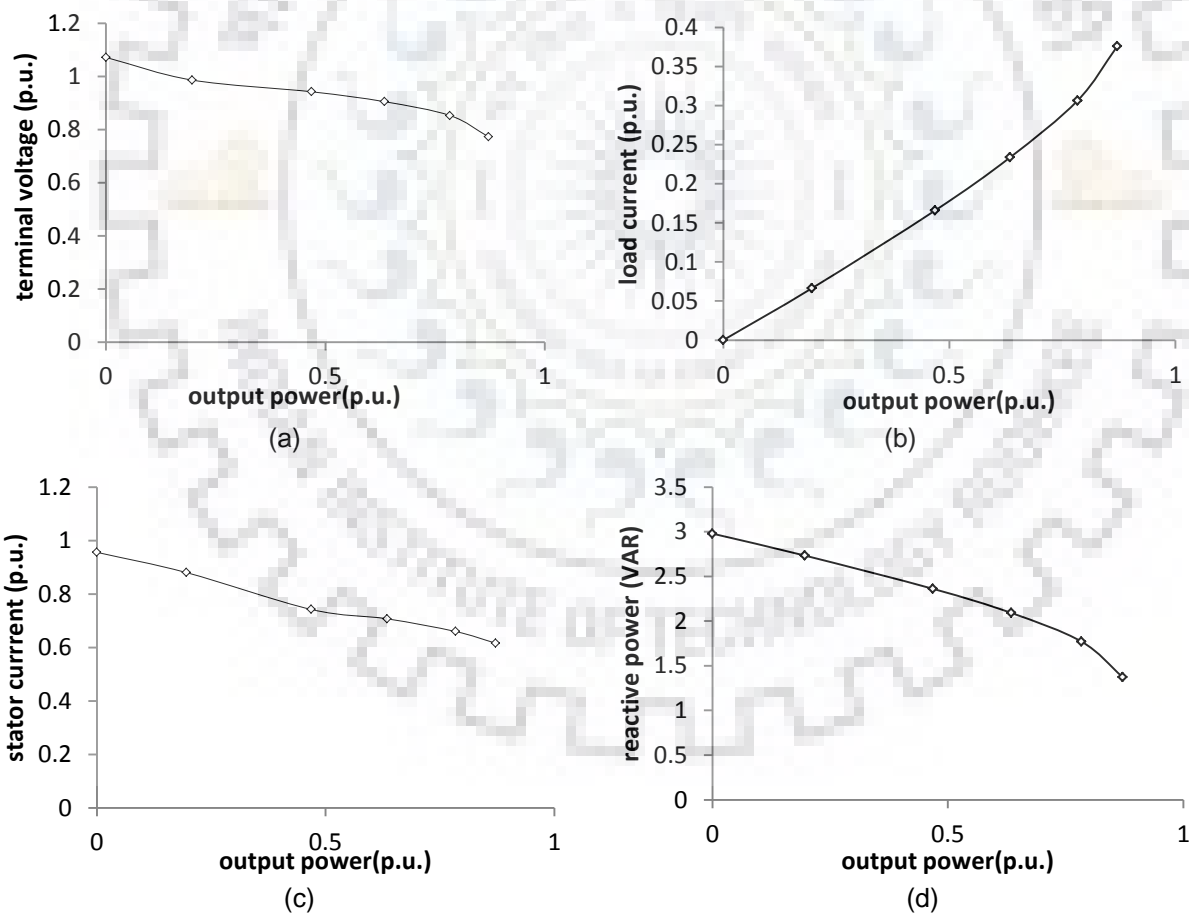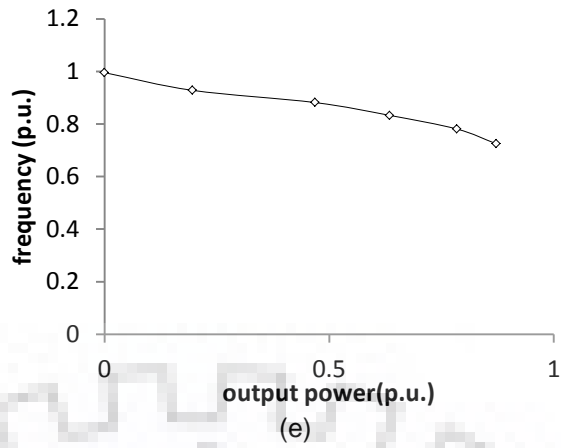
Figure 2.15: Variation of terminal voltage (a), load current (b), stator current (c), VAR (d) and frequency (e) of SP-SEIG as a function of output power when symmetrical R loading is switched on to the both excited winding sets *abc and xyz*.

(a)

(b)

(c)

(d)

37

(e)

(f)
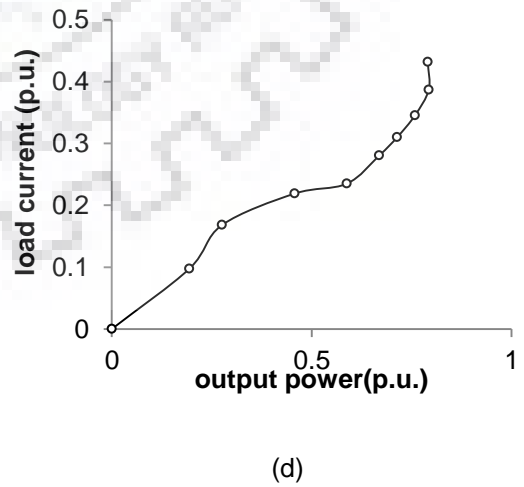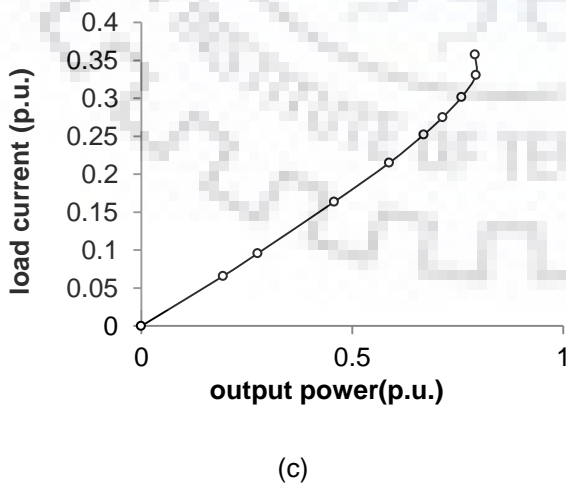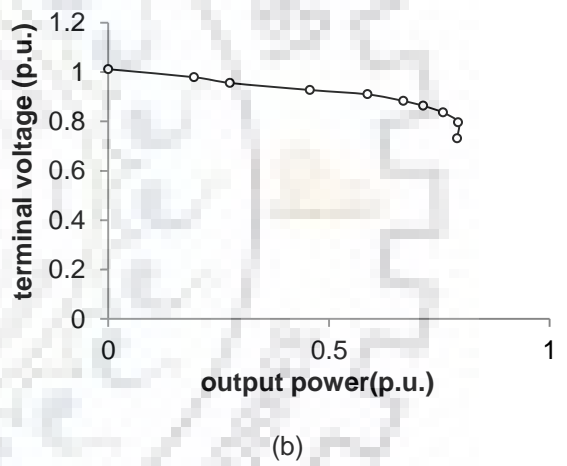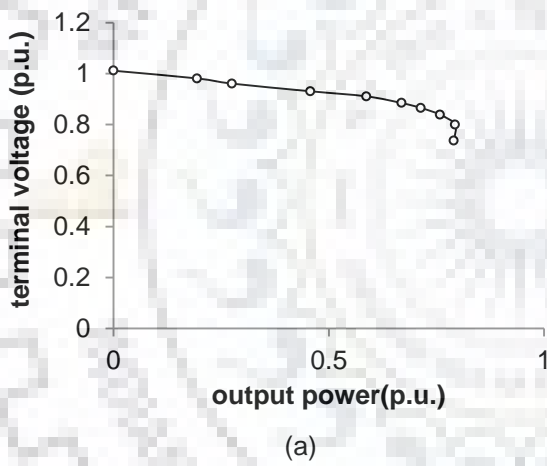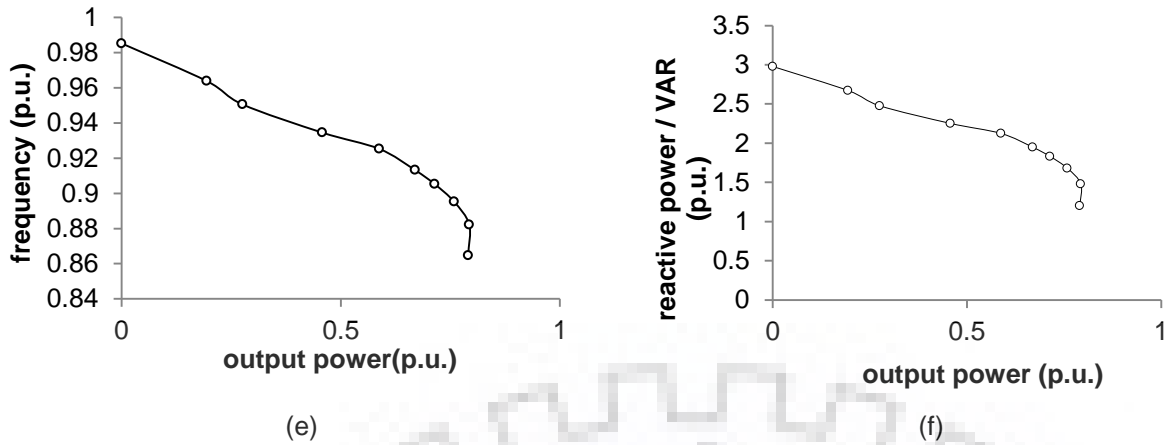
Figure 2.16: Variation of terminal voltage at *abc* set (a), terminal voltage at *xyz* set (b), load current at *abc* set (c) load current at *xyz* set (d), frequency (e) and VAR (f) of SP-SEIG as a function of output power when asymmetrical R loading is switched on to the both excited winding sets *abc and xyz.*
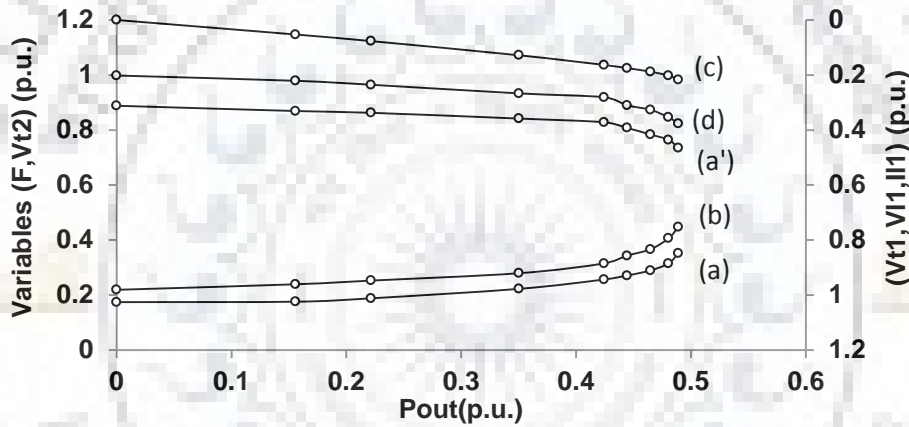
Figure 2.17: Variation of terminal voltage (*abc* set) (a) (in reverse order on secondary axis), terminal voltage (*xyz* set) (a'), load voltage (*abc* set) (b) (in reverse order on secondary axis), load current (*abc* set) (c) (in reverse order on secondary axis) and frequency (*abc* set) (d) as a function of output power when R loading is subjected to winding set *abc* with short-shunt configuration and another winding set *xyz* is kept open.
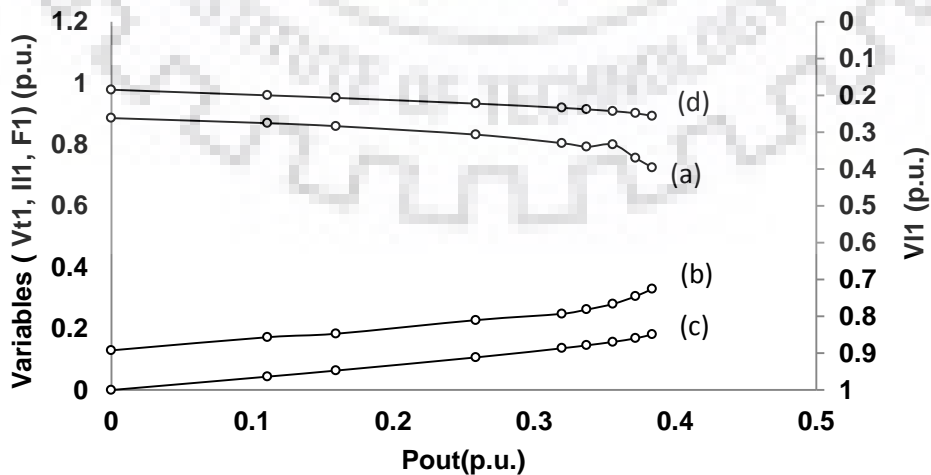
Figure 2.18: Variation of terminal voltage (a), load voltage (b) (in reverse order on secondary axis), load current (c) and frequency (d) of SP-SEIG as a function of output power when R loading is subjected to winding set *abc* with long-shunt configuration and another winding set *xyz* is kept open.

38
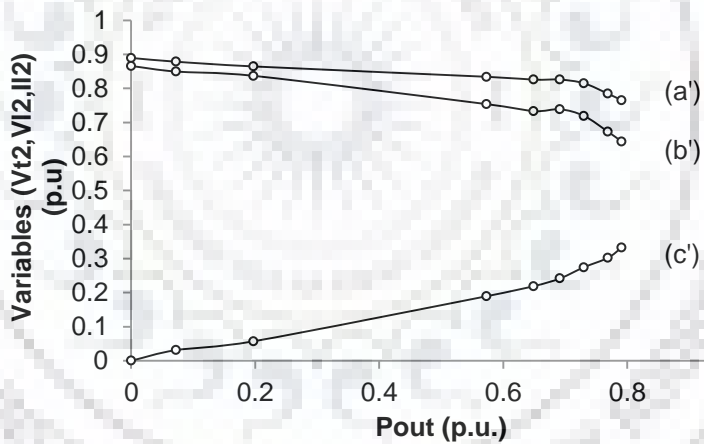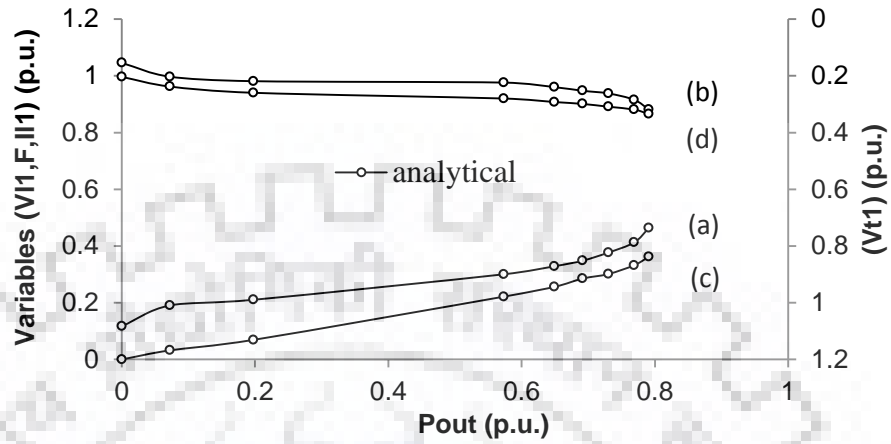
Figure 2.19: Variation of terminal voltage (*abc* set) (a) (in reverse order on secondary axis), terminal voltage (*xyz* set) (a'), load voltage (*abc* set) (b), load voltage (*xyz* set) (b'), load current (*abc* set) (c), load current (*xyz* set) (c'), and frequency (d) as a function of output power in operating mode III under short-shunt configuration.
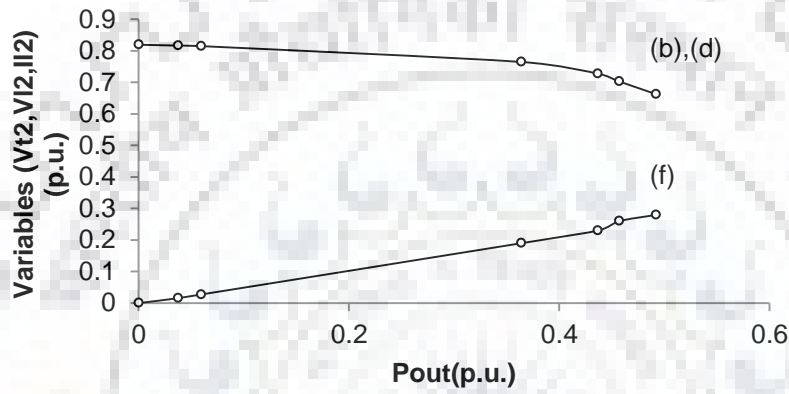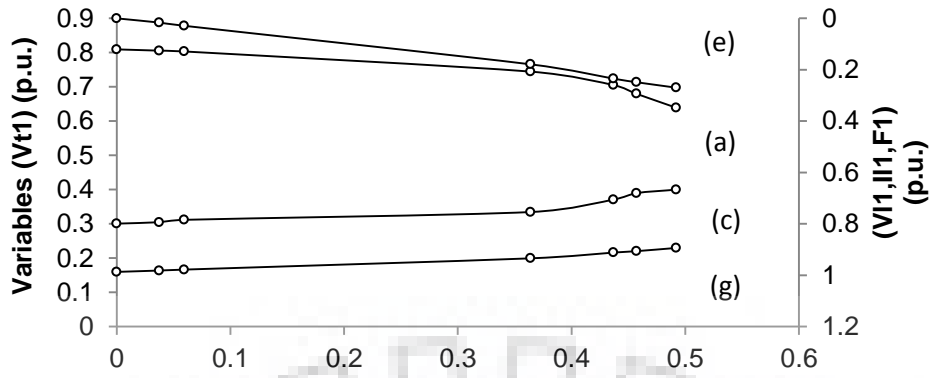
Figure 2.20: Variation of terminal voltage (a)(b), load voltage (c) (in reverse order on secondary axis), (d), load current (e) (in reverse order on secondary axis), (f) and frequency (g) (in reverse order on secondary axis) of SP-SEIG as a function of output power in operating mode III under long-shunt configuration.
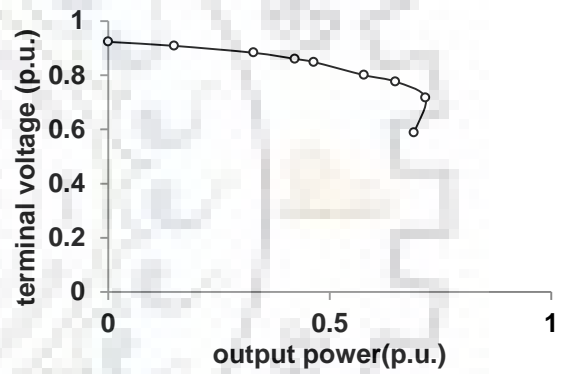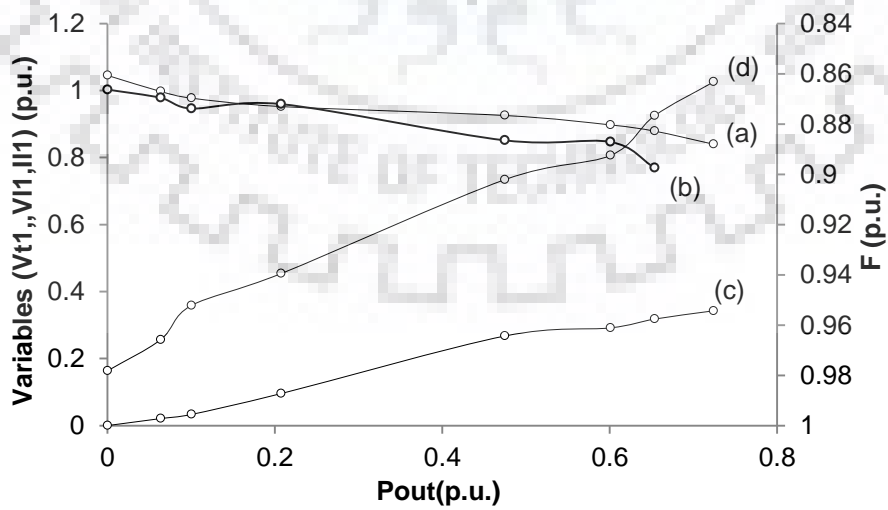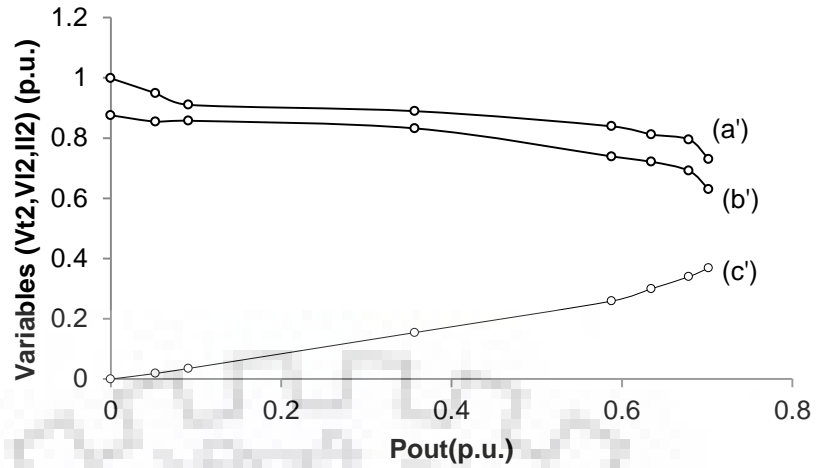
Figure 2.21: Variation of terminal voltage (*abc* set) (a), terminal voltage (*xyz* set) (a'), load voltage (*abc* set) (b), load voltage (*xyz* set) (b'), load current (*abc* set) (c), load current (*xyz* set) (c'), and frequency (d) (in reverse order on secondary axis) as a function of out put power in operating mode IV under short-shunt configuration.
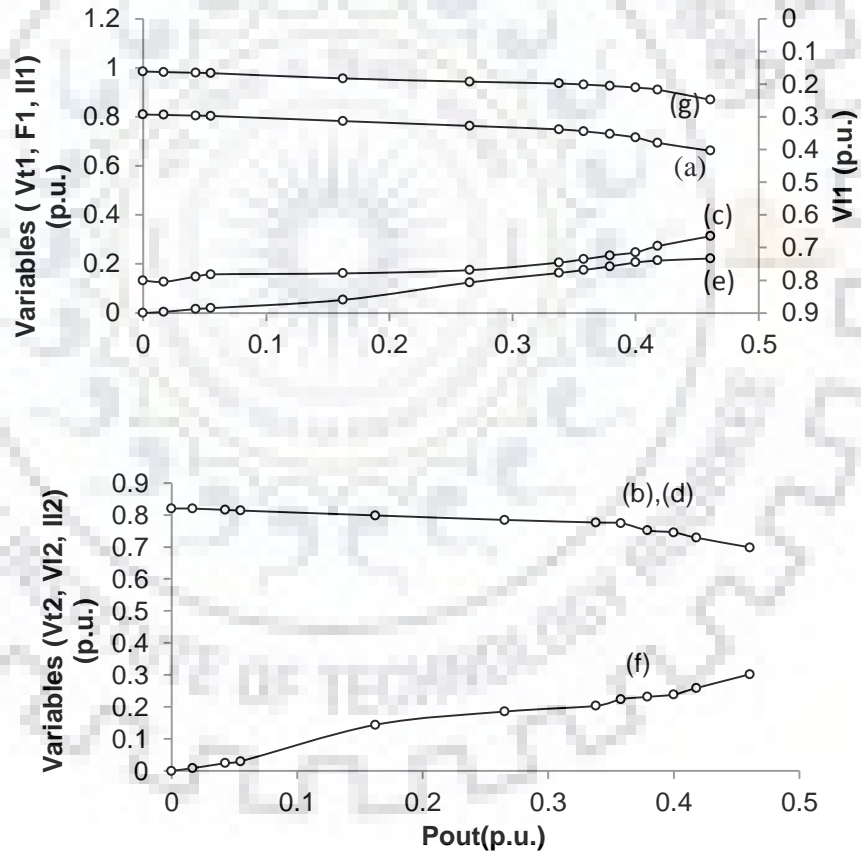
Figure 2.22: Variation of terminal voltage (a), terminal voltage (b), load voltage (c) (in reverse order on secondary axis), load voltage (d), load current (e) (f) and frequency (g) of SP-SEIG as a function of output power in operating mode IV under long-shunt configuration.

2.4.3.2 Compensated SP-SEIG Operation

Similarly, analysis of compensated configurations (short-shunt and long-shunt) has also been carried out under following operating modes:

When a single 3Φ winding set is accompanied by series compensation and subjected to R loading

In this case, excitation capacitance (in the delta) C_{P1} = C_{P2} = 63.5 µF is connected across the single 3Φ winding set of SP-SEIG operates at rated speed of 1.0 p.u. The loading transients for the series compensation when it is always on the single 3Φ winding set through the whole range of resistive load variation for different operating modes. Analysis was carried out only for the one value of short-shunt capacitance C_{ss1}= C_{ss2}=108 µF or long-shunt capacitance C_{ls1}= C_{ls2}=350 µF for series compensation.

- When loading is subjected to single 3Φ winding set *abc* accompanied series compensation and other 3Φ winding set *xyz* is kept open '*operating mode I*'

In this mode, under no load condition, it is observed that the terminal voltage developed at compensating 3Φ winding set is approximately 10% more than the terminal voltage developed at other 3Φ winding set. The performance characteristics are illustrated in Figures 2.17 and 2.18.

- When loading is subjected to 3Φ winding set *xyz*, and other winding set *abc* is kept open and accompanying series compensation '*operating mode II*'

When a single 3Φ winding set is accompanied by series compensation, and both the 3Φ winding sets are subjected to independent R loading for series compensation

- Loading performance for the shunt capacitance when it is on single 3Φ winding set *abc* along with series compensation through the whole range of equal resistive load variation on both winding sets *abc* and *xyz* '*operating mode III*'
- Loading performance for the shunt capacitance when it is on single 3Φ winding set *abc* along with series compensation through the whole range of unequal resistive load variation on both the winding sets *abc* and *xyz* '*operating mode IV*'.

The performances characteristics of both operating modes are shown in Figures 2.19 through 2.22.

*When loading is subjected to only one 3Φ set, and both winding sets are accompanying series compensation '*operating mode V*'*

Excitation capacitance (in the delta) C_{p1}=C_{p2}=38.5 µF are connected across the both winding sets when SP-SEIG operates at rated speed of 1.0 p.u. Analysis was carried out only for the one value of short-shunt capacitance C_{ss1}=C_{ss2}=108 µF or long-shunt capacitance C_{ls1}= C_{ls2}=350 µF for series compensation.

When both the 3Φ winding sets are accompanied by series compensation and subjected to independent R loading

- Loading performance for the series compensation are studied when it is on both the 3Φ winding sets through the whole range of resistive load variation of equal (symmetrical) loading condition '*operating mode VI*' and shown in Figures 2.23 and 2.24 for short-shunt and long-shunt scheme, respectively.

- Loading performance for the short-shunt compensation are studied when it is on both the 3Φ winding sets through the whole range of resistive load variation of unequal (asymmetrical) loading condition '*operating mode VII*'. In the same way, the performance characteristics of operating modes VII are also illustrated in Figures 2.25 and 2.26.

All the seven modes of operation with resistive load for simple-shunt and compensated SP-SEIG have been discussed and the performance variables variations (V_t, I_L and V_L of the machine from no-load to full load in % w.r.t. total maximum output power) have been reported in Table 2.3. All analytical results are presented in Figures 2.10 through 2.26 with their appropriate ranges in p.u. from base values of Appendix A.

A short performance evaluation of simple-shunt and compensation scheme is summarized below:

- Both compensation schemes are able to maintain the no load terminal voltage at larger load current.

- Sometimes, particularly in short-shunt configuration, series capacitors are in series with load gives rise to deep saturation and large steady state overload capability while the long-shunt SP-SEIG is able to deliver reduced output power at reduced terminal voltages.

- It is also seen that like short-shunt SP-SEIG, long-shunt SP-SEIG is also self-regulating in nature. The current rating of long-shunt series capacitors must be rated high (more than twice) as they carry machine line current unlike to the short-shunt capacitors, they carry only load current. Loading performances are also observed in a similar pattern as in the case of the simple-shunt or a short-shunt SP-SEIG.

- It is also noticed that short-shunt SP-SEIG has almost a flat output characteristic profile and improved voltage regulation, unlike a simple-shunt or uncompensated SP-SEIG configuration.
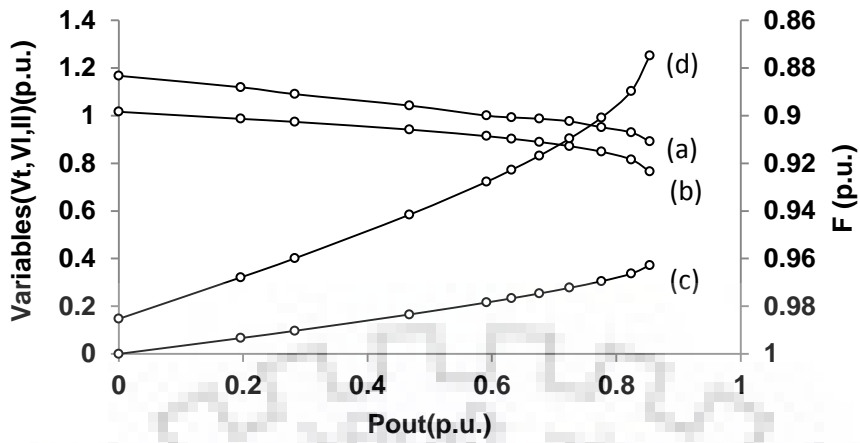
Figure 2.23: Variation of output power with: (a) terminal voltage (*abc* set), (b) load voltage (*abc* set), (c) load current (*abc* set) and (d) frequency (in reverse order on secondary axis) in operating mode VI under short-shunt configuration.
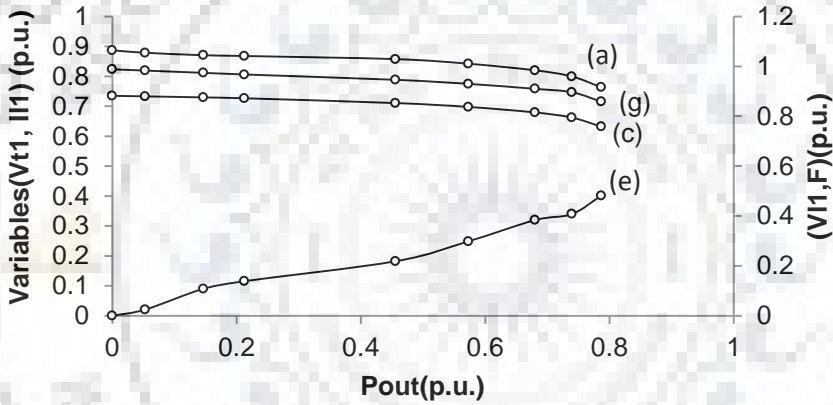
Figure 2.24: Variation of output power with: (a) terminal voltage (*abc* set), (b) load voltage (in reverse order on secondary axis), (c) load current (*abc* set) and (d) frequency (in reverse order on secondary axis) in operating mode VI under long-shunt configuration.
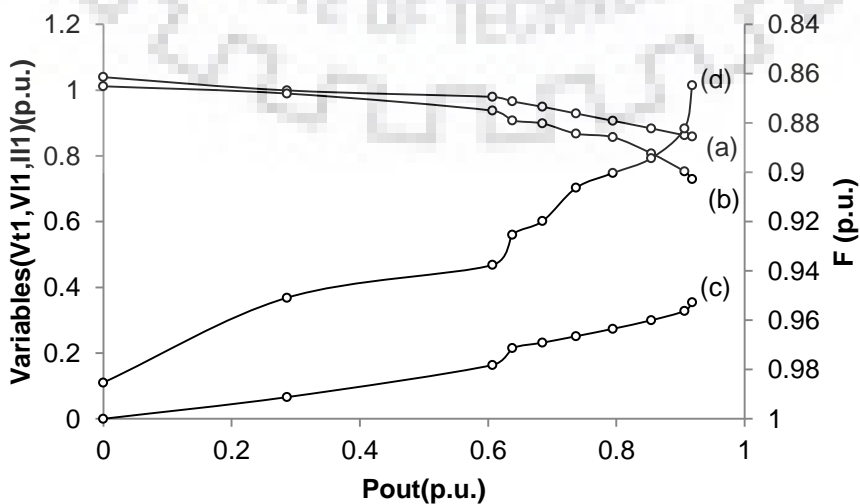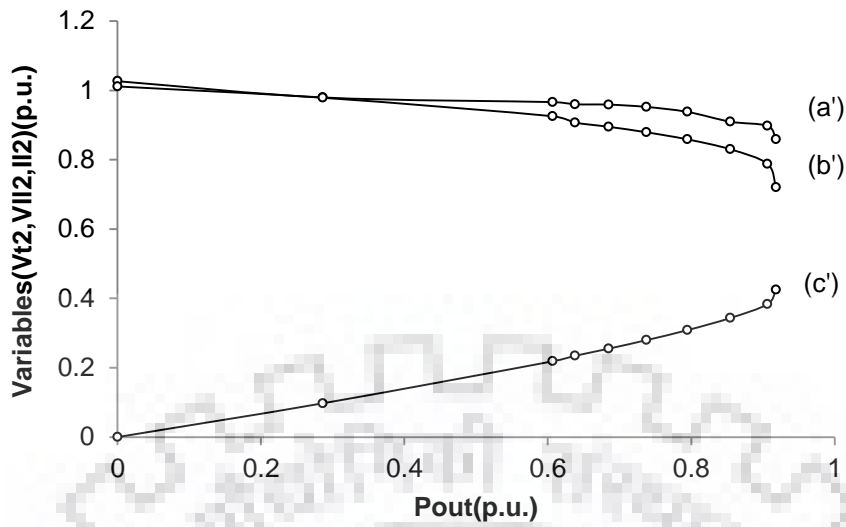
Figure 2.25: Variation of terminal voltage (*abc* set) (a), terminal voltage (*xyz* set) (a'), load voltage (*abc* set) (b), load voltage (*xyz* set) (b'), load current (*abc* set) (c), load current (*xyz* set) (c'), and frequency (d) (in reverse order on secondary axis) as a function of output power in operating mode VII under short-shunt configuration.
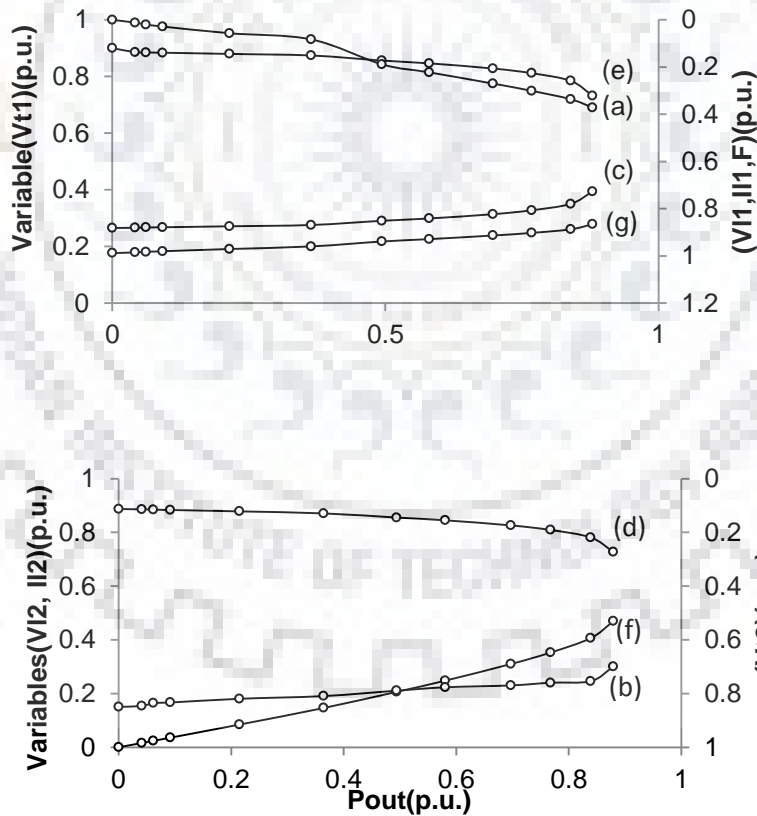
Figure 2.26: Variation of terminal voltage (*abc* set) (a), terminal voltage (*xyz* set) (b), load voltage (c) (in reverse order on secondary axis), load voltage (d) (in reverse order on secondary axis), load current (e) (in reverse order on secondary axis), load current (*xyz* set) (f), and frequency (g) (in reverse order on secondary axis) as a function of output power in operating mode VII under long-shunt configuration of SP-SEIG.

45

Table 2.3 Short comparative performance evaluation of simple and compensated SP-SEIG

S. No.	Significance of configurations	Operating modes	V_t (%)	I_L (%)	V_L (%)	Total Pout (p.u.)
1.	Simple-shunt	I	20	21	25	0.49
2.		II	29	25	24	0.46
3.		III	34	26	34	0.69
4.		IV	35	28	27	0.52
5		V	23	20	28	0.43
6.		VI	22	37	24	0.87
7.		VII	27	35	27	0.79
8.	Short-shunt compensated	I	19	21	26	0.48
9.		II	10	28	18	0.58
10.		III	16	21	25	0.79
11.		IV	12	35	27	0.72
12.		V	17	34	30	0.73
13.		VI	11	37	24	0.85
14.		VII	15	42	28	0.91
15.	Long-shunt compensated	I	16	18	16	0.37
16.		II	14	19	14	0.38
17.		III	16	21	16	0.49
18.		IV	17	27	16	0.46
19.		V	13	29	13	0.54
20.		VI	12	39	13	0.78
21.		VII	16	46	16	0.87

2.5 Concluding Remarks

In this Chapter, a simple analytical method for the determination of comparative steady state performance of the SP-SEIG in a simple-shunt and compensated schemes under different operating modes and loading conditions is presented. The model developed using loop impedance technique is based on graph theory and convenient for easy realization in computer simulation when it is in matrix form. The 'NR' technique is not so fast, but it is consistent, systematic and easily understood without any time consuming. Poor voltage regulation of SP-SEIG, even at constant rotor speed has been a major concern in its application for the static loads. For achieving and maintaining good voltage regulation of the SP-SEIG, the steady increase in reactive power demand increases with its active power delivery across the load. The aim of this chapter is also to investigate the effect of series

compensation on machine. Extra cost and complexity of several another voltage regulating schemes have been raised to various operational problems, like harmonics and switching transients. To the contrary, the inclusion of a series capacitor enables additional reactive power demand with load and become one of the attractive options to improve voltage regulation of the machine. This compensating nature of series capacitance in short-shunt or long-shunt configuration has been achieved for complexity simplification in voltage regulators, higher overload capability of the system and to avoid the loss of excitation when SP-SEIG is loaded. In this way, series capacitor compensation scheme improves the voltage profile, but also increases the maximum power delivery capability as compared to uncompensated SP-SEIG. Analysis shows that SP-SEIG can also sustain self-excitation when there is loss of excitation on one of the 3Φ winding sets. It makes the SP-SEIG more interesting and be capable of delivering output power to two independent resistive loads, and continue identical generation as earlier, even when single 3Φ winding set is only operational.

In order to meet the good agreement, computed results were proficiently verified by the competent literatures to validate the presented analytical approaches. In this way, cost effective voltage regulation technology of short-shunt and long-shunt SP-SEIG, once developed from their steady state equivalent circuits, has following crucial advantages over the simple-shunt SP-SEIG. The observations made on the basis of results reviews are summarized below:

- For fixed excitation capacitance, there exists a critical value of resistive load under which self-excitation is not possible in SP-SEIG and this critical value of resistive load corresponds to maximum steady state output power of single 3Φ winding set. Once SP-SEIG goes into the collapse, It doesn't recover even when the load is disconnected after a short period.
- On a sudden application of the resistive load, the terminal voltage is reduced to a considerable value due to the lack of reactive power that has been compensated through an additional capacitors connected in series with each phase. When a resistive load is connected in series compensated SP-SEIG, it almost maintained the no-load terminal voltage per self-regulating reactive power supplied by the additional capacitors in series.
- Many Pout (0.5 p.u.) is about 50% of total output power, which is delivered by machine when excitation capacitor is connected across only one 3 phase set along with load on excited (or unexcited) set. Apart from this, there is strong magnetic coupling between both three phase sets in SP-SEIG which affects the voltage and current of both three phase sets.
- Once in a while, application of series capacitor results in an over-voltage across the SP-SEIG terminals. The main conclusion of the study is that proper and careful selection of

shunt and series capacitors have gotten rid of this excessive voltage at the series compensated SP-SEIG terminals.

In steady state modelling and analysis of SP-SEIG, there are various methods in the available literatures. Most common and simple optimization technique has been used for steady state analysis purpose by using 'NR' technique. Steady state analysis of SP-SEIG provides initial values in simulation of its dynamic model. Proper initial and steady state values can be find out by using proper analylical technique. As we all know, 'NR' technique is an old classical method in numerical analysis problems. Newton's technique is also known as the 'NR' technique is based on a Taylor series development. To determine the comparative steady-state performance of simple and series compensated SP-SEIG in different operating modes of R loading, the developed 'NR' technique has suitability under different modes of operation and configuration in SP-SEIG. Moreover, application of loop impedance technique in conjunction with 'NR' technique is the first attempt to analyze the behavior of isolated six-phase induction generator. Though, it has been applied in case of 3Φ induction generator, However, there is no evidence of such application in steady state analysis of isolated six-phase induction generator on the basis of detailed literature review. Also, the effort is to show the relevance of old classical method that this techniques can be still used to get desired results and can't be discarded. The developed model can also be effectively utilized to analyze the machine behavior in conjunction with a stand-alone renewable energy sources.

This chapter describes detailed mathematical modelling of SP-SEIG to the research work. It will start with some background on foremost modelling and analysis problems in machine systems. Then, solutions to the problems will be discussed, through which dynamic modelling and analysis using stator current and magnetizing flux as state-space variables, and 4th order Runge - Kutta subroutine will be selected. Next, scope of work with author's contribution.

3.1 Introduction

An overall behaviour of SP-SEIG has been described by adopting the generator convention. General nomenclature and winding layouts of six-phase induction machine are also described. Two axis (dq0) modelling of six-phase induction machine was first presented by Singh et. al. around 2000, and is dedicated to any phase shift between both stator winding sets. Further other literatures were also in limelight for overall modelling and analysis of SP-SEIG (at no-load and load) in the area of renewable and non-renewable energy generation. Few findings have also reviewed progress made till 2002 and 2004, respectively, in multiphase technology particularly induction machine and SEIG for existing and proposing aspect of future planning. Some dealt mainly with the selection of capacitance for self-excitation and compensation in electric energy generation using available renewable energy sources [1, 3-9].

Reference [4] has been discussed the modelling and analysis of simple SP-SEIG, saturated SP-SEIG and multiphase induction machine in phase-redundant a.c. drive system with the help of Simulink model. It has also demonstrated dynamic modelling and analysis of simple SP-SEIG using renewable sources in wind and hydro power plants. References [6-9] have investigated steady state performance in the area of non-conventional energy. Apart from all main research work till date as mentioned in SP-SEIG, many different state-space models were also utilized during dynamic modelling of 3Φ SEIG and SP-SEIG. Main flux saturation modelling is well established by stator and rotor d-q axis currents or flux linkages variables in analytical model of saturated induction machine, on another hand mixed stator and rotor d-q axis currents-flux linkages as state-space variables are interestingly useful in integration of control system for induction machine [26].

Further, to study the transient performance characteristics of SP-SEIG during balanced and unbalanced terminal condition, it is also needed to apply accordingly the suitable control strategy after ensuring its suitability in order to get acceptable outcome. A new control strategy is admitted in Chapter 5 for this purpose. However, the overall performance of the machine can be improved by the design optimization of a SEIG. It decides voltage ratings of the machine winding sets and capacitors, so design optimization of SEIG has also been taken up for its improved steady state and dynamic state reliable operation in previous literatures. Proposed machine is embodied with asymmetrical stator and /or rotor winding structures which have ability to operate during such conditions:

- Stator phase winding's inter-turns faults
- Abnormal stator windings connections
- Broken rotor bars and their endings

Consequences of asymmetrical operations in induction machine embark upon unbalanced air gap voltages and line currents, hence, increased losses and torque pulsations in respect to decreased average torque. On that account, poor efficiency and excessive heating, eventually leads to the failure of the machine. Therefore, the accurate predictions of degradation characterization in the performance of induction machine under such conditions are also essential. Most of the transient studies of induction generators are related to voltage build-up due to self-excitation and load perturbation. The transient analysis at balanced conditions is available and scarce at unbalanced terminal conditions in the available previous literatures. The unbalanced conditions incorporate information about faults and SEIG characteristic during these faults.

However, it is further necessary to explore all these behaviour entirely. Transients are also occur during self-excitation on no load, during loading and /or unloading of electrical loads, during speed variations, variations in self-excitation capacitor value with load. Voltage build-up process during self-excitation and load perturbations is major cause of transients in SEIG. The various dynamic models have been proposed in the past since several years to study the transient behaviours of SEIG. The transient performance of an isolated configuration can be accurately predicted by d–q model in stationary reference frame which is beneficial due to the frequency variations with time and the explicitly observed effects of cross saturation.

3.2 Problem Formulation

Dynamic modelling of a SP-SEIG is mostly cultivated by using stator and rotor d-q axis currents or flux linkages as described in Chapter 4 rather than mixed stator and rotor d-q axis currents- flux linkages as state-space variables. Excluding all selected pairs of mixed variables in dynamic analysis of previous proposed machines as developed in research work [3, 5, 26, 27] here is further a need of mixed current- flux variable modelling which has been proposed using stator current and magnetizing flux as state-space variables in SP-SEIG. This pair of selected variables in dynamic analysis of SP-SEIG creates simplicity in system matrix having less number of saturation dependent members.
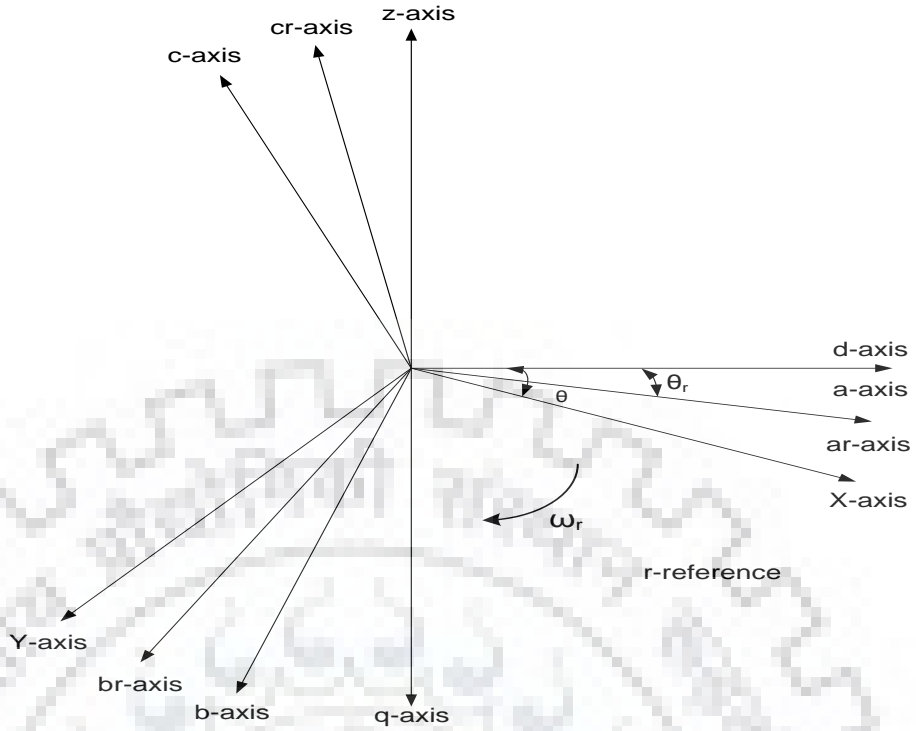
Figure 3.1: A two-pole six-phase induction machine with θ^0 displacement between two-stator winding sets.
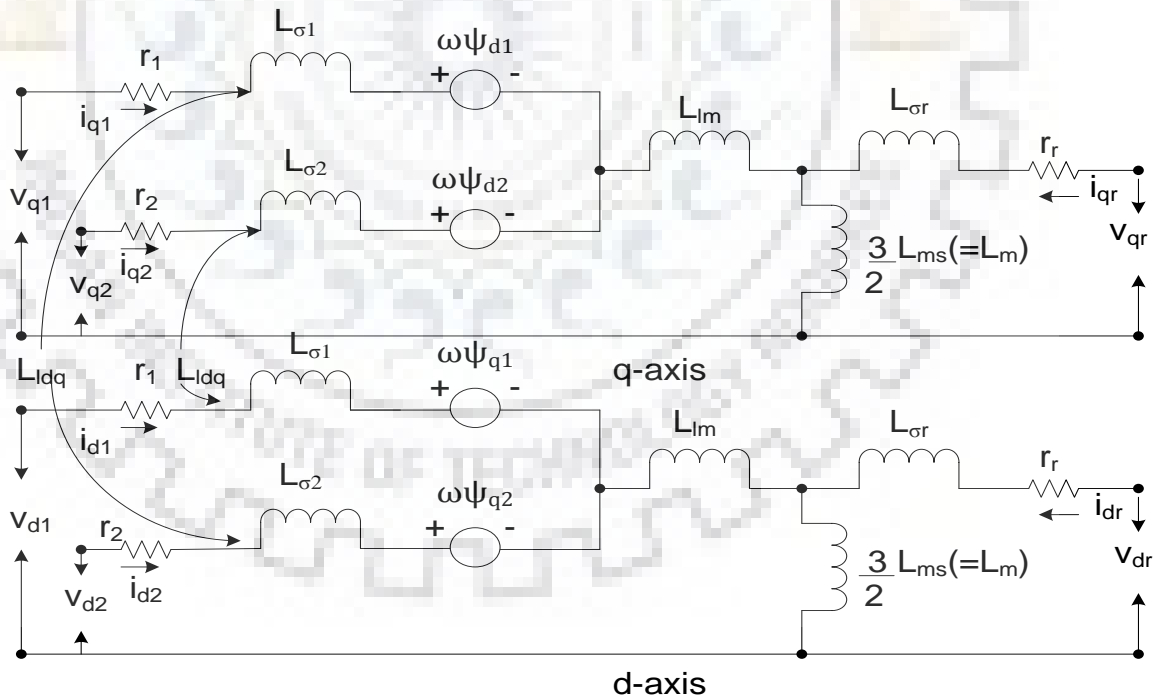
Figure 3.2: The q- and d-axis equivalent circuit of a six-phase induction machine in arbitrary reference frame.

51

Analytical model has four elements which depend on saturation only in case of consideration for dynamic analysis of SP-SEIG. Performance equations utilize the steady-state magnetizing inductance 'L_m' along with dynamic inductance 'L' against saturated magnetizing inductance 'L_m' and its derivative. Present mixed variable modelling impede the effects of common mutual leakage inductance 'L_{lm}' between the both winding sets and cross saturation coupling 'L_{ldq}' between the d and q axis of stator as shown in Figure 3.2. Modelling steps can be divided into three sections. First section delivers the modelling of saturated induction machine, second section deals with the modelling of excitation along with compensating capacitor banks and last section presents the modelling of static machine loads.

To investigate the transient behaviour of SP-SEIG, the well known reliable d-q variables modelling in stationary reference frame is preferred to study the symmetrical and asymmetrical load configuarations along with different combinations of excitation and compensating capacitor banks. The transient performances of an isolated configuration of IGs can be accurately predicted by using d–q variables model in stationary reference frame [28], so it is appreciately selected for the modelling purpose of SP-SEIG which is already presented in Section 3.3. It is solved by 'RK4' subroutine which is coded in M-file of MATLAB software for the estimation of machine performance variables under almost constant rated system speed during uncompensated and compensated SP-SEIG with their different operating modes as already mentioned in Section 2.4 and 2.5 of Chapter 2.

3.3 Modelling of Machine Dynamics

In the modelling process of phase-redundant /h.p.o (high phase order) system especially for a six-phase induction machine, six stator terminals from the same stator of 3Φ induction machine are taken out in the form of two individual 3Φ sets. Each stator set has 3Φs either connected in delta or star manner and their magnetic axes are shifted by an arbitrary angle of θ. Here, stator sets (I and II are displaced by θ=30° for asymmetrical configuration) and rotor are identified as (*abc* and *xyz*), and (a_r b_r c_r), respectively. Having a common asymmetrical set structure i.e. all air gap flux harmonics are rejected being in order of 6m ± 1; where m is an odd number; and subsequently removal of whole rotor copper losses and torque harmonics of the order of 6m; where m is even number. The winding layouts of six-phase machine being in split-phase belt connection are drawn in Figure B1 of Appendix B and preferred over true six-phase machine which needs extra insulation for coil sides. Both stator sets, and rotor are connected in star manner being displaced by 120° apart ensuring sinusoidal and uniform distribution of winding connections as shown in Figure B2 of Appendix B.

3.3.1 Modelling of SP-SEIG Dynamics

In the development of a multi-phase (six-phase) machine modelling equations, two most important assumptions are considered before the modelling. First, there must not be any physical fault propagation and second, is to restrict the flow of triplen harmonics between the both symmetrical sets of stator winding namely (*abc* and *xyz*). These presumptions are only possible when neutral of both winding sets (their magnetic axis are shifted by an angle of θ=30° for asymmetrical configuration) are separate as shown in Figure 3.1. Other fundamental assumptions are also made during the system modelling.

- Uniform machine air-gap
- Negligent of hysteresis, saturation and skin effects
- Negligent of eddy current, friction and windage losses
- Non-existence of space harmonics

The voltage and electromagnetic torque equations can be elaborated in form of machine variables for the six-phase induction generator in the arbitrary reference frame by using Stanley's transformation; which converts the nonlinear differential equations with time dependent inductance terms (3Φ axis model) into simplified equations with constant inductance terms (2Φ axis model) [28].

3.3.1.1 Addition of Stator Dynamics

The standard mathematical model of six-phase induction machine in the arbitrary reference frame are written below with the help of following set of equations by assuming rotor parameters referred to stator. Then voltage equations of SP-SEIG can be written as by using the Stanley's transformation [28]:

$$V_{q1} = -r_1 i_{q1} + \omega\psi_{d1} + p\psi_{q1} \,, \tag{3.1}$$

$$V_{d1} = -r_1 i_{d1} - \omega\psi_{q1} + p\psi_{d1} \,, \tag{3.2}$$

$$V_{q2} = -r_2 i_{q2} + \omega\psi_{d2} + p\psi_{q2} \,, \tag{3.3}$$

$$V_{d2} = -r_2 i_{d2} - \omega\psi_{q2} + p\psi_{d2} \,, \tag{3.4}$$

$$V_{qr} = r_r i_{qr} + (\omega - \omega_r)\psi_{dr} + p\psi_{qr} \,, \tag{3.5}$$

$$V_{dr} = r_r i_{dr} - (\omega - \omega_r)\psi_{qr} + p\psi_{dr} \,, \tag{3.6}$$

where,

p denotes differentiation with respect to time and rest of abbreviations symbolize their usual and listed meanings.

3.3.1.2 Addition of Main Flux Saturation

The equations of flux linkages can further be expressed from [28] for incorporating the main flux saturation in the mixed currents-flux linkages analytical model. For this purpose, stator and rotor d-q axis flux linkages can be written as addition of two components i.e. main flux and

leakage flux in whole the voltage equations (3.1) through (3.6) along with inclusion of L_{lm} and L_{ldq}.

$$\psi_{q1} = -L_{\sigma 1}i_{q1} + L_{qm}\left(-i_{q1} - i_{q2} + i_{qr}\right) - L_{lm}\left(i_{q1} + i_{q2}\right) + L_{dq}i_{d2} \ , \tag{3.7}$$

$$\psi_{d1} = -L_{\sigma 1}i_{d1} + L_{dm}\left(-i_{d1} - i_{d2} + i_{dr}\right) - L_{lm}(i_{d1} + i_{d2}) - L_{dq}i_{q2} \ , \tag{3.8}$$

$$\psi_{q2} = -L_{\sigma 2}i_{q2} + L_{qm}\left(-i_{q1} - i_{q2} + i_{qr}\right) - L_{lm}\left(i_{q1} + i_{q2}\right) + L_{dq}i_{d1} \ , \tag{3.9}$$

$$\psi_{d2} = -L_{\sigma 2}i_{d2} + L_{dm}\left(-i_{d1} - i_{d2} + i_{dr}\right) - L_{lm}\left(i_{d1} + i_{d2}\right) + L_{dq}i_{q1} \ , \tag{3.10}$$

$$\psi_{qr} = L_{\sigma r}i_{qr} + L_{qm}\left(-i_{q1} - i_{q2} + i_{qr}\right) \ , \tag{3.11}$$

$$\psi_{dr} = L_{\sigma r}i_{dr} + L_{dm}\left(-i_{d1} - i_{d2} + i_{dr}\right) \ , \tag{3.12}$$

Where,

L_{lm} is the common mutual leakage inductance between the both stator winding sets and L_{ldq} is the cross-saturation coupling between the d-q axis of stators due to saturation are expressed by [35].

$$L_{lm} = L_{lax}\cos\beta + L_{lay}\cos(\beta + 2\pi/3) + L_{laz}\sin(\beta - 2\pi/3), \tag{3.13}$$

and,

$$L_{ldq} = L_{lax}\sin\beta + L_{lay}\sin(\beta + 2\pi/3) + L_{laz}\sin(\beta - 2\pi/3), \tag{3.14}$$

The direct and quadrature axis components of magnetizing current 'i_m'and magnetizing flux linkages 'ψ_m' are also resolved in to sums of following sub-components:

$$i_{dm} = -i_{d1} - i_{d2} + i_{dr} \ , \tag{3.15}$$

$$i_{qm} = -i_{q1} - i_{q2} + i_{qr} \ , \tag{3.16}$$

$$\psi_{dm} = L_{dm}i_{dm} \ , \tag{3.17}$$

$$\psi_{qm} = L_{qm}i_{qm} \ , \tag{3.18}$$

In the expressions for stator and rotor flux linkages (3.7)-(3.12), these sub-components are already added in place of i_{dm}, i_{qm}, ψ_{dm} and ψ_{qm}. In concern of transient behaviour, it is found that neglecting the L_{lm} and L_{ldq} has no appreciable changes except slight variations in voltage harmonic distortion (VHD). It leads towards lower VHD and higher torque pulsation. In view of above, and to simplifying the analysis L_{lm} and L_{ldq} has been neglected, and also, because of uniform airgap length $L_{dm} = L_{qm} = L_m$ in the present work.

Again simplifying Equations (3.1) through (3.6) by using the Equations (3.7) through (3.12), and (3.15) through (3.18) and voltage equations can be further simplified as:

$$V_{d1} = -r_1 i_{d1} + \omega L_{\sigma 1}i_{q1} - \omega\psi_{qm} - pL_{\sigma 1}i_{d1} + p\psi_{dm} \tag{3.19}$$

$$V_{q1} = -r_1 i_{q1} - \omega L_{\sigma 1}i_{d1} + \omega\psi_{dm} - pL_{\sigma 1}i_{q1} + p\psi_{qm} \tag{3.20}$$

$$V_{d2} = -r_2 i_{d2} + \omega L_{\sigma 2}i_{q2} - \omega\psi_{qm} - pL_{\sigma 2}i_{d2} + p\psi_{dm} \tag{3.21}$$

$$V_{q2} = -r_2 i_{q2} - \omega L_{\sigma 2}i_{d2} + \omega\psi_{dm} - pL_{\sigma 2}i_{q2} + p\psi_{qm} \tag{3.22}$$

$$V_{qr} = r_r i_{qr} + (\omega - \omega_r)L_{\sigma r}i_{dr} + (\omega - \omega_r)\psi_{dm} + pL_{\sigma r}i_{qr} + p\psi_{qm}, \tag{3.23}$$

$$V_{dr} = r_r i_{dr} - (\omega - \omega_r)L_{\sigma r}i_{qr} - (\omega - \omega_r)\psi_{qm} + pL_{\sigma r}i_{dr} + p\psi_{dm}, \tag{3.24}$$

Substituting the values of currents from Equations (3.7) through (3.12), (3.15), and (3.16) in to the Equations (3.17) and (3.18) and again rewriting yields:

$$\psi_{dm} = A\left[\frac{\psi_{d1}}{L_{\sigma 1}} + \frac{\psi_{d2}}{L_{\sigma 2}} + \frac{\psi_{dr}}{L_{\sigma r}}\right] \quad , \tag{3.25}$$

$$\psi_{qm} = A\left[\frac{\psi_{q1}}{L_{\sigma 1}} + \frac{\psi_{q2}}{L_{\sigma 2}} + \frac{\psi_{qr}}{L_{\sigma r}}\right] \quad , \tag{3.26}$$

where,

$$A = 1/[(1/L_m) + (1/L_{\sigma 1}) + (1/L_{\sigma 2}) + (1/L_{\sigma r})] \quad , \tag{3.27}$$

In induction machine, rotor windings are short-circuited, hence, Equations (3.23) and (3.24) are reduced to

$V_{dr} = V_{qr} = 0;$

and,

$$0 = r_r i_{qr} + (\omega - \omega_r)L_{\sigma r}i_{dr} + (\omega - \omega_r)\psi_{dm} + pL_{\sigma r}i_{qr} + p\psi_{qm} , \tag{3.28}$$

$$0 = r_r i_{dr} - (\omega - \omega_r)L_{\sigma r}i_{qr} - (\omega - \omega_r)\psi_{qm} + pL_{\sigma r}i_{dr} + p\psi_{dm} \tag{3.29}$$

And after the substitution of rotor currents in above equation yields

$$0 = r_r i_{d1} - (\omega - \omega_r)L_{\sigma r}i_{q1} + r_r i_{d2} - (\omega - \omega_r)\ L_{\sigma r}i_{q2} + \frac{r_r}{L_m}\psi_{dm} - (\omega - \omega_r)[L_{\sigma r}/L_m + 1]\psi_{qm}$$

$$+L_{\sigma r}pi_{d1} + L_{\sigma r}pi_{d2} + [1 + L_{\sigma r}/L_{dd}]\,p\psi_{dm} + \frac{L_{\sigma r}}{L_{dq}}\,p\psi_{qm} \quad , \tag{3.30}$$

$$0 = r_r i_{q1} + (\omega - \omega_r)L_{\sigma r}i_{d1} + r_r i_{q2} + (\omega - \omega_r)\ L_{\sigma r}i_{d2} + (\omega - \omega_r)[L_{\sigma r}/L_m + 1]\psi_{dm} + \frac{r_r}{L_m}\psi_{qm}$$

$$+L_{\sigma r}pi_{q1} + L_{\sigma r}pi_{q2} + \frac{L_{\sigma r}}{L_{dq}}\,p\psi_{dm} + \left[1 + L_{\sigma r}/L_{qq}\right]p\psi_{qm} \quad , \tag{3.31}$$

The state space model using mixed current flux variables can be written in the matrix form as in Equation (3.32) from Equations (3.19) through (3.22), (3.30) and (3.31) :

$$[V_{dq}] = [E]\,d[X_{dq}]/dt + [F][X_{dq}] \tag{3.32}$$

where,

$[V_{dq}] = [V_{d1}\ V_{d2}\ V_{q1}\ V_{q2}\ 0\ 0\ ]^t$

$[X_{dq}] = [i_{d1}\ i_{q1}\ i_{d2}\ i_{q2}\ \psi_{dm}\ \psi_{qm}]^t$

and matrices [E] and [F] are given by Equations (3.33) and (3.34), respectively.

$$\begin{bmatrix} -L_{\sigma 1} & 0 & 0 & 0 & 1 & 0 \\ 0 & -L_{\sigma 1} & 0 & 0 & 0 & 1 \\ 0 & 0 & -L_{\sigma 2} & 0 & 1 & 0 \\ 0 & 0 & 0 & -L_{\sigma 2} & 0 & 1 \\ L_{\sigma r} & 0 & L_{\sigma r} & 0 & \left(1 + \frac{L_{\sigma r}}{L_{dd}}\right) & \frac{L_{\sigma r}}{L_{dq}} \\ 0 & L_{\sigma r} & 0 & L_{\sigma r} & \frac{L_{\sigma r}}{L_{dq}} & \left(1 + \frac{L_{\sigma r}}{L_{qq}}\right) \end{bmatrix} ,$$

$$\tag{3.33}$$

$$
\begin{bmatrix}
-r_1 & \omega L_{\sigma 1} & 0 & 0 & 0 & -\omega \\
-\omega L_{\sigma 1} & -r_1 & 0 & 0 & \omega & 0 \\
0 & 0 & -r_2 & \omega L_{\sigma 2} & 0 & -\omega \\
0 & 0 & -\omega L_{\sigma 2} & -r_2 & \omega & 0 \\
r_r & -(\omega - \omega_r)L_{\sigma r} & r_r & -(\omega - \omega_r)L_{\sigma r} & \dfrac{r_r}{L_m} & -(\omega - \omega_r)\left(1 + \dfrac{L_{\sigma r}}{L_m}\right) \\
(\omega - \omega_r)L_{\sigma r} & r_r & (\omega - \omega_r)L_{\sigma r} & r_r & (\omega - \omega_r)\left(1 + \dfrac{L_{\sigma r}}{L_m}\right) & \dfrac{r_r}{L_m}
\end{bmatrix}
$$

(3.34)

Also,

$$(1/L_{dd}) = (1/L_m)\sin^2\Phi + (1/L)\cos^2\Phi \,,$$

$$(1/L_{qq}) = (1/L)\sin^2\Phi + (1/L_m)\cos^2\Phi \,,$$
(3.35)

$$(1/L_{dq}) = (1/L - 1/L_m)\sin\Phi\cos\Phi,$$

where,

$$\sin\Phi = \psi_{qm}/\psi_m \; ; \; \cos\Phi = \psi_{dm}/\psi_m \,,$$

$$i_m = \sqrt{i_{dm}^2 + i_{qm}^2} \; ; \; \psi_m = \sqrt{\psi_{dm}^2 + \psi_{qm}^2} \,,$$
(3.36)

$$L = d\psi_m/di_m \; ; \; L_m = \psi_m/i_m \,,$$

Symbols (i_m and ψ_m) stands for magnetizing current and magnetizing flux amplitudes, respectively, while L_m and L denote steady-state saturated magnetizing inductance and dynamic inductance, respectively, and angle Φ describes the angular displacement of the magnetizing current space vector with respect to d-axis of the common reference frame. The magnetizing inductance L_m is a non-linear function of the magnetizing current i_m, and can be obtained from the no-load magnetization curve of the machine [4]. The value of L_m is determined by the degree of saturation, and expressed as:

$$L_m = d_1 + d_2 i_m + d_3 i_m^2 + d_4 4 i_m^3 \,,$$
(3.37)

where,

d_1, d_2, d_3, d_4 are constant and their values are given in Appendix A.

i_m is also given by

$$i_m = \sqrt{(-i_{d1} - i_{d2} + i_{dr})^2 + [(-i_{q1} - i_{q2} + i_{qr})^2]} \,,$$
(3.38)

3.3.1.3 Addition of Rotor Dynamics

Electromagnetic torque T_e of the machine is given by

$$T_e = \left(\frac{3}{2}\right)\frac{P}{\omega_b}[-(i_{q1} + i_{q2})\psi_{dm} + (i_{d1} + i_{d2})\psi_{qm}]$$
(3.39)

and, rotor dynamics equations can be written in integral form as

$$\frac{\omega_r}{\omega_b} = \frac{1}{p}\frac{P}{\omega_b}(1/J)\,(T_e - T_L)$$
(3.40)

3.3.2 Modelling of Capacitors Banks

The modelling of excitation and compensating capacitor banks are also accomplished in similar way that transforms stationary 3Φ variables in to the arbitrary reference frame by using a change of variables approach [28].

3.3.2.1 Simple-shunt Capacitor Banks

The mathematical modelling of both sets of shunt excitation capacitor banks connected across the stator terminals in conjunction with pure resistive loads can be transformed from 3Φ quantities into d-q axis equivalent-circuit model using arbitrary reference frame as written below,

$$pV_{d1} = \left(i_{d1c}/C_{p1}\right) + \omega V_{q1} \tag{3.41}$$

$$pV_{q1} = \left(i_{q1c}/C_{p1}\right) - \omega V_{d1} \tag{3.42}$$

$$pV_{d2} = \left(i_{d2c}/C_{p2}\right) + \omega V_{q2} \tag{3.43}$$

$$pV_{q2} = \left(i_{q2c}/C_{p2}\right) - \omega V_{d2} \tag{3.44}$$

Using Kirchhoff's current law at capacitor terminals, currents flowing through shunt excitation capacitors are expressed by Equations (3.49) and (3.50).

3.3.2.2 Series Capacitor Banks

In isolated mode, i.e. capacitor self-excited mode, induction generator suffers from poor voltage regulation, which necessitates appropriate voltage regulating scheme. In this regard, a comparative study of simple-shunt and compensated six-phase induction generator in different operating modes is already employed for simplifying the complexity of voltage regulators in Chapter 2.

- **Modelling of Short-Shunt Capacitors**

The current through series capacitors C_{SS1} and C_{SS2} (in case of short shunt) connected in winding set I and II respectively, is same as the load current. The load current through short shunt capacitance determines the voltage across it using arbitrary reference frame transformations as given by Equations (3.47) and (3.48)

$$\begin{aligned}
\rho V_{q1ss} &= i_{q1L} / C_{ss1} \\
\rho V_{d1ss} &= i_{d1L} / C_{ss1} \\
\rho V_{q2ss} &= i_{q2L} / C_{ss2} \\
\rho V_{d2ss} &= i_{d2L} / C_{ss2}
\end{aligned} \tag{3.45}$$

and the load terminal voltage is expressed as

$$
\begin{aligned}
V_{Lq1} &= V_{q1} - V_{q1ss} \\
V_{Ld1} &= V_{d1} - V_{d1ss} \\
V_{Lq2} &= V_{q2} - V_{q2ss} \\
V_{Ld2} &= V_{d2} - V_{d2ss}
\end{aligned}
\tag{3.46}
$$

- **Modelling of Long-Shunt Capacitors**

   In the same way, currents through series capacitors C_{ls1} and C_{ls2} (in case of long-shunt) connected in winding set I and II, respectively, are machine currents. The machine current through long-shunt capacitance determines corresponding voltage across it by using Equations (3.49) and (3.50)

$$
\begin{aligned}
\rho V_{q1ls} &= i_{q1}/C_{ls1} \\
\rho V_{d1ls} &= i_{d1}/C_{ls1} \\
\rho V_{q2ls} &= i_{q2}/C_{ls2} \\
\rho V_{d2ls} &= i_{d2}/C_{ls2}
\end{aligned}
\tag{3.47}
$$

and, the load terminal voltage is expressed as

$$
\begin{aligned}
V_{Lq1} &= V_{q1} + V_{q1ls} \\
V_{Ld1} &= V_{d1} + V_{d1ls} \\
V_{Lq2} &= V_{q2} + V_{q2ls} \\
V_{Ld2} &= V_{d2} + V_{d2ls}
\end{aligned}
\tag{3.48}
$$

3.3.3 Modelling of Static Loads

   Assume that the loads are pure resistive 'R' and balanced 3Φ reactive (RL) /resistive-inductive 'R-L'. The modelling of these static loads is given in the following equation. According to Kirchhoff's current law and the relation between voltage and current of capacitances, different current equations at excitation shunt capacitor terminals are as:

$$
i_{d1c} = i_{d1} - i_{d1L}; \; i_{q1c} = i_{q1} - i_{q1L}; \; i_{d2c} = i_{d2} - i_{d2L}; \; i_{q2c} = i_{q2} - i_{q2L};
\tag{3.49}
$$

$$
i_{d1c} = C_{p1}pV_{d1}; \; i_{q1c} = C_{p1}pV_{q1}; i_{d2c} = C_{p2}pV_{d2}; \; i_{q2c} = C_{p2}pV_{q2}
\tag{3.50}
$$

If, pure resistive loads are considered across the terminals of generator, its load current equations can be given by

$$
i_{d1L} = V_{d1}/R_{L1}; \; i_{q1L} = V_{q1}/R_{L1}; \; i_{d2L} = V_{d2}/R_{L2}; \; i_{q2L} = V_{q2}/R_{L2}
\tag{3.51}
$$

hence, with pure resistive loads, terminal voltages can be modified as:

$$
pV_{d1} = (i_{d1}/C_{P1}) - (V_{d1}/R_{L1}C_{P1}) + \omega V_{q1}
\tag{3.52}
$$

58

$$pV_{q1} = (i_{q1}/C_{P1}) - (V_{q1}/R_{L1}C_{P1}) - \omega V_{d1} \tag{3.53}$$

$$pV_{d2} = (i_{d2}/C_{P2}) - (V_{d2}/R_{L2}C_{P2}) + \omega V_{q2} \tag{3.54}$$

$$pV_{q2} = (i_{q2}/C_{P2}) - (V_{q2}/R_{L2}C_{P2}) - \omega V_{d2} \tag{3.55}$$

where, R_{L1} and R_{L2} are the load resistances connected across the winding set I and II, respectively.

When assume balanced 3Φ reactive loads, R_1L_1 and R_2L_2 (per phase values) connected across winding set I and II, respectively, hence voltage equations are given by,

$$pV_{d1} = (i_{d1}/C_{p1}) - (i_{d1L}/C_{p1}) + \omega V_{q1} \tag{3.56}$$

$$pV_{q1} = (i_{q1}/C_{p1}) - (i_{q1L}/C_{p1}) - \omega V_{d1} \tag{3.57}$$

$$pV_{d2} = (i_{d2}/C_{p2}) - (i_{d2L}/C_{p2}) + \omega V_{q2} \tag{3.58}$$

$$pV_{q2} = (i_{q2}/C_{p2}) - (i_{q2L}/C_{p2}) - \omega V_{d2} \tag{3.59}$$

Where, the load currents are expressed as:

$$\begin{aligned}
pi_{d1L} &= (V_{d1}/L_1) - (R_{L1}/L_1)(i_{d1L}) \\
pi_{q1L} &= (V_{q1}/L_1) - (R_{L1}/L_1)(i_{q1L}) \\
pi_{d2L} &= (V_{d2}/L_2) - (R_{L2}/L_2)(i_{d2L}) \\
pi_{q2L} &= (V_{q2}/L_2) - (R_{L2}/L_2)(i_{q2L})
\end{aligned} \tag{3.60}$$

A couple of models, obtained from different sets of state-space variables to unify main flux saturation d-q axis models of induction machines have been reported by [26]. In general, two common approaches are most frequently used either by selecting stator and rotor d-q axis currents or stator and rotor d-q axis flux linkages as state-space variables in to main flux saturation modelling [3-8]. Mathematical model selected here is developed with a different approach i.e. stator current d-q axis components and magnetizing flux d-q axis components as state–space variables without taking into account the common mutual leakage inductance between both the stator sets and dynamic cross saturation across the d-q axis of stator set [26].

3.4 Simulation of SP-SEIG Model

The computer based analytical transient study has been carried out on SP-SEIG by using RK4 subroutine coded in MATLAB M-file and its program algorithm is shown in Figure 3.3. In this section, a numerical method is introduced for the solution of Equations (3.32), (3.39) and (3.40). In the case, where the ordinary differential equations are linear can be solved by the

analytical methods. Unfortunately, the differential Equation (3.32) is nonlinear and cannot be solved exactly with high expectation. Approximate solutions can be estimated by using computer approximations and concentrated on the case where Equation (3.32) is solved numerically by RK4 algorithm. An explicit MATLAB program for the implementation of RK subroutine of order 4 is constructed in M-file. The theoritical analysis using RK4 subroutine on MATLAB platform has been carried out in simple-shunt and compensated configuration of SP-SEIG. The dynamic performance of the SP-SEIG were determined, under no load and loading condition when both the winding sets are self-excited and /or compensated. If the speed of SP-SEIG is kept constant, terminal voltage depends on the values of capacitances and the load connected across its terminals. The voltage of SP-SEIG decreases with the increase in load for a fixed value of the capacitance. The following transient or dynamic responses are considered for the validity of analytical approach proposed in this Chapter.

- Dynamic response of simple-shunt SP-SEIG under no load condition when both 3Φ sets are excited.
- Transient response of simple-shunt SP-SEIG under a resistive loading condition on only single winding set when both 3Φ sets are excited.
- Transient response of simple-shunt SP-SEIG under equal resistive loading condition on both excited 3Φ winding sets.
- Transient response of simple-shunt SP-SEIG under an unequal resistive loading condition on both excited 3Φ winding sets.

The transient response under following operating conditions have also been performed for series compensated SP-SEIG which were determined during no load, R load and R-L loading condition in the single mode of excitation capacitor bank when it is simultaneously connected across both 3Φ winding sets, and in both configuarations of compensating series capacitor bank connection.

- During R and R-L loading with short shunt compensation.
- During R and R-L loading with long shunt compensation.

3.5 Analytical Treatment

The estimated analytical responses are given in detail here. An algorithm for Runge -Kutta method for the operation of the SP-SEIG is also shown in chronological order in the form of flowchart in Figure 3.3. The chronological order which are used in the flowchart of Figure 3.3 is similar to the constructed M-file for the estimation of the machine variables under constant rated speed of the studied system. The flowchart for the algorithm of the Runge-Kutta method is coded in M-file for estimation of the performance under constant rated speed. The machine

60

variables of SP-SEIG were estimated by the analytical approach using RK4 method under proposed particular mode, i.e. when both winding sets are self-excited (with fixed value)

```
                        ╱‾‾‾‾‾‾‾‾╲
                       ╱  Start   ╲
                       ╲          ╱
                        ╲_____╱
                            │
                            ▼
      ╱───────────────────────────────────────────╱
     ╱ Read r₁,r₂,lϭ₁,lϭ₂, l'ϭᵣ, Cₚ , Cₛₛ  and Cₗₛ for simple-  ╱
    ╱   shunt, short-shunt and long-shunt respectively.      ╱
   ╱───────────────────────────────────────────╱
                            │
                            ▼
   ┌───────────────────────────────────────────────┐
   │ Take Cp₁= Cp₂= Cp, Cₛₛ₁= Cₛₛ₂= Cₛₛ, Cₗₛ₁= Cₗₛ₂= Cₗₛ, R_L1=R_L2= R_L (for equal │
   │ resistive load), L₁=L₂=L (for equal inductive load). │
   └───────────────────────────────────────────────┘
                            │
                            ▼
   ┌───────────────────────────────────────────────┐
   │ Set the constant value of rotor speed (Nr), prescribed values of Ψdm and │
   │ Ψqm with initialization id1=iq1=id2=iq2=vd1=vq1=vd2=vq2=Imm=0; │
   └───────────────────────────────────────────────┘
                            │
                            ▼
   ┌───────────────────────────────────────────────┐
   │ Calculate also the initial value for Lm, L, Fm, Ldd, Lqq, Ldq, cosu, sinu as │
   │ per configuration used │
   └───────────────────────────────────────────────┘
                            │
                            ▼
   ┌───────────────────────────────────────────────┐
   │ Assume step size h=0.0001, tsim=10, imax = tsim /h; │
   └───────────────────────────────────────────────┘
                            │
                            ▼
            ┌──────────────────────────┐
            │ Iteration no. i =1 │
            └──────────────────────────┘
                            │
                            ▼
   ┌───────────────────────────────────────────────┐
   │ Compute at every iteration, all four slopes for every machine variable │
   │ as per configuration used │
   └───────────────────────────────────────────────┘
                            │
                            ▼
   ┌───────────────────────────────────────────────┐
   │ Compute at every iteration, averaging of all four slopes for every │
   │ machine variable under considered configuration │
   └───────────────────────────────────────────────┘
                            │
                            ▼
   ┌───────────────────────────────────────────────┐
   │ Update every time all machine variables by averaging of all │
   │ four slopes by runge-kutta method │
   └───────────────────────────────────────────────┘
                            │
                            ▼
                       ╱‾‾‾‾‾‾‾‾╲
                      ╱  Check   ╲
         ┌───────────╱  i < imax   ╲──────────┐
         │           ╲            ╱           │
     yes │            ╲_____╱         no  │
         │                                    ▼
         │        ┌─────────────────────────────────────┐
         │        │ Print vd1, vd2, vq1, vq2, id1, id2, iq1, iq2, Ψdm, Ψqm │
         │        │ and all other required machine variables │
         │        └─────────────────────────────────────┘
         ▼                                    │
   ┌──────────────┐                           ▼
   │ i=i+1 │                          ╱‾‾‾‾‾‾‾‾╲
   └──────────────┘                  ╱  End   ╲
         │                           ╲_____╱
         └───────────────
```
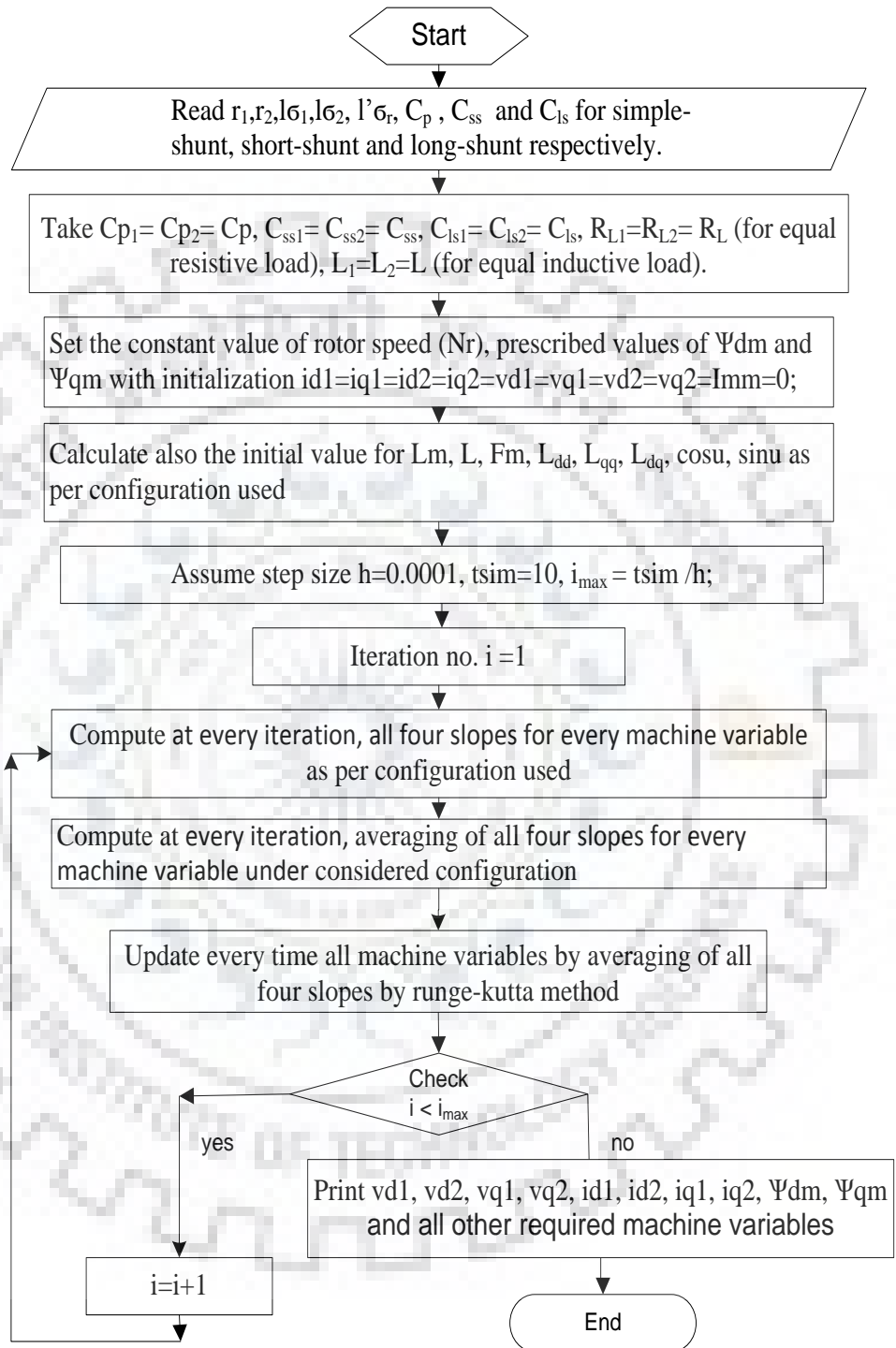
Figure 3.3: Algorithm for Runge-Kutta method implemented for SP-SEIG under constant rated speed at 1000 r.p.m.

in simple-shunt and compensated configuration with or without load as shown in Figure 3.4 through 3.7.

3.5.1 Simple-Shunt SP-SEIG

The following transient responses under different operating load conditions have been performed:

- *No load performance with both of the 3Φ winding sets in simple-shunt configuration*

For this no load operation, both winding sets were excited by fixed shunt capacitance of 38.5 μF (in delta bank connection) and simulation performance curves are shown in Figure 3.4. The peak value of simulated voltage in each terminal phase is 181 V as shown in Figure 3.4 (a). Similar variations in other variables (i.e. per phase flux, mutual inductance, dynamic inductance, magnetizing flux, angular displacements of the magnetizing current) with the time were observed and are shown in Figure 3.4. In the balanced condition, the generated voltage in each winding set (*abc* and *xyz*) will be equal and also 90⁰ phase shift between d and q axis of set I and II. So, there is phase difference of 90⁰ between the V_{d1} and V_{q1} as shown in Figure 3.4 (i). But, both three phase winding sets are physically displaced by θ =30⁰ as shown in Figure 3.1. Hence, the generated voltage across winding set II is establishing the phase shift of 30 degree with respect to winding set I between V_a and V_x as shown in Figure 3.4 (j).

- *Single loading performance with both of the 3Φ winding sets in simple-shunt configuration*

When the machine was resistively loaded with 200 Ω on only single 3Φ set I at t=2s, it gives a reduced steady state terminal voltage about 100 V on set I and 107 V on another set II from its no load voltage of 200V are shown in Figures 3.5 (a) and (b), respectively. Likewise, variations in remaining performance variables are also shown in Figure 3.5.

- *Equal loading performance with both of the 3Φ winding sets in simple-shunt configuration*

In loading performance, first the simple-shunt excited SP-SEIG was operated under no load conditions and self-excitation is initiated at t=0s at rated speed of 1000 RPM. When equal resistive loads of 200Ω per phase were applied at t=2s, a sudden drop was found in terminal voltage values of machine as shown in Figure 3.6. A sudden equal resistive loading of 200 Ω at t=2s gives a reduced steady state terminal voltage about 90V from its initial value as shown in Figure 3.6.

(a)

(b)

(c)

(d)

(e)

(f)

64
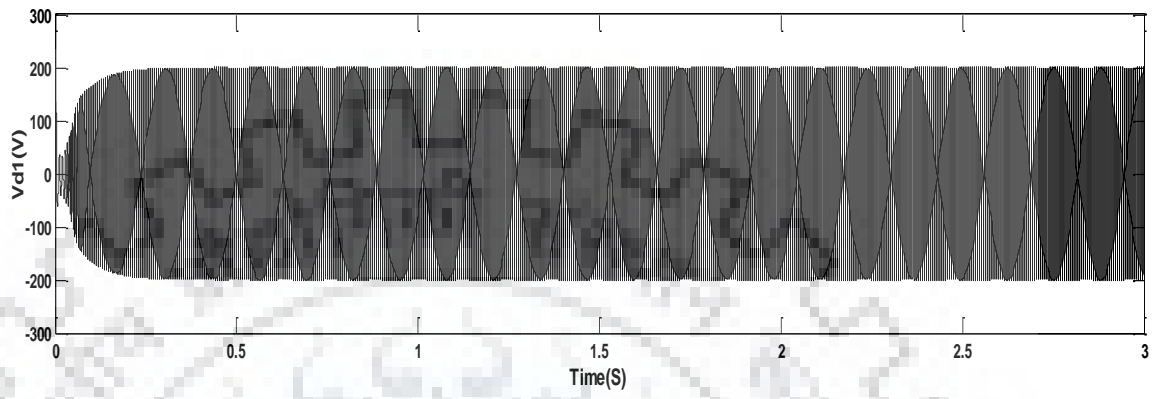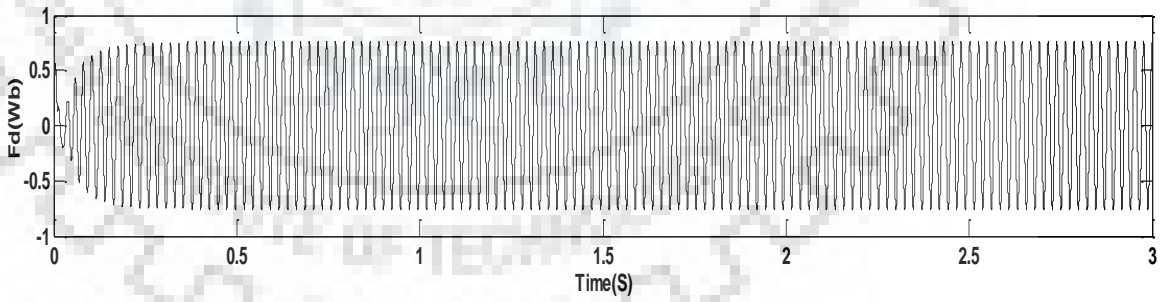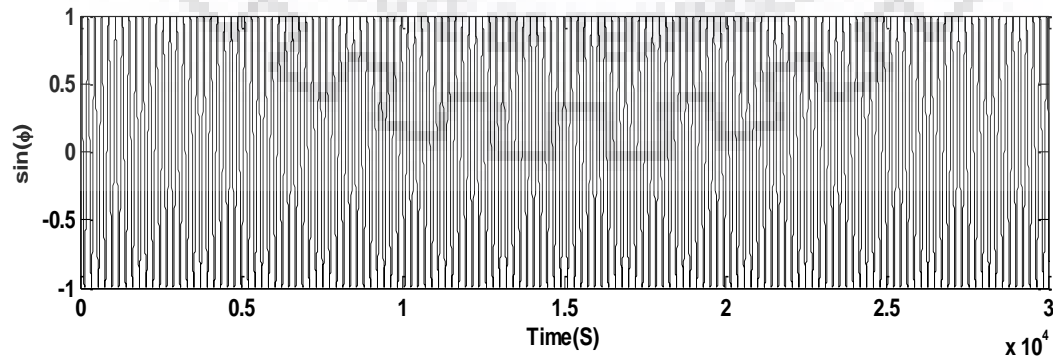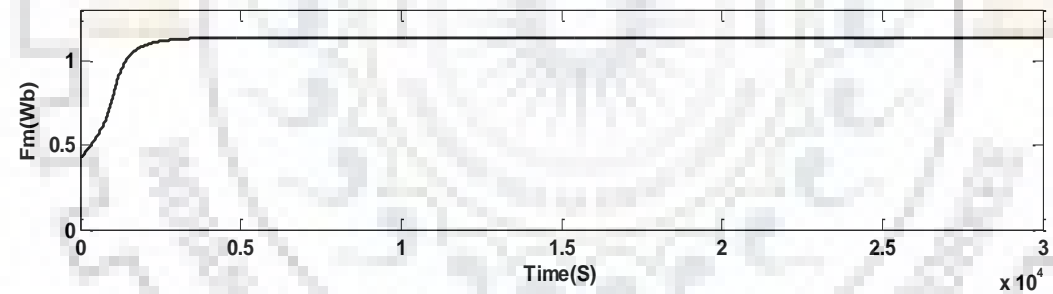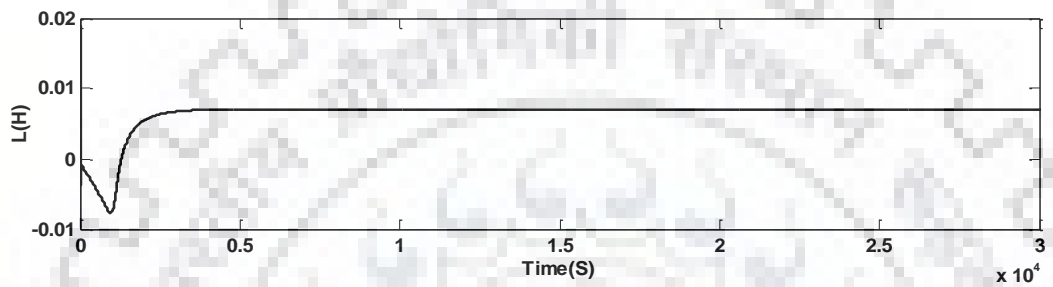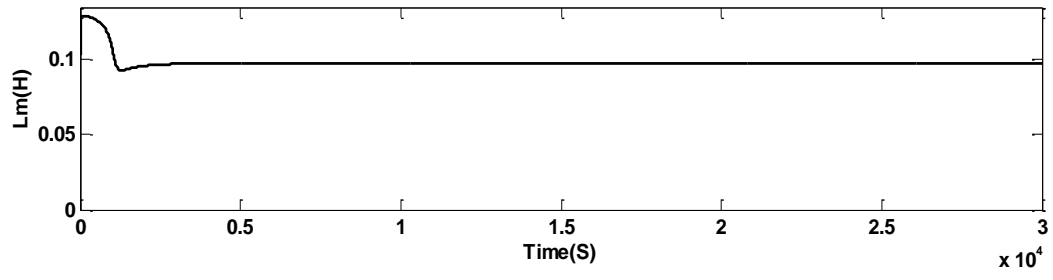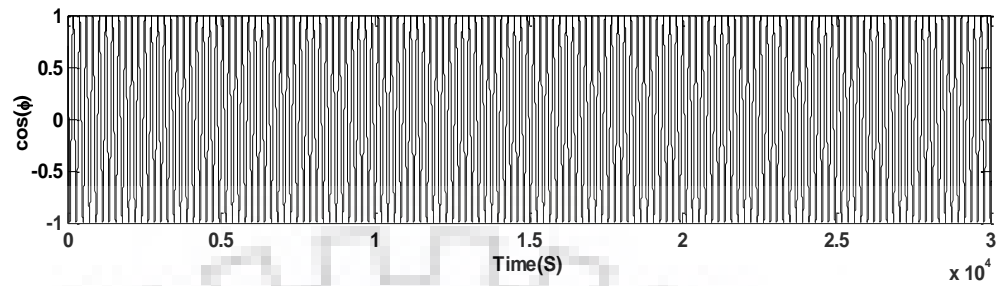
(g)
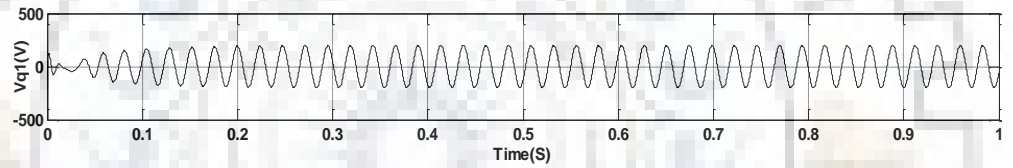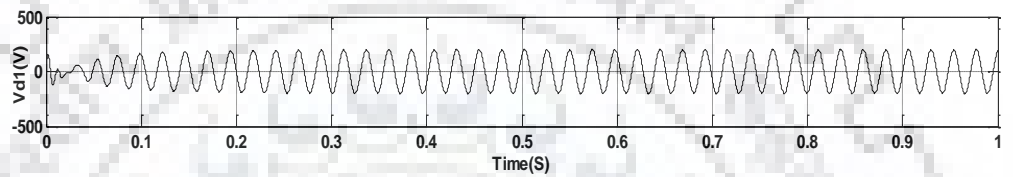
(h)
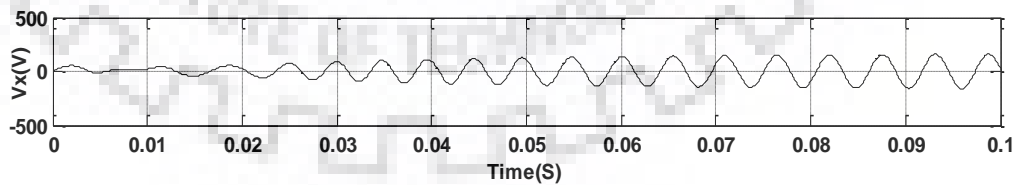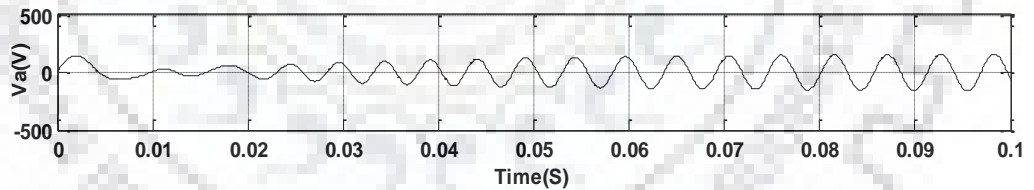
(i)

Figure 3.4: Estimated response of (a) per phase voltage across set I (b) per phase flux across set I (c) variation of mutual inductance with time (d) variation of dynamic inductance with time (e) variation of magnetizing flux with time (f) and (g) angular displacements of the magnetizing current (h) 90⁰ phase shift between V_{d1} (or V_{d2}) and V_{q1} (or V_{q2}) of set I (or set II) (i) 30⁰ displacement between generated voltages of set I and II; when no load on SP-SEIG at constant rated speed of 1000 r.p.m.

65

- *Unequal loading performance with both of the 3Φ winding sets in simple-shunt configuration*

In the same way, when both of the 3Φ winding sets are self-excited with 38.5 µF and on unequal loads, the machine terminal voltages were estimated by the analytical approach using RK4 method are shown in Figure 3.7. When the machine was unequally resistive loaded (200Ω & 400 Ω) at t=2s, a sudden drops occur in the previous estimated steady state no load terminal voltages across both sets at rated speed of about 1000 RPM. A sudden resistive loading of 200 Ω at t=2s gives a reduced steady state voltage about 80V on set I, and on another set II, it gives a reduced steady state terminal voltage about 70V with 400 Ω of loading.

3.5.2 Compensated SP-SEIG

Analytical waveforms of d-q axis terminal voltage, d-q axis load current, d-q axis magnetizing flux, d-q axis series capacitor voltage and magnetizing current during sudden switching of R load of 200 Ω and a balanced 3Φ R-L load (200 Ω in series with 500mH) at t= 2s with both (short-shunt and long-shunt) compensation in 3Φ winding sets are shown in Figures 3.8 through 3.11. In the case of R-L load, generated voltage amplitude is dropped by few more volts compared to R load. Combined amplitude of magnetizing flux, steady-state saturated magnetizing inductance and dynamic (tangent slope) inductance along with the combined amplitude waveform of d-axis stator current and load current during no-load and sudden switching of resistive load of 200 Ω at t= 2s are also shown in Figures 3.8 through 3.11. The application of short-shunt capacitor results in overvoltage across the generator terminal at no-load before sudden switching of R and R-L load at t= 2s as compared to long-shunt capacitor results in reduced terminal voltage. While long-shunt SP-SEIG is also able to deliver output power at reduced terminal voltages. In proposing, stator current and magnetizing flux as state-space variables in mixed model, it has been observed that terminal voltage build-up from its initial value to steady state value completely depends upon initial few Weber values of residual flux, and rotor speed.

3.5.2.1 Short-Shunt Series Compensated SP-SEIG

Analysis of short-shunt SP-SEIG along with a single mode of excitation and the series capacitor banks of 38.5 µF and 108 µF respectively, have been computed and predicted from the explicit MATLAB program using RK4 subroutine are shown in Figures 3.8 and 3.9. The application of short-shunt scheme results in overvoltage across the generator terminals. As it is shown in Figure 3.8a, the per phase voltage level is more than the voltage level of Figure 3.10a and it is equal to about 50V as shown in Figure 3.8b.
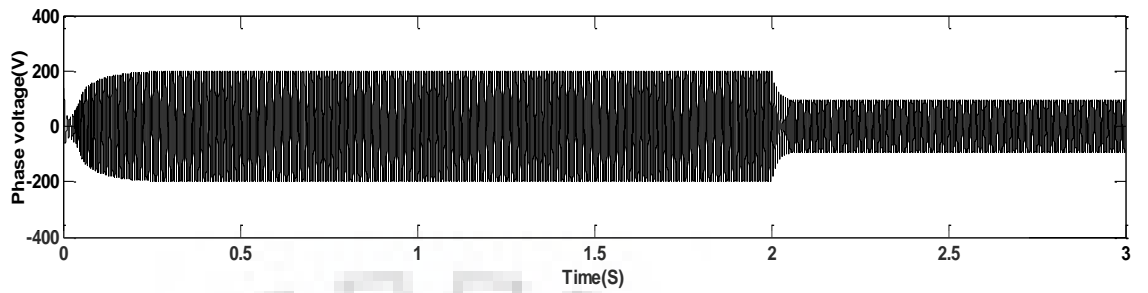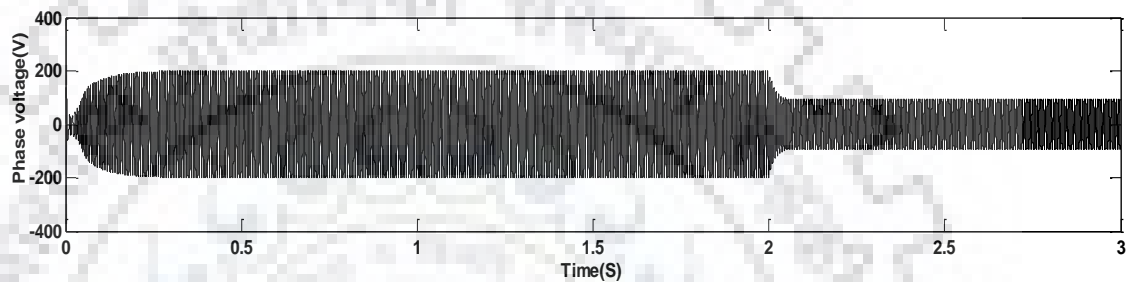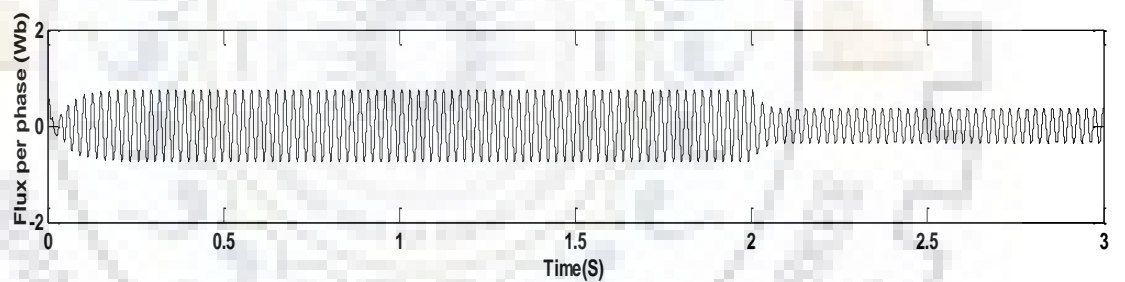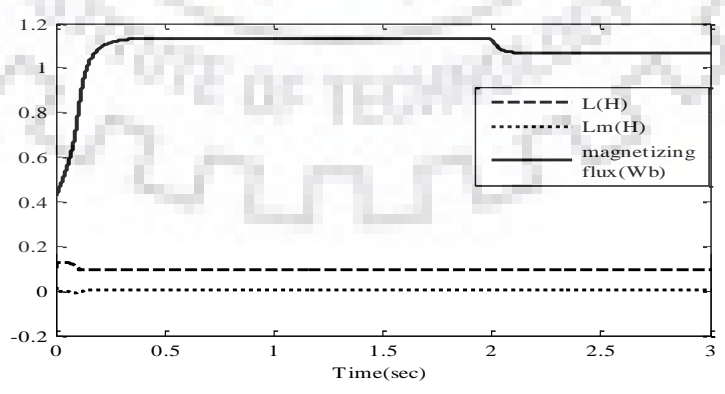
Figure 3.5: The estimated response of (a) per phase voltage across set I (b) per phase voltage across set II (c) per phase winding flux (d) variations of mutual inductance, dynamic inductance and magnetizing flux linkages with the time when a single load of 200 Ω at only single 3Φ set I of SP-SEIG at constant rated speed of 1000 r.p.m.
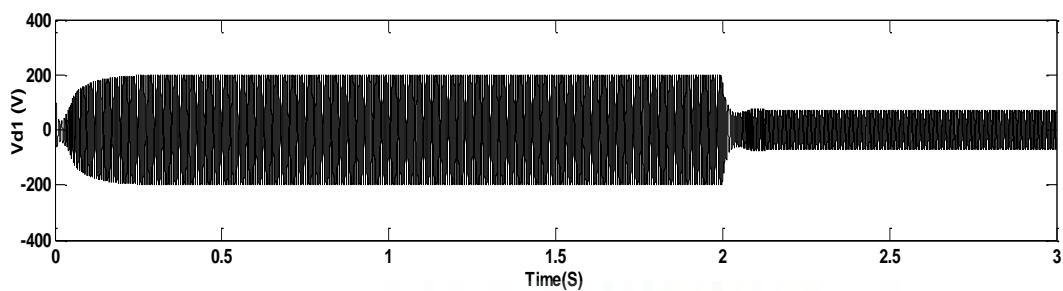
(a)
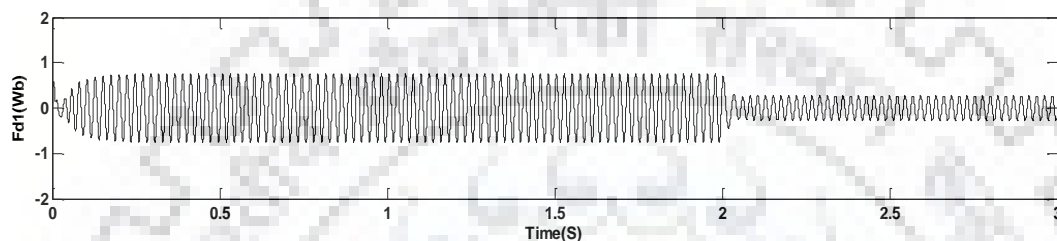
(b)

Figure 3.6: Estimated response of (a) per phase voltage (b) per phase flux with time across set I of SP-SEIG when equal resistive loads at t=2s at constant rated speed of 1000 r.p.m.
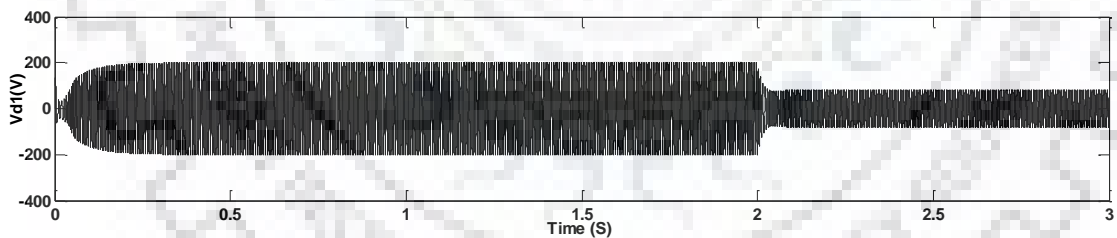
(a)
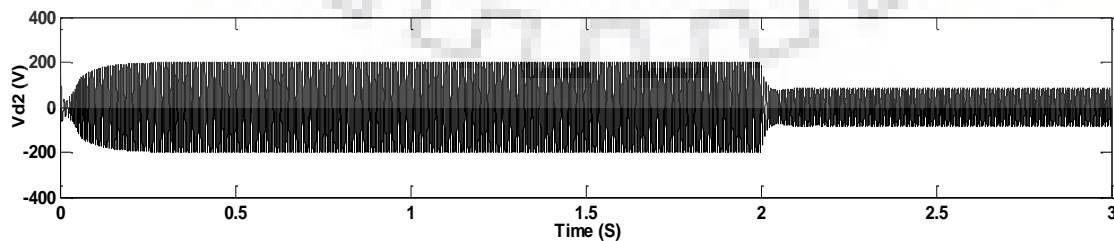
(b)

Figure 3.7: Estimated response of per phase voltages across set I and II, respectively, when unequal resistive loads (200Ω & 400 Ω) at t=2s on the SP-SEIG at constant rated speed of 1000 r.p.m.

(a)

(b)

(c)

(d)
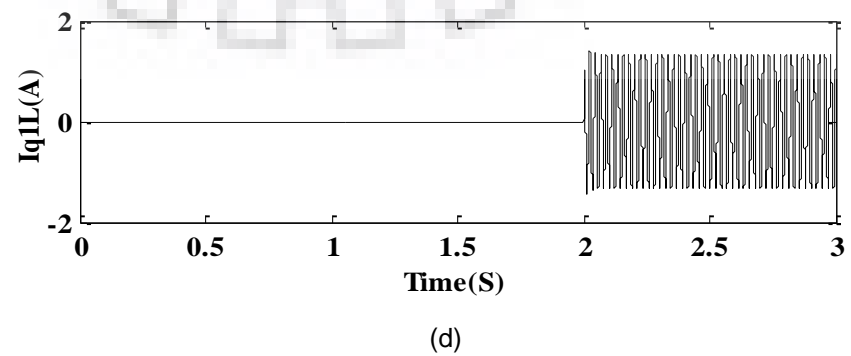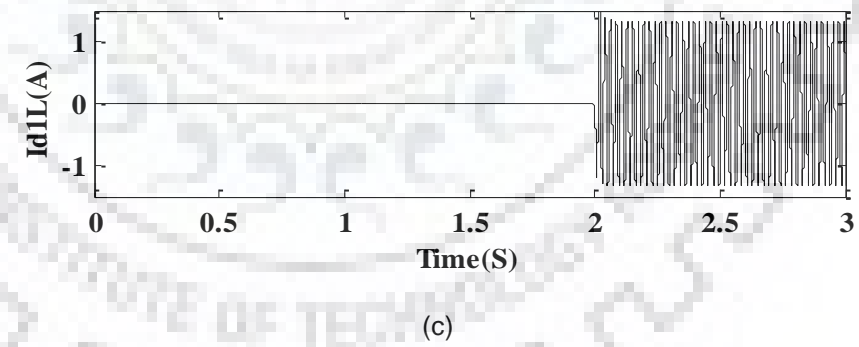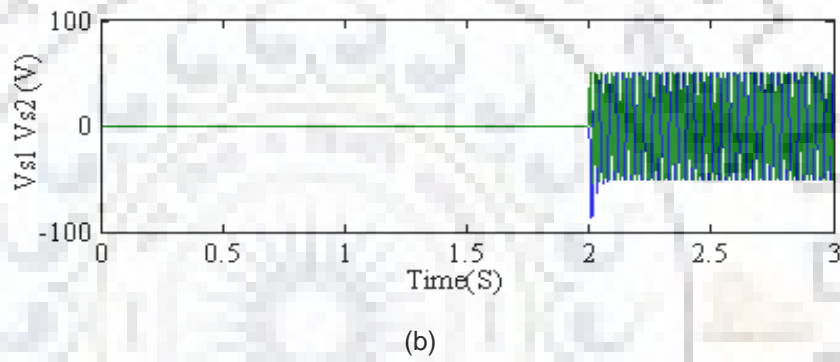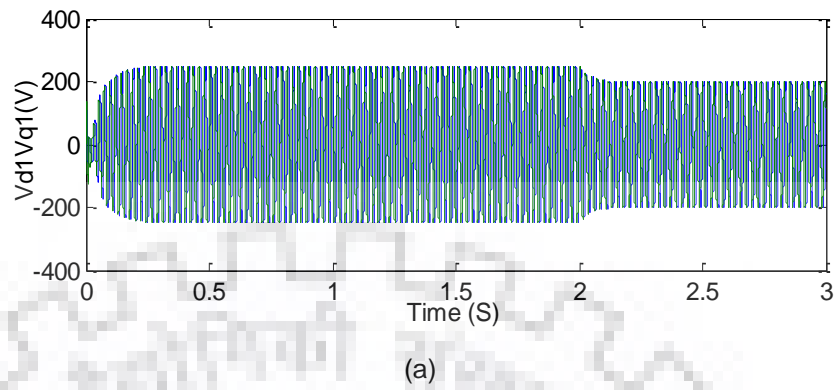
Figure 3.8. Analytical waveforms during sudden switching of R loads of 200 Ω at t= 2s.

- *When both the 3Φ winding sets are accompanied by short-shunt configuration and subjected to independent R loadings*

The analytical d-q waveform of voltage during no-load and sudden switching of resistive loads of 200 Ω at t=2s with short-shunt compensation for both 3Φ winding sets are shown in Figure 3.8a. In addition, The combined d-q axis voltage drops across the series short-shunt capacitors is also given in Figure 3.8b. The d- and q-axis load currents are also depicted in Figures 3.8c and d, respectively, during sudden switching of resistive loads of 200 Ω at t= 2s and equal to about 1.4 A. The steady state generated no-load voltage is about 240V at rated speed of 1000 RPM. While, it reduces to 200V at rated speed of 1000 RPM on switching of 200 Ω resistive loads at t= 2s. The reduced terminal voltage value is almost no load voltage. So, inclusion of series capacitor in each line gives self-regulation by supplying additional reactive powers during sudden load connections.

- *When both the 3Φ winding sets are accompanied by short-shunt configuration and subjected to independent R-L loadings*

Similarly, in the same order of Figure 3.8, all analytical waveforms are also shown in Figure 3.9 during sudden switching of R-L load of 200 Ω in series with 500mH at t= 2s. Hence, the reduced steady state voltage generated is about 190V at rated speed of 1000 RPM at t=2s. The drops in lagging load currents (d-and q-axis) are also given by Figures 3.9c and d.

3.5.2.2 Long-Shunt Series Compensated SP-SEIG

It is also seen that like short-shunt configuration, long-shunt configuration is also self-regulating in nature. In same manner, analysis of long-shunt SP-SEIG along with a single mode of excitation and the series capacitor banks of $38.5\,\mu\text{F}$ and $350\,\mu\text{F}$, respectively, have also been computed and predicted by using the RK4 subroutine and given in Figures 3.10 and 3.11. Here, the value of series capacitor is more than the twice of short-shunt series capacitor.

- *When both the 3Φ winding sets are accompanied by long-shunt configuration and subjected to independent R loadings*

The analytical waveforms of voltage during no-load and sudden switching of resistive load of 200 Ω at t=2s with long-shunt compensation for two 3Φ winding sets are respectively shown in Figure 3.10a. The application of the long-scheme results in less overvoltage or reduced terminal voltage across the generator terminals. As it is shown in Figure 3.10a, the per phase voltage level is less than the voltage level of Figure 3.8a.

70
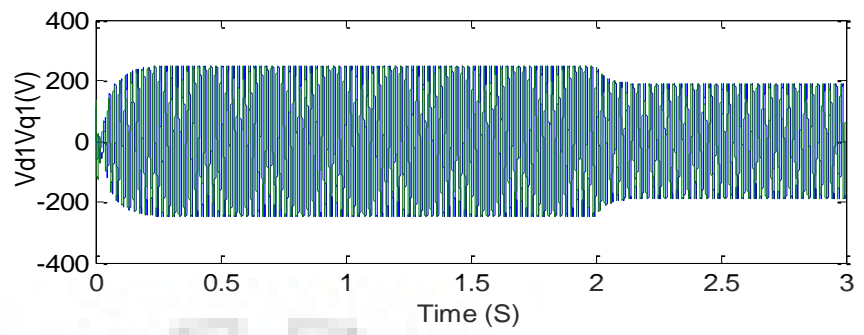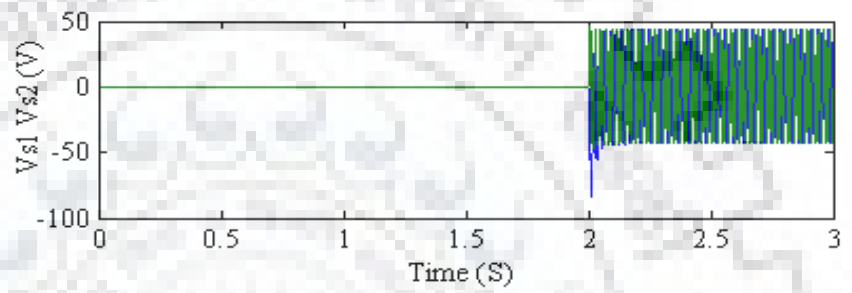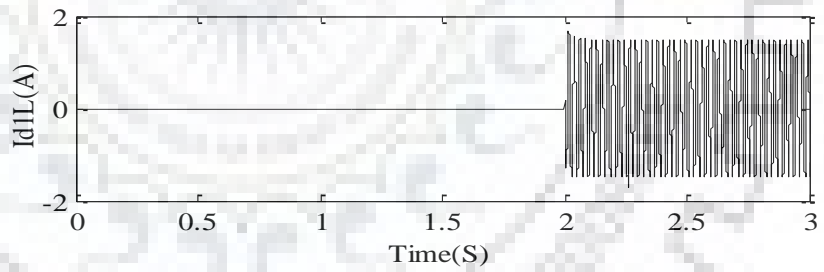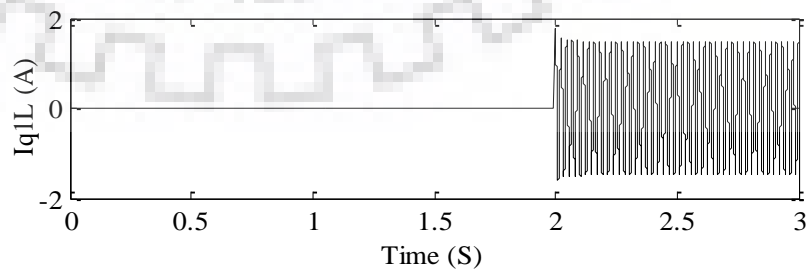
Figure 3.9: Analytical waveforms during sudden switching of R-L loads at t= 2s.
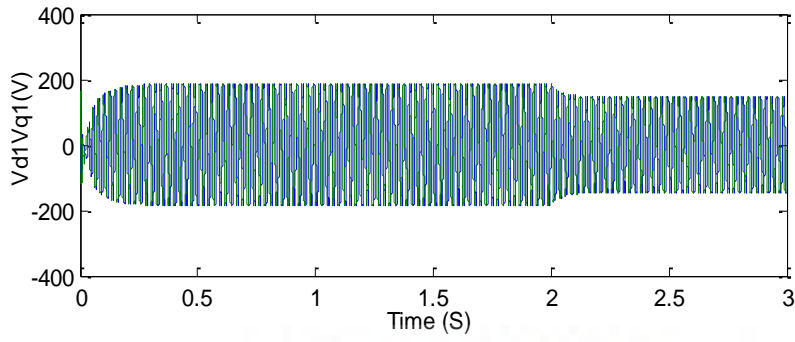
(a)
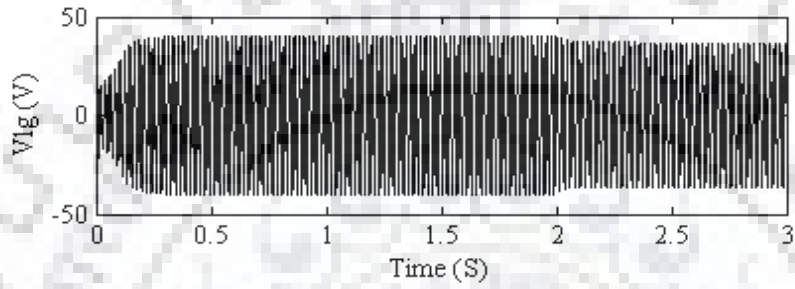
(b)
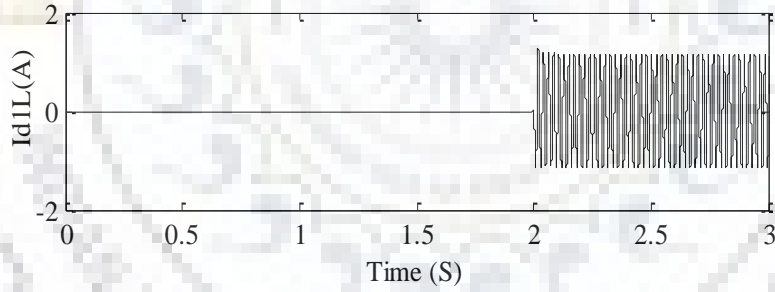
(c)
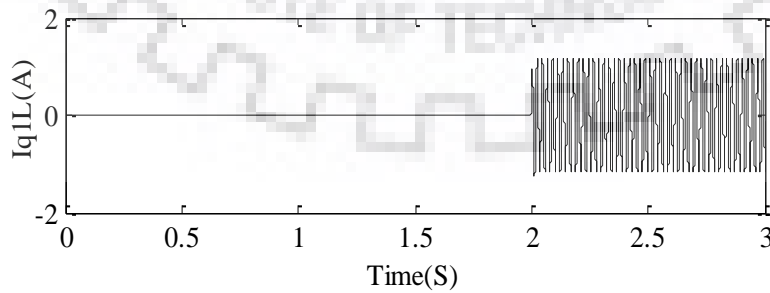
(d)

Figure 3.10: Analytical waveforms during sudden switching of R loads of 200 Ω at t= 2s.
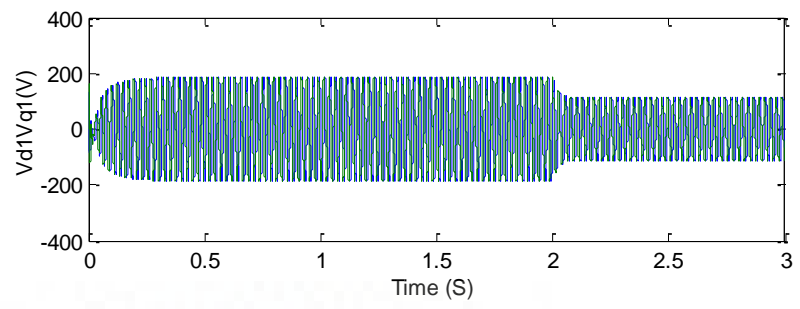
(a)
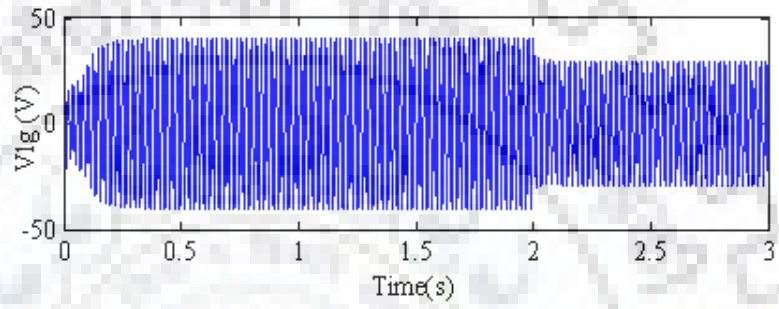
(b)
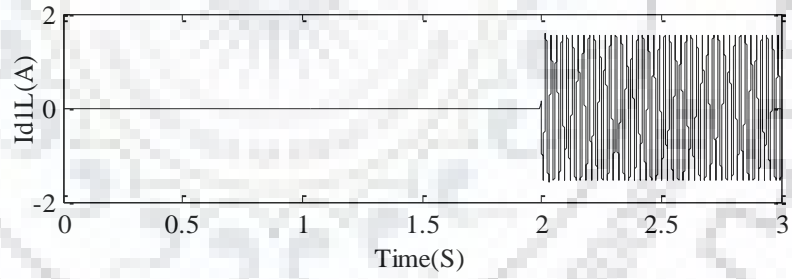
(c)
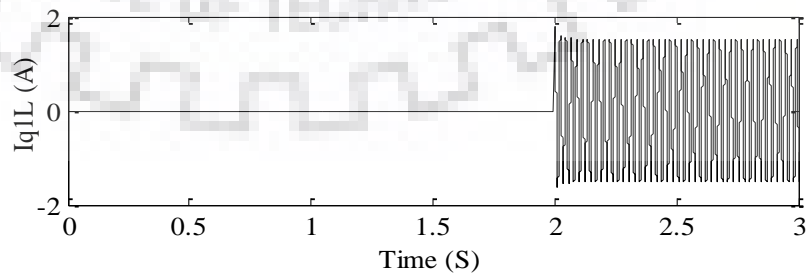
(d)

Figure 3.11: Analytical waveforms during sudden switching of R-L loads at t= 2s.

73

It gives evidence that long-shunt SP-SEIG is able to deliver output power at reduced terminal voltages, that voltage drop across the long shunt capacitor is equal to about 40V as shown in Figure 3.10b. The combined d-q axis voltage drop across the series long-shunt capacitor is given in Figure 3.10b. The d- and q-axis load currents are also depicted in Figures 3.10c and d respectively, during sudden switching of resistive loads of 200 Ω at t= 2s. The steady state no-load voltage generated is about 190V at rated speed of 1000 RPM. While it is 170V at rated speed of 1000 RPM on switching of 200 Ω resistive load at t= 2s.

- *When both the 3Φ winding sets are accompanied by long-shunt configuration and subjected to independent R-L loadings*

Similarly, in the same order of Figure 3.10, all analytical waveforms are also shown in Figure 3.11 during sudden switching of R-L load (200 Ω resistance in series with 500mH inductor) at t= 2s. Hence, the reduced steady state voltage generated is about 160V at rated speed of 1000 RPM at t=2s. Same like of Section 3.5.2.1, the drops in lagging load currents (d-and q-axis) are also given by Figures 3.11c and d.

The analytical dynamic performance study of SP-SEIG and its simulation have been accomplished by an explicit MATLAB program using mixed variable approach.

3.6 Concluding Remarks

Mixed stator current and air-gap flux state space model possesses the advantage of having variable speed operation under the variable magnetizing flux level in the machine. The state space model matrix equations are simpler than the d and q axis current state space model. Similarly, for finding out the machine variables, the computation of matrix equations is also an easy task using RK4 subroutine. The transient analysis of SP-SEIG demonstrates machine behaviour during the static loadings. A careful selection of the shunt capacitor values also avoids the excessive voltage at the terminals of SP-SEIG under loading condition. A careful value selection of the combination, i.e. shunt and series capacitors may also avoid the excessive voltages at the terminals of SP-SEIG under the loads and can maintain the no-load terminal voltage due to extra reactive power supplied by the series capacitors. The involvement of different series capacitors satisfied the requirement of the voltage regulation when load is suddenly switched on after few second and retains the no-load terminal voltage as per self-regulating nature. In both the cases (R and R-L loading), less voltage drops were occurred with series compensation when variation from no load to full load.

After getting the initial values from steady state analysis of SP-SEIG, One's responsibility is towards choice of proper set of state-space variables for dynamic and (or) transient analysis.

74

This analysis can also determine the extent, to which, suitability of winding insulation and its stress, rotor shaft oscillations, unreasonable heating, and extra losses has taken placed. In dynamic modelling of SP-SEIG, there are various methods in the available literatures. One simple and mixed variable approach has been used for dynamic modelling purpose by using stator current and magnetizing flux as state-space variables. So, dynamic modelling can also be improved little more than before by using mixed current-flux state-space variables. It includes main (airgap or magnetizing) flux saturation which has valuable consideration in the current source fed variable speed induction motor drives.

Although, mixed model analysis leads to more computational efforts in its state-space matrix model by having only non-zero members and the selected pair of stator current and magnetizing flux as state-space variables. However, simple matrix model than other existing and available mixed variable models in literatures. Under variable speed operating conditions, flux level in the machine needs to be modelled accordingly that accounts for the main flux saturation. This saturated machine model is mostly applied in air-gap flux field orientation vector control strategy. Mixed state-space variable approach (includes stator current and magnetizing flux) is beneficial in study of vector-controlled induction machines. The mixed stator current and air-gap flux as a state-space variables model belongs to one of the more complex types and preserves the information about both stator and rotor parameters.

The study on inclusion of series capacitances to serve additional VAR is an inviting alternative during improvement of voltage regulations of SP-SEIG. Additionally, an effect of long-shunt series capacitors in load terminal voltage regulation prepares SP-SEIG as simple and cost effective. Short-shunt compensation will be used in improved voltage regulation during loaded condition, while long-shunt compensation serves effect of parameter 'k' (which is ratio of series capacitive reactance to shunt capacitive reactance) on the performance of machine during different loading condition and also maintains load voltages under different load currents.

This chapter describes the stability of SP-SEIG to the research work. Foremost, It will start with some background on stability problems in machine systems. Then, the solutions to the problems will be discussed through which stability analysis using eigenvalue criteria along with derived transfer functions will be selected. Next, scope of work with author's contribution are explained.

4.1 Introduction

Several utilization of symmetrical induction machine, i.e. accurate performance predictions of system over a wide range of operating frequencies, have a need of low speed (5 to 10 percent of the rated speed) and may become unstable against constant and balanced applied stator voltages. As induction generators have abrupt increase in the speed with sudden reduction in their electrical torque during short circuits, so its dynamic behaviour requires more attention during faults. Consequence, increase in reactive power further leads to a system voltage collapse. The terminal voltage and frequency of isolated SEIG power source are appreciably influenced by rotor speed, excitation capacitors and connected loads in renewable energy applications. So, it is necessary to develop analytical techniques of stability analysis. The stability studies have been presented in detail for six-phase induction machine, but no such study has been carried out for six-phase induction generator [20, 28, 35].

Stability of electrical machine is an important factor to be considered, and is directly affected by the many design parameters of it during the steady state operation. As per the study, the first overall scenario on the stability of AC machines was developed in 1965 using the root locus technique. Instability of induction motor which is fed by frequency inverter was analyzed. Other evidences have analyzed an induction motor drive with different schemes of rectifier-inverter, single cage, controlled current, current source inverter, double cage and voltage source inverter using Nyquist stability criterion, root-locus technique, transfer function technique, a linearized small signal model, decoupled boundary layer model and Liapunov's first method, respectively. All above works demonstrated the analysis of 3Φ induction motor drive in account with different schemes [34].

In the last year of the past decade, only limited literatures were available on the dynamic stability of isolated 3Φ induction generators. But these works are insufficient as compared with the well documented 3Φ induction motor as discussed above. Some deals with the steady state analysis of 3Φ isolated induction generator feeding an IM load using predictor-corrector-type continuation method. The eigenvalue analysis is also used to examine the stability of induction generator. While the phase-plane plot, eigenvalue and root-locus technique was used to analyze the dynamic stability of two parallel operated autonomous induction generators supplying an induction motor with long-shunt compensation. The stability of 3Φ synchronous machine has been examined by using the small signal analysis, Nyquist stability criteria and root-locus technique.

To the best of the author's knowledge, the stability analysis of 3Φ AC machine has been carried out in detail in mentioned available literatures, such analysis was not developed for multi-phase AC machines till 2002. Stability issue using a small - signal analysis of a multi-phase machine was recognized first by Singh et al [35] in 2003 followed by Duran et al in 2008, and Singh et al in 2013 [20] followed 2014 [14]. Singh et al [35] have analyzed the stability of a six-phase induction machine, keeping the effect of common mutual leakage reactance and harmonics, between the both 3Φ stator winding sets. Whereas Duran et al and Singh et al [20], have analyzed five-phase motor with an injection of third harmonic and six-phase synchronous generator connected to the utility grid, respectively. Reference [34] deals with the stability of asymmetrical synchronous motor. Such analysis has no evidence so far for six-phase induction generator in isolated mode.

Small signal analysis with eigenvalue approach focuses on a simple, stable and successful operation at any balanced operating condition during small excursion behavior of a machine. Eigenvalue analysis is also employed to determine the critical operating conditions of the studied machine. The behaviour of SP-SEIG can be described by a set of non-linear differential equations [4]. However, the study of small displacement behaviour requires the linearized equations. The linearized two axis model of SP-SEIG in synchronously rotating reference frame is developed using Taylor's expansion about a fixed point from the voltage equations of multi-phase induction machine [28]. An eleventh order linearized model has been developed for small excursion stability analysis w.r.t eleven state variables corresponding to eleven eigenvalues. Whereas, eigenvalue calculations and transfer functions formulations have been performed by linear system theory.

Stability is investigated under perturbation of any one variable from the placement of the eigenvalues of the machine. In the present eleventh-order linearized model of a SP-SEIG, the effects of common mutual leakage inductance (L_{lm}) between two winding sets and cross-saturation coupling (L_{ldq}) between d- and q-axis of individual stator have not been considered. This avoids the complexity of the solution and only effect of magnetizing inductance (L_m) has been considered. This analysis also presents the effect of magnetizing inductance during the process of self-excitation and also finds that speed too plays an important role which is necessary to initiate, and to sustain the self-excitation process in an isolated SP-SEIG for a given value of capacitance, and load. Magnetizing inductance (L_m) also plays an important role in the dynamics of voltage build up and stabilization of SP-SEIG.

4.2 Problem Formulation

In order to have detailed investigation of eigenvalues behaviour, first of all, characteristic roots /eigenvalues are determined from linearized model of SP-SEIG for fundamental machine parameters and variables. Secondly, Eigenvalue approach establishes an opportunity to correlate eigenvalues with machine parameters. The eigenvalues are varied in accordance with the machine variables and gives focus about stabilization of SP-SEIG. Lastly, nature of whole complex and real eigenvalues "corresponding of the stator, rotor, capacitor and rotor inertia closely" along the complex s-plane would also signify the stability of SP-SEIG using Root-locus graphical tool. This section is mainly divided in to three sub sections as discussed below.

4.2.1 Fundamental Nonlinear SP-SEIG Model

The behavior of induction machines is nonlinear, so there is a need of linearization of these nonlinear equations and to be rewritten in the state variable form for further small signal analysis. The nonlinear fundamental model is derived in following manner in below sub sections.

4.2.1.1 Modelling of Stator Dynamics

An ac machine can have as many phases as coils per pole pair. Generally, all the 3Φ machines are designed with 60^0 phase belts, but sometimes these machines are also wound with 120^0 phase belts. A 3Φ machine can be easily converted to six-phase by 'splitting' the 60^0 phase belts into two portion each spanning 30^0 without any additional cost. The detailed design of six-phase machine is given in [4].

The equivalent circuit of SP-SEIG is shown in Figure 4.1. The voltage and electromagnetic torque equations can be elaborated in form of single variable i.e. current in arbitrary reference frame [28] in to simplified two-phase axis model in similar manner of Chapter 3:

$$V_{q1} = -r_1 i_{q1} + \omega \psi_{d1} + p\psi_{q1} \; ; \tag{4.1}$$

$$V_{d1} = -r_1 i_{d1} - \omega \psi_{q1} + p\psi_{d1} \; ; \tag{4.2}$$

$$V_{q2} = -r_2 i_{q2} + \omega \psi_{d2} + p\psi_{q2} \; ; \tag{4.3}$$

$$V_{d2} = -r_2 i_{d2} - \omega \psi_{q2} + p\psi_{d2}; \tag{4.4}$$
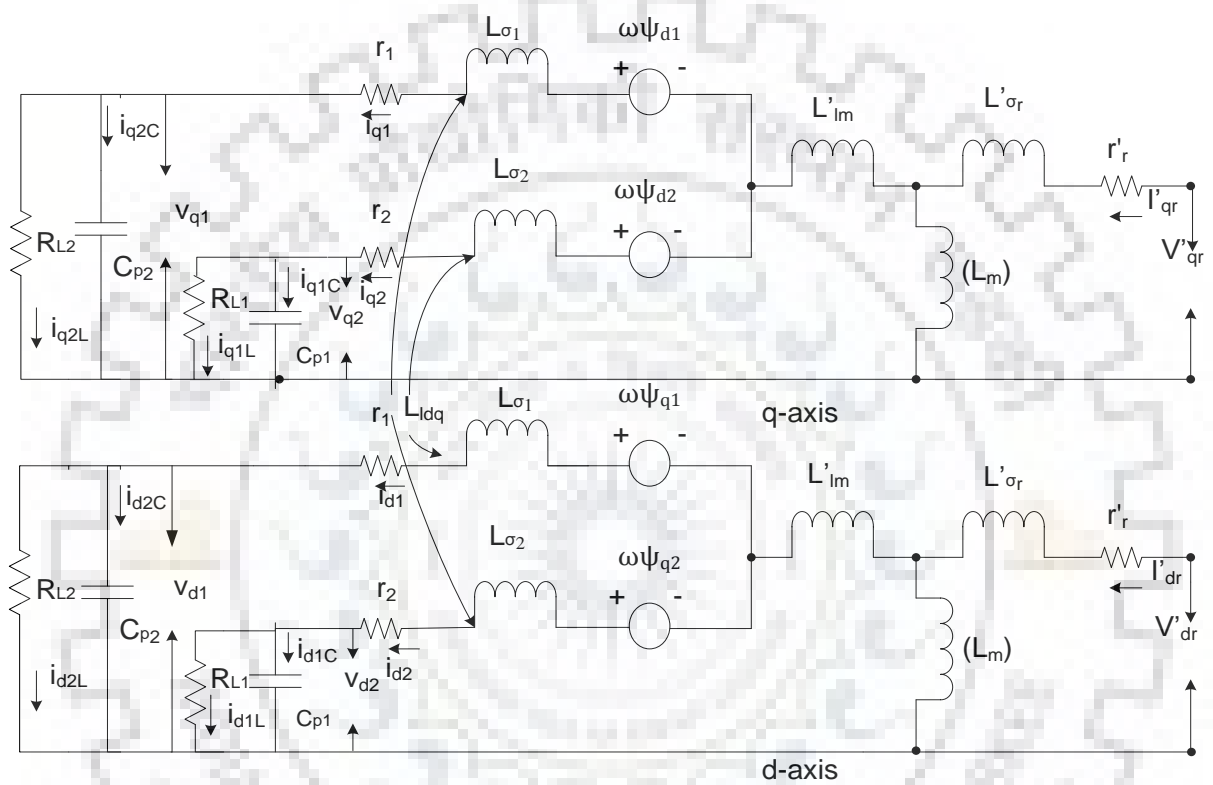
Figure 4.1: Equivalent circuit of SP-SEIG in dq-axis

$$V'_{qr} = r'_r i'_{qr} + (\omega - \omega_r)\psi'_{dr} + p\psi'_{qr} \; ; \tag{4.5}$$

$$V'_{dr} = r'_r i'_{dr} - (\omega - \omega_r)\psi'_{qr} + p\psi'_{dr}; \tag{4.6}$$

$$\psi_{q1} = -L_{\sigma 1} i_{q1} + \psi_{qm} \;; \;\; \psi_{d1} = -L_{\sigma 1} i_{d1} + \psi_{dm} \;; \;\; \psi_{q2} = -L_{\sigma 2} i_{q2} + \psi_{qm} \; ; \tag{4.7}$$

$$\psi_{d2} = -L_{\sigma 2} i_{d2} + \psi_{dm} \;; \;\; \psi'_{qr} = L'_{\sigma r} i'_{qr} + \psi_{qm} \;; \;\; \psi'_{dr} = L'_{\sigma r} i'_{dr} + \psi_{dm}; \tag{4.8}$$

Where,

$$\psi_{dm} = L_{dm} i_{dm} \;; \;\; \psi_{qm} = L_{qm} i_{qm} \;; \;\; i_{dm} = -i_{d1} - i_{d2} + i'_{dr}; \; i_{qm} = -i_{q1} - i_{q2} + i'_{qr};$$

Thus simplifying the Equations (4.1)-(4.6) by using Equations (4.7) and (4.8), and rewritten them as follows:

$$V_{d1} = -r_1 i_{d1} + \omega(L_{l1} + L_{dm})i_{q1} + \omega L_{qm} i_{q2} - \omega L_{qm} i'_{qr} - p(L_{l1} + L_{dm})i_{d1} - pL_{dm} i_{d2} + pL_{dm} i'_{dr} \tag{4.9}$$

$$V_{q1} = -r_1 i_{q1} - \omega(L_{l1} + L_{dm})i_{d1} - \omega L_{dm} i_{d2} + \omega L_{dm} i'_{dr} - p(L_{l1} + L_{qm})i_{q1} - pL_{qm} i_{q2} + pL_{qm} i'_{qr} \tag{4.10}$$

$$V_{d2} = r_2 i_{d2} + \omega(L_{l2} + L_{qm})i_{q2} + \omega L_{qm} i_{q1} - \omega L_{qm} i'_{qr} - p(L_{l2} + L_{dm})i_{d2} - pL_{dm} i_{d1} + pL_{dm} i'_{dr} \tag{4.11}$$

$$V_{q2} = -r_2 i_{q2} - \omega(L_{l2} + L_{dm})i_{d2} - \omega L_{dm} i_{d1} + \omega L_{dm} i'_{dr} - p(L_{l2} + L_{qm})i_{q2} - pL_{qm} i_{q1} + pL_{qm} i'_{qr} \tag{4.12}$$

In induction machine, rotor windings are short-circuited, hence, $V'_{dr} = V'_{qr} = 0$

$$0 = r'_r i'_{qr} + (\omega - \omega_r)(L'_{lr} + L_{dm})i'_{dr} - (\omega - \omega_r)L_{dm} i_{d1} - (\omega - \omega_r)L_{dm} i_{d2} + p(L'_{lr} + L_{qm})i'_{qr} - pL_{qm} i_{q1} - pL_{qm} i_{q2} \tag{4.13}$$

$$0 = r'_r i'_{dr} - (\omega - \omega_r)(L'_{lr} + L_{qm})i'_{qr} + (\omega - \omega_r)L_{qm} i_{q1} + (\omega - \omega_r)L_{qm} i_{q2} + p(L'_{lr} + L_{dm})i'_{dr} - pL_{dm} i_{d1} - pL_{dm} i_{d2} \tag{4.14}$$

Considering the uniform air gap length, and $L_{dm} = L_{qm} = L_m$, equation of L_m is nonlinear function of i_m as given in Appendix A and i_m is given by Equation (3.38).

4.2.1.2 Modelling of Shunt Excitation Capacitor Bank and Load

The mathematical modelling of both sets of shunt excitation capacitor bank connected in parallel with pure resistive loads can be introduced by Sections 3.3.2.1 and 3.3.3.

4.2.1.3 Modeling of Torque and Rotor Dynamics

The electromagnetic torque and rotor speed of the SP-SEIG can be expressed in terms of selected state-space variables as:

$$T_e = (3/2)(P/2)(L_m/L_r)\left[(i_{q1}+i_{q2})\Psi''_{dr}-(i_{d1}+i_{d2})\Psi''_{qr}\right] \tag{4.15}$$

$$\omega_r = (1/p)(P/2)(1/J)(T_m - T_e) \tag{4.16}$$

where, T_e is electromagnetic torque, T_m is mechanical input torque and $L_r = L'_{lr} + L_m$. After combining Equations (3.54) through (3.57) and Equations (4.9) through (4.16), It is convenient to write the system equations in synchronously rotating reference frame by setting $\omega = \omega_e$ and rewritten in matrix form as given in Equation (4.17).

4.2.2 Development of Linearized SP-SEIG Model

The procedure, which is involved in the linearization of nonlinear differential equations of SP-SEIG has included following assumptions for a small displacement: first, the product terms of two or more deviations must be neglected. Second, flux levels have little variation for keeping the inductances terms constant. In the process of linearization, first of all each variable is replaced by its value, and then both the assumptions are applied for simplifying the linearized differential equations. In this way, a small-displacement linear equations are developed from the fixed operating point. The linear differential equations of SP-SEIG becomes as given in Equation (4.18).

The linearized machine equations are conveniently derived from the voltage equations with currents as state variables during steady-state balanced conditions. This selection is generally determined by a particular application and resulting set of differential equations are linear with regard to small disturbances and available for the stability study of SP-SEIG. For convenience, the derivative terms are put on one side and the Equation (4.18) in the state space form is written as:

$$Apx = Bx + u \tag{4.19}$$

where, $x = [i_{d1}\ i_{q1}\ i_{d2}\ i_{q2}\ i'_{dr}\ i'_{qr}\ V_{d1}\ V_{q1}\ V_{d2}\ V_{q2}\ \omega_r]^T$, $u = [0\ 0\ 0\ 0\ V'_{dr}\ V'_{qr}\ 0\ 0\ 0\ 0\ T_m]^T$

and A and B is given by the Equations (4.20) and (4.21).

It is also suitable to indicate the Equation (4.19) in to elementary form of linear differential equation (state equation). This standard state equation can be written as:

$$px = A^{-1}Bx + A^{-1}u \tag{4.22}$$

where,

$$E= A^{-1}B \tag{4.23}$$

$$F= A^{-1} \tag{4.24}$$

The linear differential equations written in standard or state variable form in the Equation (4.22) can be rewritten as

$$px=Ex+Fu \tag{4.25}$$

where, u is input vector and if it is equal to zero, the solution of linear differential Equation (4.22) can be given by Equation (4.26). The characteristic equation of A is determined by Equation (4.27) from Reference [28].

$$x = Ke^{At} \tag{4.26}$$

and
$$\det\left(A - \zeta I\right)=0 \tag{4.27}$$

where, the roots ζ of the Equation (4.27) is referred to as eigenvalues, characteristic roots, or latent roots and I is an identity matrix.
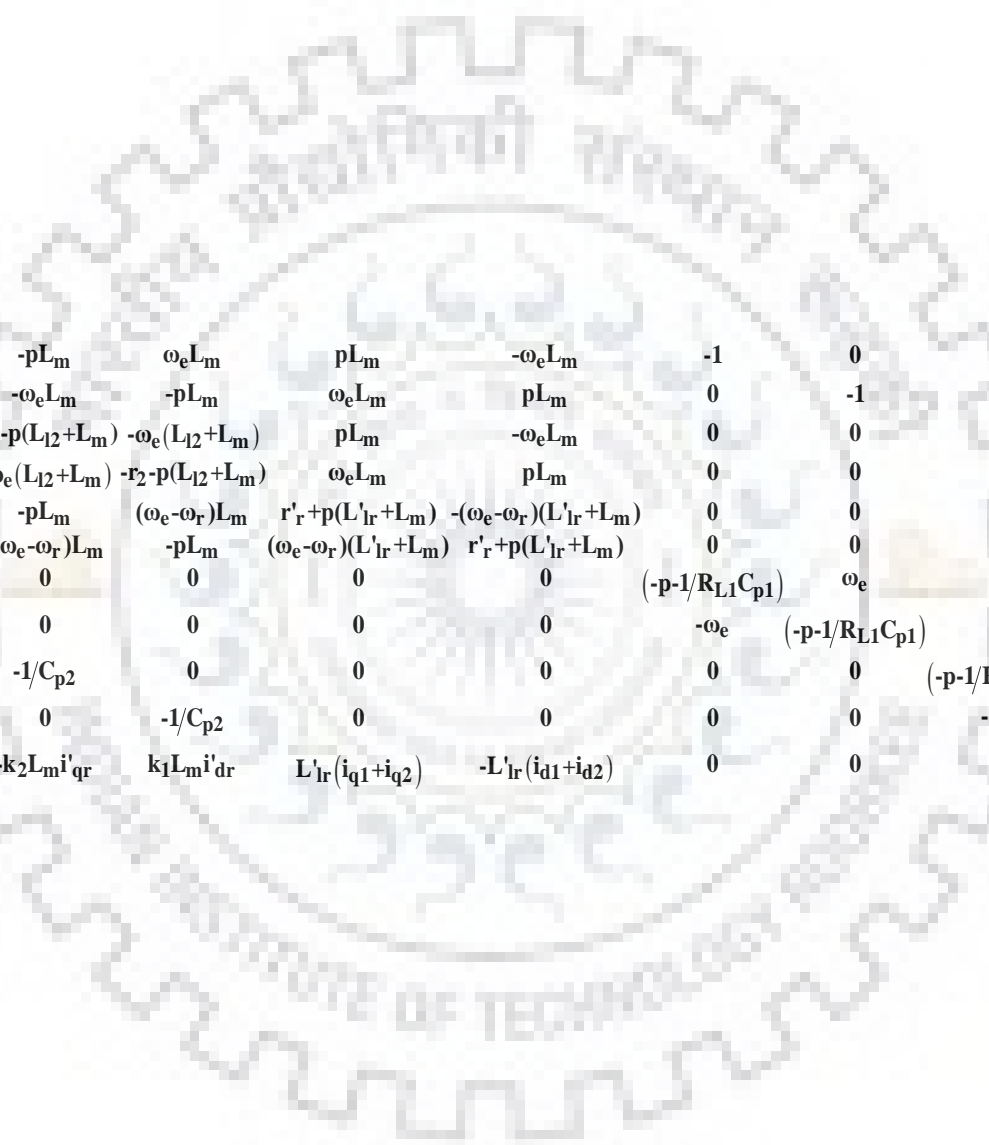
4.3 Simulation of Linear Small Signal Model

Two simple techniques are involved in the stability analysis of linearized SP-SEIG model using the eigenvalue approach and transfer functions in following subsections.

4.3.1 Eigenvalue Analysis of Small Signal Model

Eigenvalues allow a direct and effective approach for stability analysis of SP-SEIG at any small displacement. These are either real or complex values obtained from characteristic equation of the studied system. Real values correlate with a non-oscillatory mode of the state variables. Positive and negative real values indicate a periodic instability and a decaying mode, respectively. Whereas, when they are complex, occur as a pair of complex-conjugate eigenvalues that signifies a mode of oscillation of the state variables. The real part of complex-conjugate eigenvalue corresponds to damping while the imaginary part corresponds to the frequency of oscillations. Real parts may be either positive value or negative value. Positive, and negative values indicate an exponential increase with time; an unstable condition, and an exponential decrease with time; a stable condition, respectively. Basic linear system theory can be used to calculate the eigenvalues [14, 28].

The eigenvalues of SP-SEIG can be obtained by using a standard eigenvalue computer routine. To calculate the roots of matrix [E] given by Equation (4.27) i.e. the eigenvalues of SP-

$$
\begin{bmatrix} 0 \\ 0 \\ 0 \\ 0 \\ 0 \\ V'_{dr} \\ V'_{qr} \\ 0 \\ 0 \\ 0 \\ 0 \\ T_m \end{bmatrix}
=
\begin{bmatrix}
-r_1-p(L_{l1}+L_m) & \omega_e(L_{l1}+L_m) & -pL_m & \omega_e L_m & pL_m & -\omega_e L_m & -1 & 0 & 0 & 0 & 0 \\
-\omega_e(L_{l1}+L_m) & -r_1-p(L_{l1}+L_m) & -\omega_e L_m & -pL_m & \omega_e L_m & pL_m & 0 & -1 & 0 & 0 & 0 \\
-pL_m & \omega_e L_m & -r_2-p(L_{l2}+L_m) & -\omega_e(L_{l2}+L_m) & pL_m & -\omega_e L_m & 0 & 0 & -1 & 0 & 0 \\
-\omega_e L_m & -pL_m & -\omega_e(L_{l2}+L_m) & -r_2-p(L_{l2}+L_m) & \omega_e L_m & pL_m & 0 & 0 & 0 & -1 & 0 \\
-pL_m & (\omega_e-\omega_r)L_m & -pL_m & (\omega_e-\omega_r)L_m & r'_r+p(L'_{lr}+L_m) & -(\omega_e-\omega_r)(L'_{lr}+L_m) & 0 & 0 & 0 & 0 & 0 \\
-(\omega_e-\omega_r)L_m & -pL_m & -(\omega_e-\omega_r)L_m & -pL_m & (\omega_e-\omega_r)(L'_{lr}+L_m) & r'_r+p(L'_{lr}+L_m) & 0 & 0 & 0 & 0 & 0 \\
-1/C_{p1} & 0 & 0 & 0 & 0 & 0 & (-p-1/R_{L1}C_{p1}) & \omega_e & 0 & 0 & 0 \\
0 & -1/C_{p1} & 0 & 0 & 0 & 0 & -\omega_e & (-p-1/R_{L1}C_{p1}) & 0 & 0 & 0 \\
0 & 0 & -1/C_{p2} & 0 & 0 & 0 & 0 & 0 & (-p-1/R_{L2}C_{p2}) & \omega_e & 0 \\
0 & 0 & 0 & -1/C_{p2} & 0 & 0 & 0 & 0 & -\omega_e & (-p-1/R_{L2}C_{p2}) & 0 \\
-k_2 L_m i'_{qr} & k_1 L_m i'_{dr} & -k_2 L_m i'_{qr} & k_1 L_m i'_{dr} & L'_{lr}(i_{q1}+i_{q2}) & -L'_{lr}(i_{d1}+i_{d2}) & 0 & 0 & 0 & 0 & p(2J/P)
\end{bmatrix}
\begin{bmatrix} i_{d1} \\ i_{q1} \\ i_{d2} \\ i_{q2} \\ i'_{dr} \\ i'_{qr} \\ V_{d1} \\ V_{q1} \\ V_{d2} \\ V_{q2} \\ \omega_r \end{bmatrix}
\quad (4.17)
$$

$$
\begin{bmatrix}
0 \\ 0 \\ 0 \\ 0 \\ 0 \\ V'_{dr} \\ V'_{qr} \\ 0 \\ 0 \\ 0 \\ 0 \\ T_m
\end{bmatrix}
=
\begin{bmatrix}
-r_1-p(L_{l1}+L_m) & \omega_e(L_{l1}+L_m) & -pL_m & \omega_e L_m & pL_m & -\omega_e L_m & -1 & 0 & 0 & 0 & 0 \\
-\omega_e(L_{l1}+L_m) & -r_1-p(L_{l1}+L_m) & -\omega_e L_m & -pL_m & \omega_e L_m & pL_m & 0 & -1 & 0 & 0 & 0 \\
-pL_m & \omega_e L_m & -r_2-p(L_{l2}+L_m) & -\omega_e(L_{l2}+L_m) & pL_m & -\omega_e L_m & 0 & 0 & -1 & 0 & 0 \\
-\omega_e L_m & -pL_m & -\omega_e(L_{l2}+L_m) & -r_2-p(L_{l2}+L_m) & \omega_e L_m & pL_m & 0 & 0 & 0 & -1 & 0 \\
-pL_m & (\omega_e-\omega_r)L_m & -pL_m & (\omega_e-\omega_r)L_m & r'_r+p(L'_{lr}+L_m) & -(\omega_e-\omega_r)(L'_{lr}+L_m) & 0 & 0 & 0 & 0 & -L_m(i_{q10}+i_{q20})+(L'_{lr}+L_m)i'_{qr0} \\
-(\omega_e-\omega_r)L_m & -pL_m & -(\omega_e-\omega_r)L_m & -pL_m & (\omega_e-\omega_r)(L'_{lr}+L_m) & r'_r+p(L'_{lr}+L_m) & 0 & 0 & 0 & 0 & L_m(i_{d10}+i_{d20})+(L'_{lr}+L_m)i'_{dr0} \\
-1/C_{p1} & 0 & 0 & 0 & 0 & 0 & (-p-1/R_1 C_{p1}) & \omega_e & 0 & 0 & 0 \\
0 & -1/C_{p1} & 0 & 0 & 0 & 0 & -\omega_e & (-p-1/R_1 C_{p1}) & 0 & 0 & 0 \\
0 & 0 & -1/C_{p2} & 0 & 0 & 0 & 0 & 0 & (-p-1/R_2 C_{p2}) & \omega_e & 0 \\
0 & 0 & 0 & -1/C_{p2} & 0 & 0 & 0 & 0 & -\omega_e & (-p-1/R_2 C_{p2}) & 0 \\
-k_2 L_m i'_{qr0} & k_1 L_m i'_{dr0} & -k_2 L_m i'_{qr0} & k_1 L_m i'_{dr0} & (L'_{lr}(i_{q10}+i_{q20})) & (-L'_{lr}(i_{d10}+i_{d20})) & 0 & 0 & 0 & 0 & p(2J/P)
\end{bmatrix}
\begin{bmatrix}
i_{d1} \\ i_{q1} \\ i_{d2} \\ i_{q2} \\ i'_{dr} \\ i'_{qr} \\ V_{d1} \\ V_{q1} \\ V_{d2} \\ V_{q2} \\ \omega_r
\end{bmatrix}
\quad (4.18)
$$

Where,

$$\kappa_1 = \left(\left(\frac{3P}{4}\right)\left(\frac{L_m}{L_m+L'_{lr}}\right)\right)$$

$$\kappa_2 = \left(\left(\frac{3P}{4}\right)\left(\frac{L_m}{L_m+L'_{lr}}\right)\right)$$

$$A = - \begin{bmatrix} -(L_{l1}+L_m) & 0 & -L_m & 0 & L_m & 0 & 0 & 0 & 0 & 0 & 0 \\ 0 & -(L_{l1}+L_m) & 0 & -L_m & 0 & L_m & 0 & 0 & 0 & 0 & 0 \\ -L_m & 0 & -(L_{l2}+L_m) & 0 & L_m & 0 & 0 & 0 & 0 & 0 & 0 \\ 0 & -L_m & 0 & -(L_{l2}+L_m) & 0 & L_m & 0 & 0 & 0 & 0 & 0 \\ -L_m & 0 & -L_m & 0 & (L'_{lr}+L_m) & 0 & 0 & 0 & 0 & 0 & 0 \\ 0 & -L_m & 0 & -L_m & 0 & (L'_{lr}+L_m) & 0 & 0 & 0 & 0 & 0 \\ 0 & 0 & 0 & 0 & 0 & 0 & 1 & 0 & 0 & 0 & 0 \\ 0 & 0 & 0 & 0 & 0 & 0 & 0 & 1 & 0 & 0 & 0 \\ 0 & 0 & 0 & 0 & 0 & 0 & 0 & 0 & 1 & 0 & 0 \\ 0 & 0 & 0 & 0 & 0 & 0 & 0 & 0 & 0 & 1 & 0 \\ 0 & 0 & 0 & 0 & 0 & 0 & 0 & 0 & 0 & 0 & (2J/P) \end{bmatrix} \quad (4.20)$$

$$B = \begin{bmatrix}
-r_1 & \omega_e(L_{l1}+L_m) & 0 & \omega_e L_m & 0 & -\omega_e L_m & -1 & 0 & 0 & 0 & 0 \\
-\omega_e(L_{l1}+L_m) & -r_1 & -\omega_e L_m & 0 & \omega_e L_m & 0 & 0 & -1 & 0 & 0 & 0 \\
0 & \omega_e L_m & -r_2 & -\omega_e(L_{l2}+L_m) & 0 & -\omega_e L_m & 0 & 0 & -1 & 0 & 0 \\
-\omega_e L_m & 0 & -\omega_e(L_{l2}+L_m) & -r_2 & \omega_e L_m & 0 & 0 & 0 & 0 & -1 & 0 \\
0 & (\omega_e-\omega_r)L_m & 0 & (\omega_e-\omega_r)L_m & r'_r & -(\omega_e-\omega_r)(L'_{lr}+L_m) & 0 & 0 & 0 & 0 & -L_m(i_{q10}+i_{q20})+(L'_{lr}+L_m)i'_{qr0} \\
-(\omega_e-\omega_r)L_m & 0 & -(\omega_e-\omega_r)L_m & 0 & (\omega_e-\omega_r)(L'_{lr}+L_m) & r'_r & 0 & 0 & 0 & 0 & L_m(i_{d10}+i_{d20})+(L'_{lr}+L_m)i'_{dr0} \\
-1/C_{p1} & 0 & 0 & 0 & 0 & 0 & -(1/R_1 C_{p1}) & \omega_e & 0 & 0 & 0 \\
0 & -1/C_{p1} & 0 & 0 & 0 & 0 & -\omega_e & -(1/R_1 C_{p1}) & 0 & 0 & 0 \\
0 & 0 & -1/C_{p2} & 0 & 0 & 0 & 0 & 0 & -(1/R_2 C_{p2}) & \omega_e & 0 \\
0 & 0 & 0 & -1/C_{p2} & 0 & 0 & 0 & 0 & -\omega_e & -(1/R_2 C_{p2}) & 0 \\
\left(-k_2 L_m i'_{qr0}\right) & \left(k_1 L_m i'_{dr0}\right) & \left(-k_2 L_m i'_{qr0}\right) & \left(k_1 L_m i'_{dr0}\right) & \left(L'_{lr}(i_{q10}+i_{q20})\right) & \left(-L'_{lr}(i_{d10}+i_{d20})\right) & 0 & 0 & 0 & 0 & 0
\end{bmatrix} \quad (4.21)$$

and subscript '0' denotes steady state values.

87

Table 4.1

Eigenvalue variations with small perturbation in stator resistance at load at rated speed

Stator resistance (Ω)	Stator Eigenvalue I	Stator Eigenvalue II	Rotor Eigenvalue	Capacitor Eigenvalue I	Capacitor Eigenvalue II	Real Eigenvalue
3.99	-16. 501 ± 1162.20i	-151.09 ± 902.07i	-41.098 ± 636.46i	-74.460 ± 323.34i	-141.788 -87.078	-1.8752+ 0.000i
4.04	-16.946 ± 1162.50i	-152.62 ± 901.49i	-41.126 ± 636.49i	-75.290 ± 322.97i	-141.961 -87.068	-1.8752 + 0.000i
4.12	-17.668± 1163.10i	-155.06 ± 900.56i	-41.173 ± 636.52i	-76.618 ± 322.38i	-142.239 -87.053	-1.8753 + 0.000i
4.20	-18.401 ± 1163.70i	-157.49± 899.63i	-41.221 ± 636.56i	-77.945 ± 321.79i	-142.519 -87.038	-1.8755 + 0.000i
4.24	-18.772 ± 1163.90i	-158.70 ± 899.16i	-41.246 ± 636.58i	-78.608 ± 321.49i	-142.661 -87.030	-1.8755+ 0.000i

$i_{q1} = i_{q2}$; $i_{d1} = i_{d2} = 1.5$ A

Table 4.2

Eigenvalue variations with small perturbation in stator leakage inductance at load at rated speed

Stator leakage inductance (mH)	Stator Eigenvalue I	Stator Eigenvalue II	Rotor Eigenvalue	Capacitor Eigenvalue I	Capacitor Eigenvalue II	Real Eigenvalue
20.9	-18.619 ± 1181.60i	-160.04 ± 911.62i	-41.629 ± 638.58i	-78.271 ± 326.04i	-141.533	-1.876+ 0.000i
					-87.121	
21.2	-18.202 ± 1173.50i	-157.87 ± 906.82i	-41.433± 637.70i	-77.561 ± 324.47i	-141.835	-1.876 + 0.000i
					-87.091	
21.6	-17.668± 1163.10i	-155.06 ± 900.56i	-41.173 ± 636.52i	-76.618 ± 322.38i	-142.239	-1.875 + 0.000i
					-87.053	
22.0	-17.159 ± 1152.90i	-152.37 ± 894.48i	-40.916 ± 635.36i	-75.680 ± 320.31i	-142.648	-1.875+ 0.000i
					-87.014	
22.3	-16.792 ± 1145.50i	-150.41 ± 890.03i	-40.725 ± 634.49i	-74.980 ± 318.77i	-142.957	-1.874+ 0.000i
					-86.985	

$i_{q1} = i_{q2}$; $i_{d1} = i_{d2} = 1.5$ A

Table 4.3

Eigenvalue variations with small perturbation in rotor resistance at load at rated speed

Rotor resistance (Ω)	Stator Eigenvalue I	Stator Eigenvalue II	Rotor Eigenvalue	Capacitor Eigenvalue I	Capacitor Eigenvalue II	Real Eigenvalue
8.52	-17.669 ± 1163.10i	-154.76 ± 900.55i	-39.978± 636.94i	-76. 868± 322.95i	-137.297 -84.251	-1.936 + 0.000i
8.61	-17.669 ± 1163.10i	-154.86 ± 900.56i	-40.377 ± 636.80i	-76.786± 322.76i	-138.942 -85.184	-1.915 + 0.000i
8.79	-17.668 ± 1163.10i	-155.06 ± 900.56i	-41.173 ± 636.52i	-76.618 ± 322.38i	-142.239 -87.053	-1.875 + 0.000i
8.97	-17.667 ± 1163.10i	-155.26± 900.57i	-41.967 ± 636.24i	-76.443 ± 322.01i	-145.549 -88.926	-1.837 + 0.000i
9.05	-17.667 ± 1163.10i	-155.35 ± 900.57i	-42.319± 636.11i	-76.364 ± 321.85i	-147.024 -89.759	-1.820 + 0.000i

$i_{q1} = i_{q2}$; $i_{d1} = i_{d2} = 1.5$ A

Table 4.4

Eigenvalue variations with small perturbation in rotor leakage inductance at load at rated speed

Rotor leakage inductance (mH)	Stator Eigenvalue I	Stator Eigenvalue II	Rotor Eigenvalue	Capacitor Eigenvalue I	Capacitor Eigenvalue II	Real Eigenvalue
42.00	-17.725 ± 1163.10i	-155.25 ± 901.93i	-42.726 ± 640.10i	-77.417 ± 321.75i	-145.829	-1.804 + 0.000i
					-88.249	
42.43	-17.706 ± 1163.10i	-155.19 ± 901.47i	-42.202 ± 638.90i	-77.151 ± 321.96 i	-144.621	-1.828 + 0.000i
					-87.849	
43.30	-17.668 ± 1163.10i	-155.06 ± 900.56i	-41.173 ± 636.52i	-76.618 ± 322.38i	-142.239	-1.875 + 0.000i
					-87.053	
44.17	-17.631 ± 1163.10i	-154.95 ± 899.68i	-40.182 ± 634.21i	-76.093 ± 322.79i	-139.938	-1.923 +0.000i
					-86.271	
45.03	-17.597± 1163.10i	-154.85 ± 898. 84i	-39.239 ± 631.98 i	-75.582 ± 323.17i	-137.738	-1.971+ 0.000i
					-85.512	

$i_{q1} = i_{q2}$; $i_{d1} = i_{d2} = 1.5$ A

SEIG, a computer program has been developed from the state Equation (4.26). The eleven state variables contribute to a set of eleven eigenvalues.

4.3.1.1 Effect of Machine Parameters

Variation of eigenvalues with machine parameters has also been determined. These parameters are stator resistance, rotor resistance, stator leakage inductance, rotor leakage As it is difficult to relate analytically the eigenvalues with machine parameters, so the eigenvalues have been obtained by the deviation in every machine parameters at definite interval and by varying only one parameter at a time and keeping remaining parameters constant. Generator eigenvalues are calculated for its operation at load at rated speed when both winding sets are connected to 38.5 μF per phase (verified experimentally) which can also be optimized by using another methods [3, 25].

First the eigenvalues have been calculated for different proposed machine parameters and small machine variables variation. Then the small parameter and variable variations have been related to calculated eigenvalues of the studied machine and the results are given in Tables 4.1 through 4.7 and also shown in Figures 4.2 nd 4.3 respectively. The pair of eigenvalues, which are less sensitive and less affected by the change in rotor parameters and inertia constant has been termed as *stator eigenvalue*. On the other hand, complex conjugate pairs of eigenvalues, which are more sensitive and more affected by the change in rotor parameters and inertia constant have been termed as *rotor eigenvalue*. In other words, all the stator eigenvalues are highly affected by the change in stator parameters i.e. stator resistance and stator inductance. Changes in stator parameters also slightly affect the rotor eigenvalues, capacitor eigenvalues and real part [28, 34]. The most prominent effect was found to be caused by small perturbation in magnetizing inductance 'L_m' of the machine.

- **Variations in Stator Parameters:**

    Tables 4.1 and 4.2 show the eigenvalues variation with small perturbation in stator parameters, i.e. stator resistance and stator leakage inductance. In Table 4.1 the complex pair of rotor eigenvalues has very slight deviations from its previous value, but complex pairs of capacitor eigenvalues I and II have very small changes in real and imaginary parts while real eigenvalue is not affected. Whereas, the stator eigenvalue I and II have a considerable variations in their real and complex conjugate parts. In Table 4.2 all the eigenvalues were found to be varied at more or less extent in the same pattern for the variations in stator leakage inductance, as depicted in Table 4.1

Table 4.5

Eigenvalue variations with small perturbation in inertia-constant at load at rated speed

Inertia-constant (kg/m^2)	Stator Eigenvalue I	Stator Eigenvalue II	Rotor Eigenvalue	Capacitor Eigenvalue I	Capacitor Eigenvalue II	Real Eigenvalue
0.0128	-17.668 ± 1163.10i	-155.06 ± 900.56i	-41.171± 636.53i	-76.619 ± 322.38i	-142.223 -87.011	-1.935 +0.000i
0.0129	-17.668 ± 1163.10i	-155.06 ± 900.56i	-41.172± 636.52i	-76.619 ± 322.38i	-142.227 -87.022	-1.919 +0.000i
0.0132	-17.668 ± 1163.10i	-155.06 ± 900.56i	-41.173 ± 636.52i	-76.618 ± 322.38i	-142.239 -87.053	-1.875+ 0.000i
0.0135	-17.668 ± 1163.10i	155.06 ± 900.56i	-41.174 ± 636.52i	-76.618 ± 322.39i	-142.252 -87.082	-1.833 +0.000i
0.0136	-17.668 ± 1163.10i	-155.06 ± 900.56i	-41.175 ± 636.52i	-76.618 ± 322.39i	-142.255 -87.092	-1.819 +0.000i

$i_{q1} = i_{q2}$; $i_{d1} = i_{d2} = 1.5$ A

Table 4.6

Eigenvalue variations with small perturbation in magnetizing inductance at load at rated speed

Magnetizing inductance (mH)	Stator Eigenvalue I	Stator Eigenvalue II	Rotor Eigenvalue	Capacitor Eigenvalue I	Capacitor Eigenvalue II	Real Eigenvalue
0.101	-18.088 ± 1163.20i	-155.34 ± 904.30i	-40.831 ± 638.21 i	-79.583 ± 338.66i	-135.453 / -88.036	-1.845 +0.000i
0.102	-17.946 ± 1163.20i	-155.25 ± 903.05i	-40.946 ± 637.64 i	-78.674 ± 333.31i	-137.553 / -87.703	-1.856 +0.000i
0.104	-17.668 ± 1163.10i	-155.06 ± 900.56i	-41.173 ± 636.52i	-76.618 ± 322.38i	-142.239 / -87.053	-1.875 + 0.000i
0.106	-17.396 ± 1163.00i	-154.87 ± 898.12i	-41.394 ± 635.44i	- 74.196 ± 311.16i	-147.675 / -86.423	-1.894 +0.000i
0.107	-17.263± 1162.90i	-154.76± 896.91i	-41.503 ± 634.92i	-72.827± 305.44i	-150.714 / -86.116	-1.902 +0.000i

$i_{q1} = i_{q2}$; $i_{d1} = i_{d2} = 1.5$ A

- **Variations in Rotor Parameters:**

Similarly, Tables 4.3 and 4.4 depict the variations in eigenvalues with small perturbation in rotor parameters, i.e. rotor resistance and rotor leakage inductance. Stator eigenvalues are less sensitive to rotor parameters as depicted in Tables 4.3 and 4.4 for small perturbations in rotor resistance and rotor leakage inductance. In both the Tables, capacitor eigenvalues I and II have a small but considerable change, whereas rotor eigenvalues have highly variation in their complex conjugate pairs along with little deviations in real eigenvalue of the machine.

- **Variations in Moment of Inertia:**

In the same way, Table 4.5 depicts the variations in eigenvalues with small perturbation in inertia constant. Only last and real eigenvalue has significant changes in their values and remaining eigenvalues are minutely affected.

- **Variations in Magnetizing Inductance:**

Table 4.6 depicts variations in eigenvalues with small perturbation in magnetizing inductance. With small changes in magnetizing inductances, almost all the eigenvalues are definitely affected either slightly or greatly. Table 4.6 depicts the variation in eigenvalues with small perturbations in magnetizing inductance. In Table 4.6, capacitor eigenvalues I and II are more affected by the change in magnetizing inductance 'L_m' along with very little effects on remaining eigenvalues. This pattern of effect has signified that the most critical parameter is small perturbation in magnetizing inductance 'L_m' in the dynamics of voltage build-up in SP-SEIG.

4.3.2 Transfer Functions of Linearized System

The linearized SP-SEIG model has been further utilized to determine the transfer function at a given specified operating point. The linearized equations relating the output (active power, P and reactive power, Q) to input (mechanical input torque, T_m) are convenient for the establishment of transfer function.

The instantaneous active and reactive power of SP-SEIG is given by the following relation:

$$P = Vq1iq1 + Vd1id1 + Vq2iq2 + Vd2id2 \ldots, \tag{4.28}$$

and,

$$Q = Vq1id1 - Vd1iq1 + Vq2id2 - Vd2iq2 \ldots, \tag{4.29}$$

respectively.

Table 4.7

Values of Zeros and Poles of transfer functions $\Delta P / \Delta Tm$, and $\Delta Q / \Delta Tm$

At full load				At half load			
$\Delta P / \Delta Tm$		$\Delta Q / \Delta Tm$		$\Delta P / \Delta Tm$		$\Delta Q / \Delta Tm$	
Zeros	Poles	Zeros	Poles	Zeros	Poles	Zeros	Poles
1.0e+016 * -(8.6984)	1.0e+003 * (-0.0177 + 1.1631i)	1.0e+017 * -(5.1299)	1.0e+003 * (-0.0177 + 1.1631i)	1.0e+016 * (7.5457)	1.0e+003 * (-0.0177 + 1.1631i)	1.0e+017 * (-6.3438)	1.0e+003 * (-0.0177 + 1.1631i)
1.0e+016 * (-0.0000)	1.0e+003 * (-0.0177 - 1.1631i)	1.0e+017 * (-0.0000 + 0.0000i)	1.0e+003 * (-0.0177 - 1.1631i)	1.0e+016 * -(0.0000 + 0.0000i)	1.0e+003 * (-0.0177 - 1.1631i)	1.0e+017 * -(0.0000 + 0.0000i)	1.0e+003 * (-0.0177 - 1.1631i)
1.0e+016 * (-0.0000)	1.0e+003 * (-0.1536 + 0.9003i)	1.0e+017 * (-0.0000 - 0.0000i)	1.0e+003 * (-0.1536 + 0.9003i)	1.0e+016 * -(0.0000 - 0.0000i)	1.0e+003 * (-0.1544 + 0.9004i)	1.0e+017 * -(0.0000 - 0.0000i)	1.0e+003 * (-0.1544 + 0.9004i)
1.0e+016 * (0.0000 + 0.0000i)	1.0e+003 * (-0.1536 - 0.9003i)	1.0e+017 * (-0.0000 + 0.0000i)	1.0e+003 * (-0.1536 - 0.9003i)	1.0e+016 * -(0.0000 + 0.0000i)	1.0e+003 * (-0.1544 - 0.9004i)	1.0e+017 * -(0.0000 + 0.0000i)	1.0e+003 * (-0.1544 - 0.9004i)
1.0e+016 * (0.0000 - 0.0000i)	1.0e+003 * (-0.0472 + 0.6346i)	1.0e+017 * (-0.0000 - 0.0000i)	1.0e+003 * (-0.0472 + 0.6346i)	1.0e+016 * -(0.0000 - 0.0000i)	1.0e+003 * (-0.0439 + 0.6358i)	1.0e+017 * -(0.0000 - 0.0000i)	1.0e+003 * (-0.0439 + 0.6358i)
1.0e+016 * (0.0000 + 0.0000i)	1.0e+003 * (-0.0472 - 0.6346i)	1.0e+017 * (0.0000 + 0.0000i)	1.0e+003 * (-0.0472 - 0.6346i)	1.0e+016 * -(0.0000 + 0.0000i)	1.0e+003 * (-0.0439 - 0.6358i)	1.0e+017 * (0.0000 + 0.0000i)	1.0e+003 * (-0.0439 - 0.6358i)
1.0e+016 * (0.0000 - 0.0000i)	1.0e+003 * (-0.0779 + 0.3250i)	1.0e+017 * (0.0000 - 0.0000i)	1.0e+003 * (-0.0779 + 0.3250i)	1.0e+016 * -(0.0000 - 0.0000i)	1.0e+003 * (-0.0769 + 0.3237i)	1.0e+017 * (0.0000 - 0.0000i)	1.0e+003 * (-0.0769 + 0.3237i)
1.0e+016 * (0.0000 + 0.0000i)	1.0e+003 * (-0.0779 - 0.3250i)	1.0e+017 * (-0.0000 + 0.0000i)	1.0e+003 * (-0.0779 - 0.3250i)	1.0e+016 * -(0.0000 + 0.0000i)	1.0e+003 * (-0.0769 - 0.3237i)	1.0e+017 * -(0.0000 + 0.0000i)	1.0e+003 * (-0.0769 - 0.3237i)
1.0e+016 * (0.0000 - 0.0000i)	1.0e+003 * (-0.1039 + 0.0463i)	1.0e+017 * (-0.0000 - 0.0000i)	1.0e+003 * (-0.1039 + 0.0463i)	1.0e+016 * -(0.0000 - 0.0000i)	1.0e+003 * -0.1258	1.0e+017 * -(0.0000 - 0.0000i)	1.0e+003 * -0.1258
1.0e+016 * -(0.0000)	1.0e+003 * (-0.1039 - 0.0463i)	1.0e+017 * (-0.0000)	1.0e+003 * (-0.1039 - 0.0463i)	1.0e+016 * -(0.0000)	1.0e+003 * -0.0981	1.0e+017 * -(0.0000)	1.0e+003 * -0.0981
K , gain = -1.9327e-12	1.0e+003 * (-0.0117)	**K , gain = -3.7517e-012**	1.0e+003 * (-0.0117)	**K , gain = 3.1832e-12**	1.0e+003 * -0.0026	**K , gain = -1.4779e-012**	1.0e+003 * -0.0026

The expression for developed electromagnetic torque, T_e is already given in Equation (4.15). The linearized active and reactive power equations are

$$\Delta P = Vq1\Delta iq1 + \Delta Vq1iq1 + Vd1\Delta id1 + \Delta Vd1id1 + Vq2\Delta iq2 + \Delta Vq2iq2 + Vd2\Delta id2 + \Delta Vd2id2 \qquad (4.30)$$

and,

$$\Delta Q = Vq1\Delta id1 + \Delta Vq1id1 - Vd1\Delta iq1 - \Delta Vd1iq1 + Vq2\Delta id2 + \Delta Vq2id2 - Vd2\Delta iq2 - \Delta Vd2iq2 \qquad (4.31)$$

respectively. Further, Equations (4.30) and (4.31) are rewritten in form of output equation y of linear dynamical system i.e.

$$\Delta P = Cx + Du \,, \qquad (4.32)$$

and,

$$\Delta Q = Mx + Nu \,, \qquad (4.33)$$

From Equations (4.32) and (4.33), matrices C, D, M, N, x and u can also be written as:

$$C = \begin{bmatrix} Vd1 & Vq1 & Vd2 & Vq2 & 0 & 0 & id1 & iq1 & id2 & iq2 & 0 \end{bmatrix},$$

$$D = \begin{bmatrix} 0 & 0 & 0 & 0 & 0 & 0 & 0 & 0 & 0 & 0 & 0 \end{bmatrix},$$

$$M = \begin{bmatrix} Vq1 & -Vd1 & Vq2 & -Vd2 & 0 & 0 & -iq1 & id1 & -iq2 & id2 & 0 \end{bmatrix},$$

$$N = \begin{bmatrix} 0 & 0 & 0 & 0 & 0 & 0 & 0 & 0 & 0 & 0 & 0 \end{bmatrix},$$

$$x = \begin{bmatrix} \Delta id1 & \Delta iq1 & \Delta id2 & \Delta iq2 & \Delta idr & \Delta iqr & \Delta Vd1 & \Delta Vq1 & \Delta Vd2 & \Delta Vq2 & \Delta\omega \end{bmatrix}$$

and

$$u = \begin{bmatrix} 0 & 0 & 0 & 0 & \Delta Vdr & \Delta Vqr & 0 & 0 & 0 & 0 & Tm \end{bmatrix}.$$

Root-locus of the both transfer functions ($\Delta P / \Delta Tm$ and $\Delta Q / \Delta Tm$) is shown in Figures 4.2 and 4.3, when both the winding sets of SP-SEIG are carrying full load current and half load current, respectively. The computational data of both transfer functions ($\Delta P / \Delta Tm$ and $\Delta Q / \Delta Tm$) are also given in Table 4.7 for two specified operating points. The contours shown in Figures 4.2 and 4.3 suggest that the studied SP-SEIG is stable, since all the poles are placed in the left half of s-plane i.e. the negative x-axis. As, for a linear system stability, all poles must have negative real parts i.e. all poles must lie inside the left-half of the s-plane.
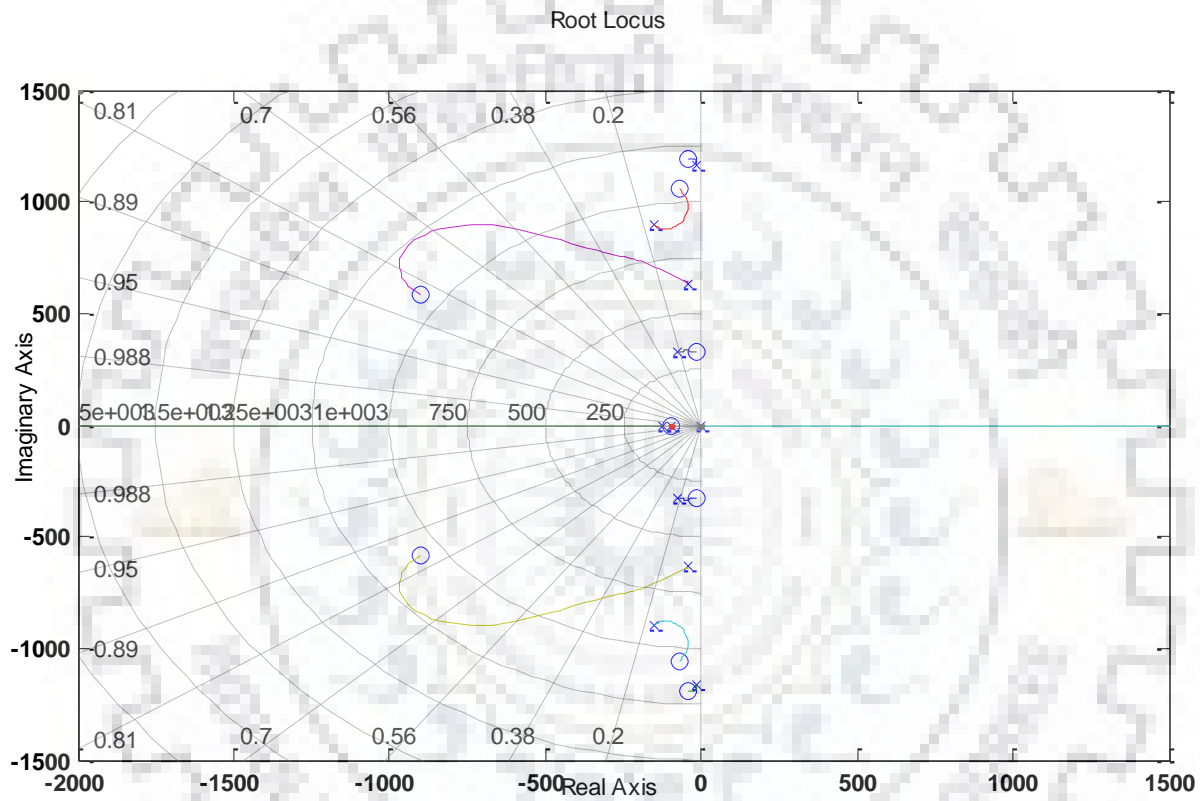
(a)
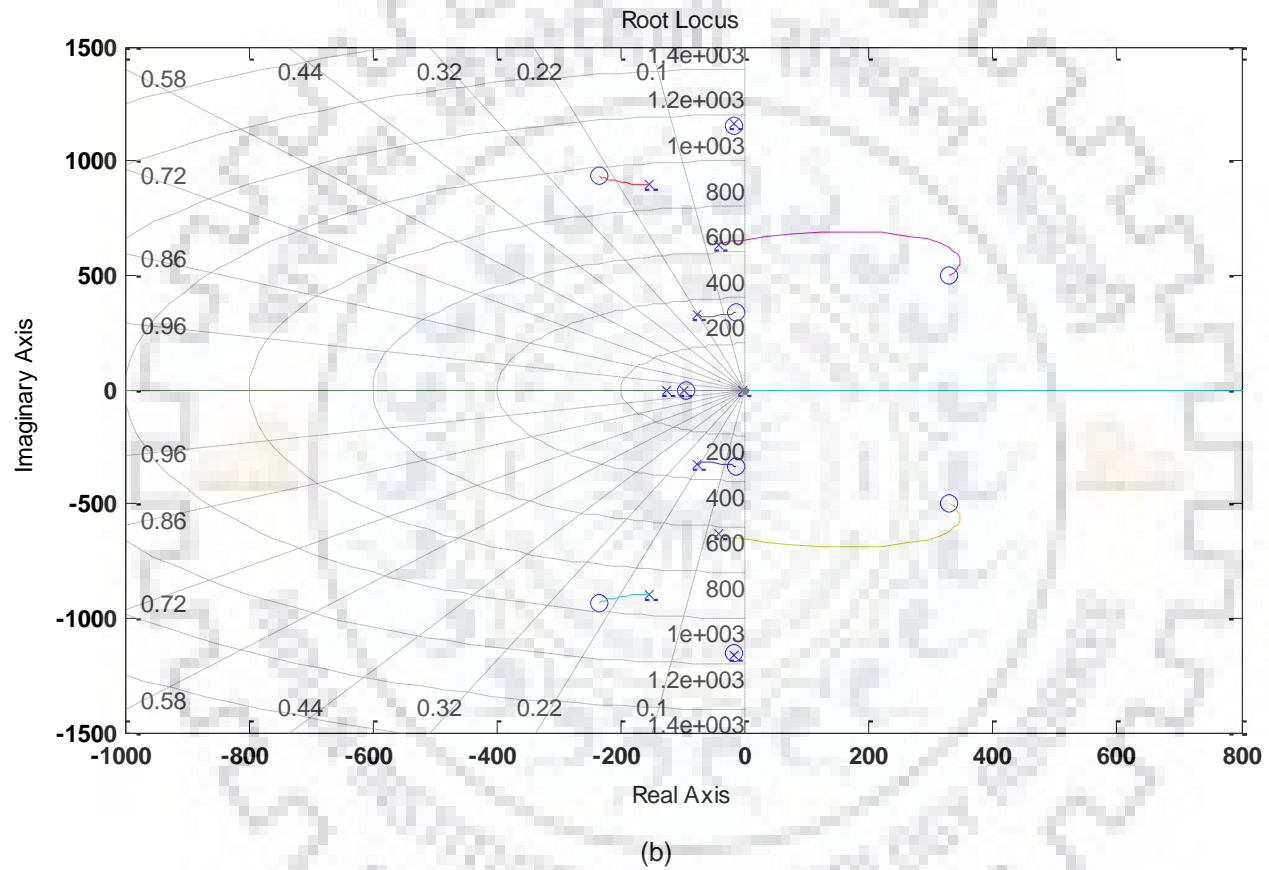
Figure 4.2. Root locus of $\Delta P / \Delta Tm$ (a); Root locus of $\Delta Q / \Delta Tm$ (b); when both the winding sets are carrying full load current.

(a)
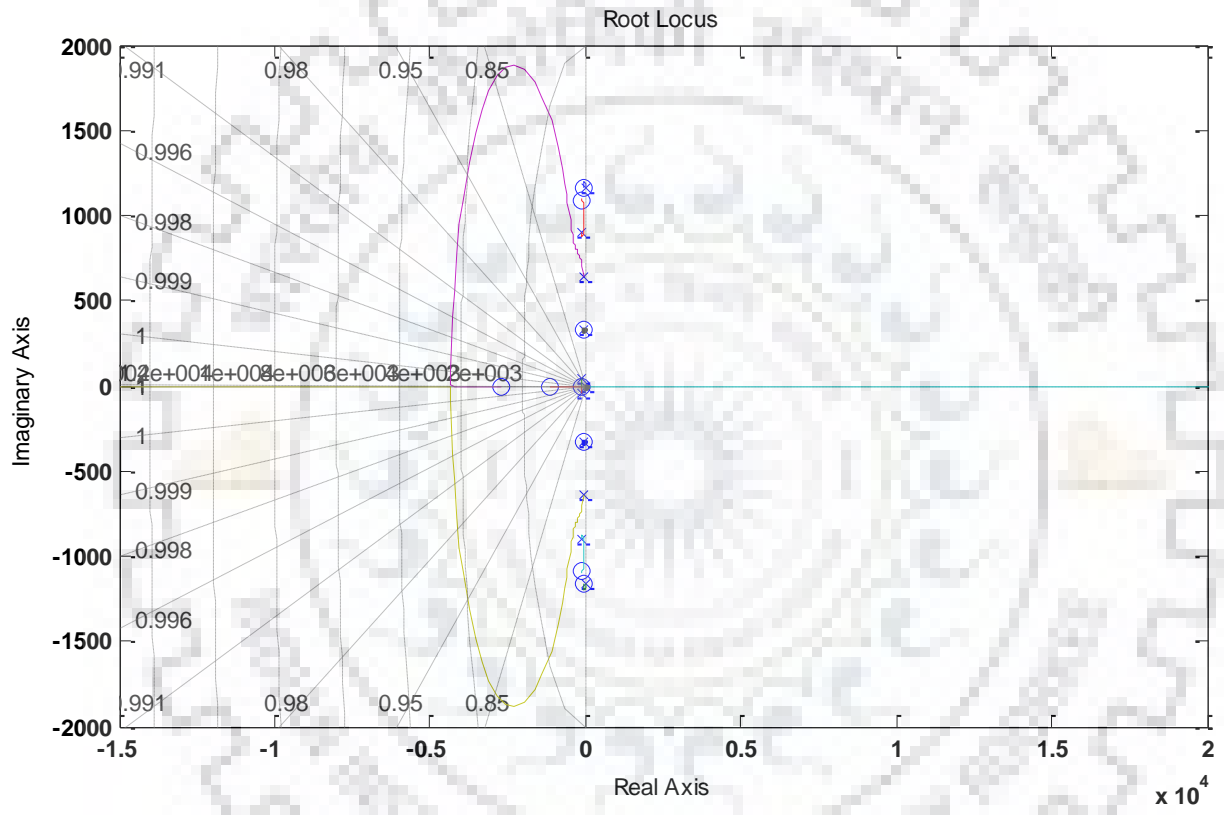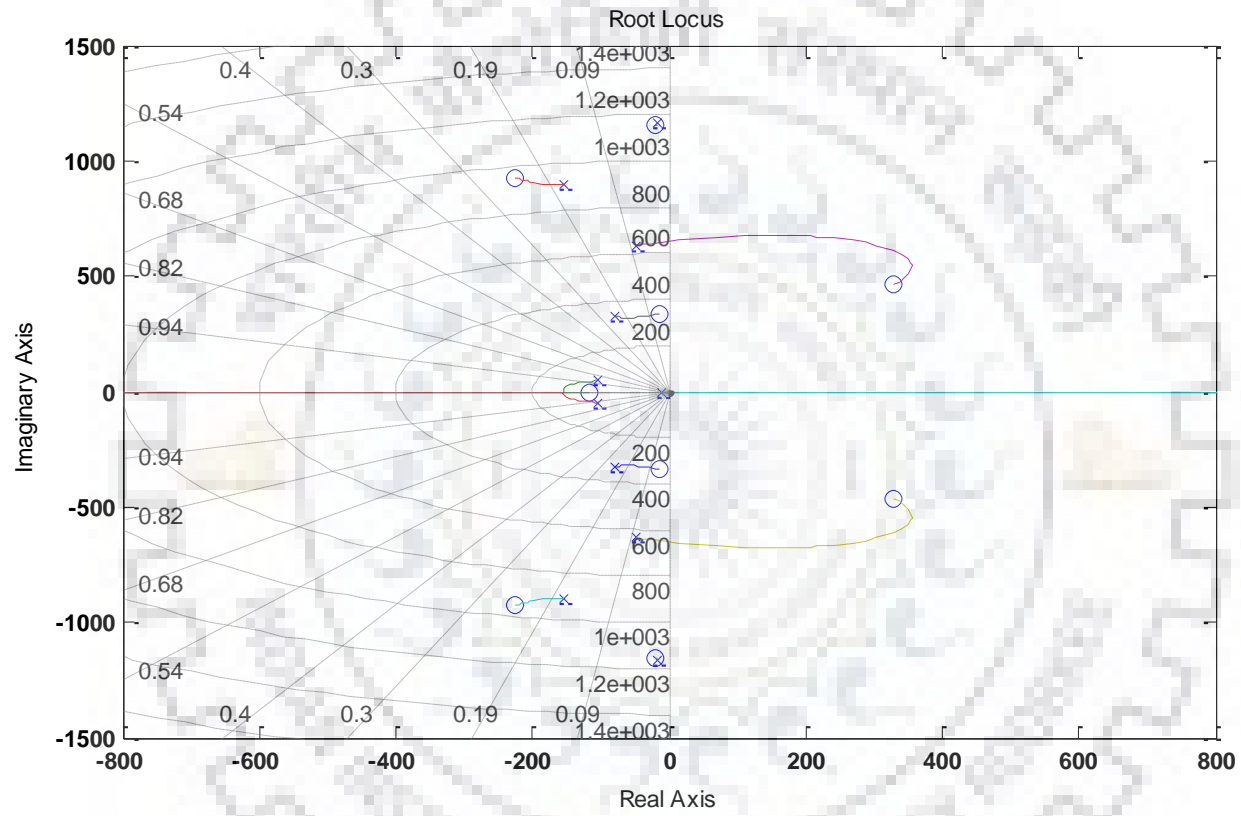
Root Locus

Figure 4.3 Root locus of $\Delta P / \Delta T_m$ (a); Root locus of $\Delta Q / \Delta T_m$ (b); when both the winding sets are carrying half load current.

101

4.4 Result and Discussion

To summarize the results investigated on SP-SEIG for eigenvalue analysis, a task of the discussion has been initiated from Table 4.1 through 4.6, which shows the eigenvalue variations with machine parameters. For more clarity in stability study of SP-SEIG, two transfer functions are derived. Contours of both the transfer functions using root-locus technique are shown in Figures 4.2 and 4.3, and the values of their gains, zeros and poles are also tabulated in Table 4.7. All contours have their poles (eigenvalues or characteristic or latent, roots) placements in negative left half of the s-plane and in this way, the graphical tool (Root- locus contour) is satisfying the basic condition of an absolute system stability. For investigating the stability analysis of SP-SEIG, the machine parameters of squirrel cage induction machine are given in Appendix A and used throughout the thesis work to validate the proposed analytical approach of this Chapter.

4.5 Concluding Remarks

Stability studies of SP-SEIG are developed by using a simple method based on eigenvalue analysis. A detailed investigation is carried out to adjudge the eigenvalues behaviour of the machine for small and definite deviations in machine parameters. From the analysis, it is evinced that all the eigenvalues are affected by the change in magnetizing inductance (L_m), and this shows that most critical parameter is a small perturbation in magnetizing inductance (L_m) in the dynamics of SP-SEIG. Location of eigenvalues (poles) in the left half of the s - plane also gives an opportunity to know about the SP-SEIG absolute stability using Root-locus graphical tool in the derivation of transfer functions having relation between single input variable and single output state variable. The nature of real components in complex, and real eigenvalues represents its location on the complex s - plane. As the real components in studied machine eigenvalues (poles or characteristic or latent, roots) are in left half of the s - plane, it would signify the absolute stability of SP-SEIG from the contours of Root-locus diagram.

This stability study of SP-SEIG demonstrates machine behaviour during small perturbation of machine parameters and variables. Todays general consciousness of finite and limited sources of energy on earth has created the favourable situation for the revival of induction generator. More recently, power electronics and micro-controller technology have also given a decisive boost to induction generators as an energy converter in conjunction with renewable energy sources. So, the stability analysis has been a major concern for electrical engineers in stand-alone or self-excited induction generators during small perturbation in the machine

system variables. Eigenvalue also plays an important role in the selection of minimum capacitance required for self-excitation and the condition at which excitation will be initiated and sustained.

This chapter explores the use of SP-SEIG as variable speed drive system to the research work. Foremost, it will start with some background on voltage and frequency regulation problems in machine systems. Then, the solutions to the problems will be discussed through which new V and F control strategy using a simple and moderate simulink model will be selected. Next, scope of work with author's contribution are explained.

5.1 Introduction

When an induction machine is directly connected to power supply, it runs only at its rated speed. On the other hand, many applications require variable speed in its operation. Efficiently, driving and controlling of induction machines are prime concerns in today's energy conscious world. In order to maintain the quality of power in distributed power generation associated with locally available renewable energy sources, it is necessary to maintain the simplicity, reliability and user-friendliness of a generating scheme. To meet the requirement of desired consumer power quality, it is also important to develop a suitable controller for 6Φ IG to avoid the two most important drawbacks which are associated with its isolated mode besides its benefits mentioned in [10]. Two main well known drawbacks that are associated with isolated induction generator i.e.

- Need of more reactive power support during faults
- Poor voltage and frequency regulation during variations in rotor speed, excitation capacitance and connected loads

There are mainly three schemes which are in use to control the voltage and frequency of induction machine in variable speed drives.

- Voltage and frequency (Volts and Hz) control
- Constant slip control
- Field oriented control

Basically, a V and F (Volts and Hz) is a simple and popular scheme of speed regulation in induction machine usually used in industries for several decades. This scheme preserves the constant magnitude of flux i.e. ratio of voltage to frequency during voltage and frequency regulation at varying speed and load, and disregarding any drop across stator resistance. There are various literatures in the past, which tells about improvement of voltage and frequency regulation of SEIG by using additional series capacitors in its short and long shunt configurations as explained in Chapter 2. Variety of solid-state controllers were also investigated for improving the voltage and frequency regulation. There is also a need for frequency regulation under varying prime mover speed, excitation capacitance and load characteristics. A considerable amount of work [27, 30 - 32] has been directed towards the design and analysis of voltage and frequency regulators for the 3Φ induction generator. Some more prior investigation on different types of controllers are
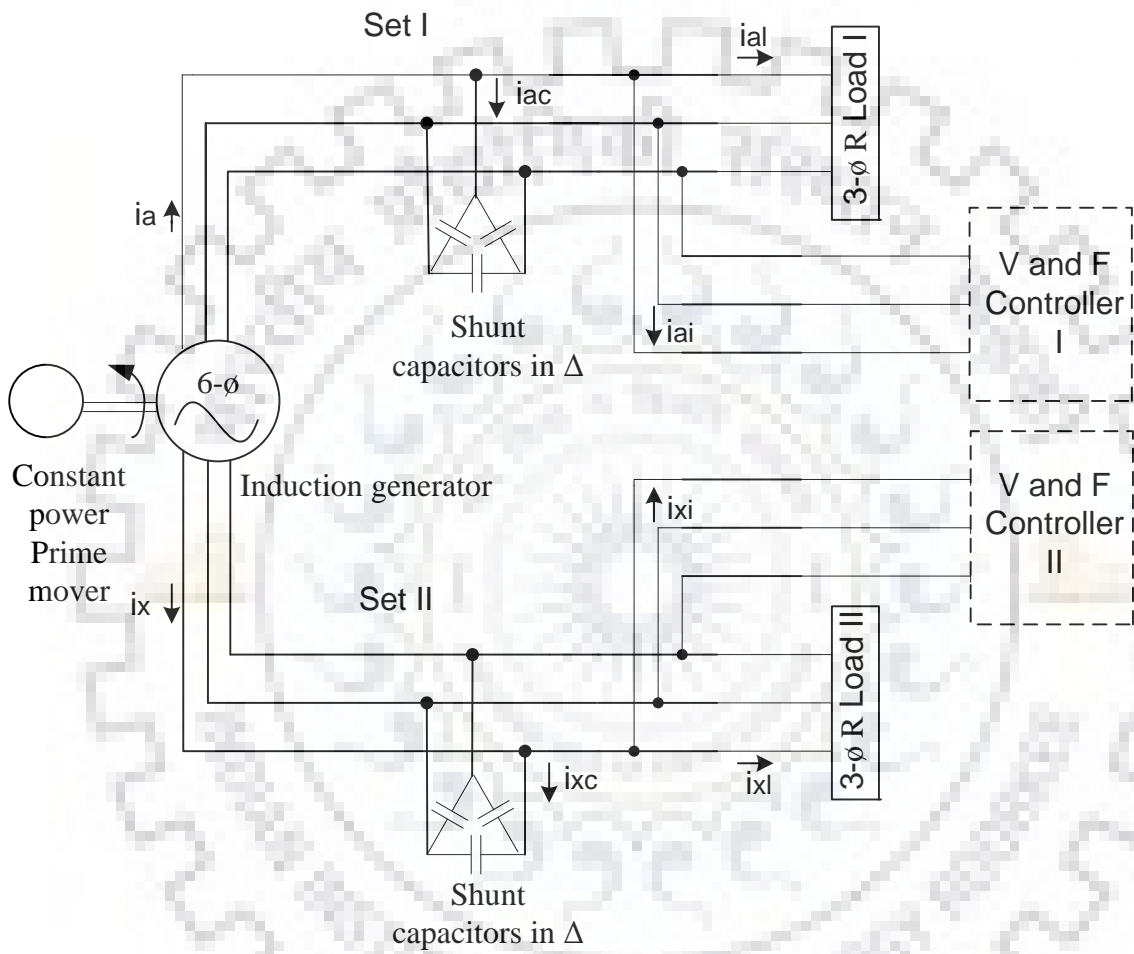
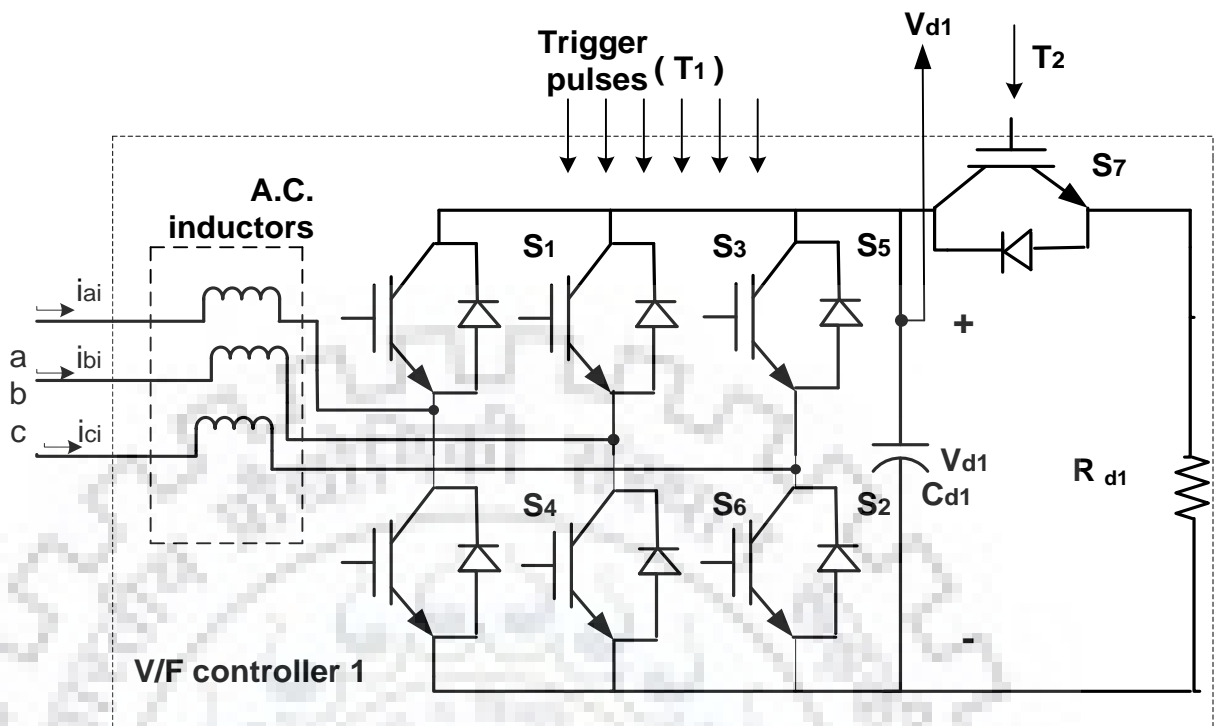Figure 5.1: Block Diagram of V and F controller cum SP-SEIG

Figure 5.2: Block Diagram of V and F controller on set I
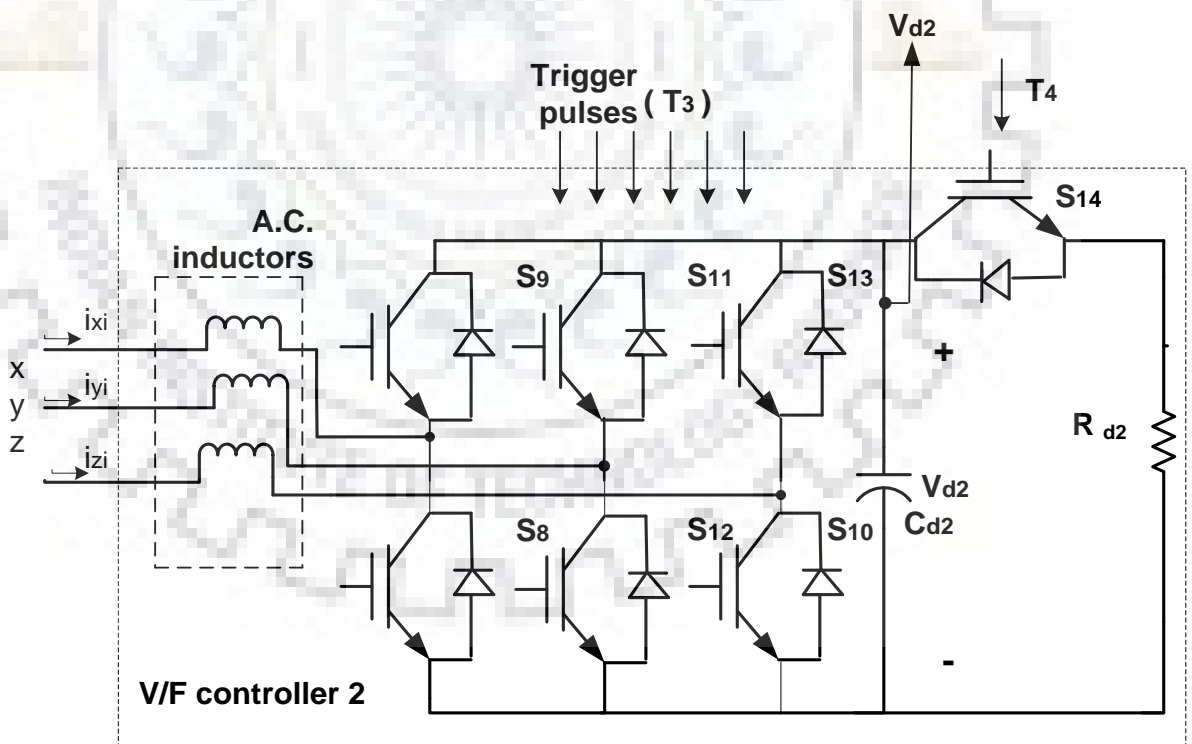
Figure 5.3: Block Diagram of V and F controller on set II

107
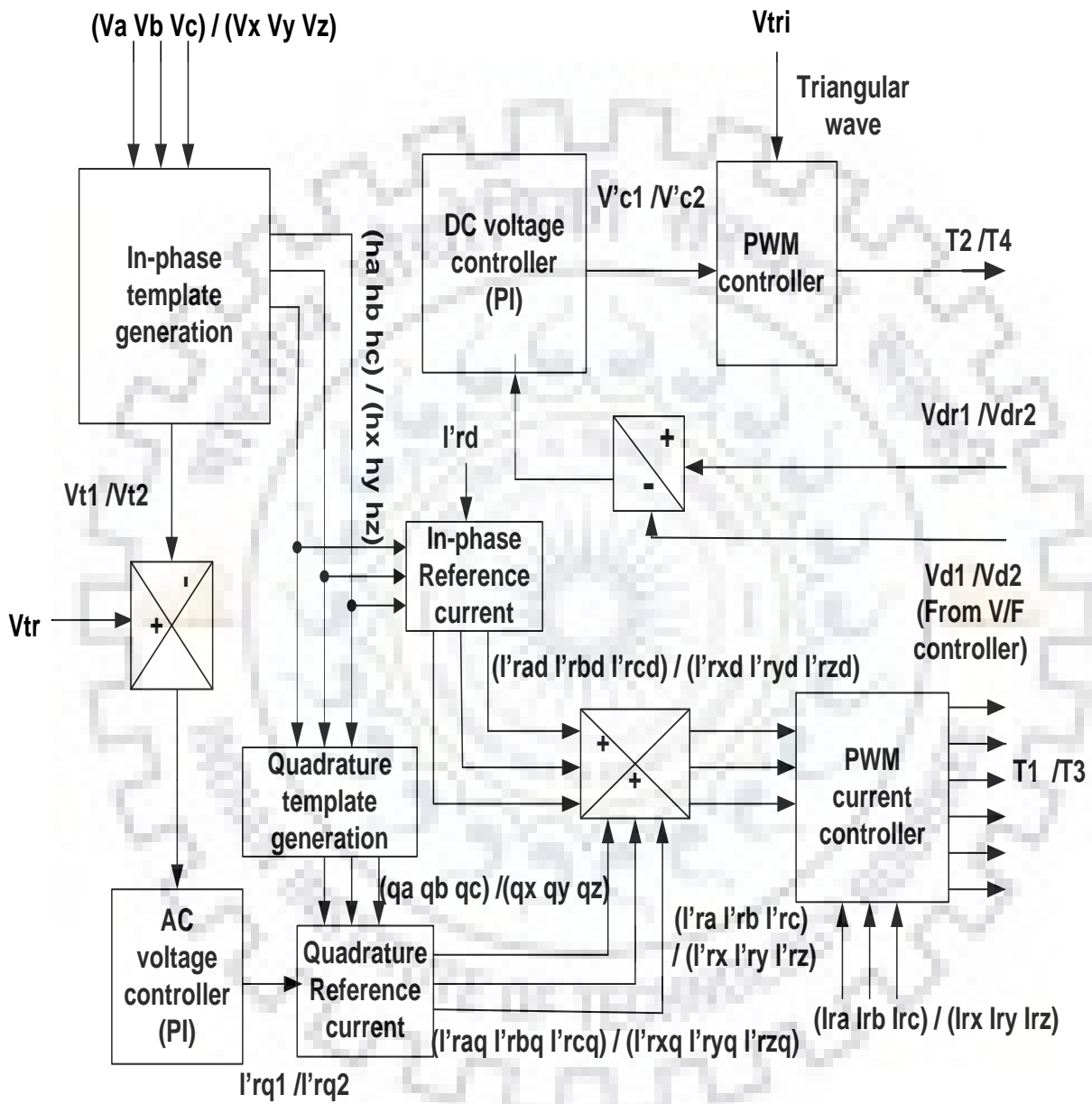
Figure 5.4: Combined Block Diagram of SP-SEIG - V and F controller scheme for set I and II

already mentioned in literature review of Chapter 1, but no such work is available on voltage and frequency (Volts and Hz) control of multiphase induction generator (SP-SEIGs) till now in available literatures on the basis of detailed review.

5.2 Planing for Problem Formulation

Block diagram of whole new control system is shown in Figure 5.1, which consist of SP-SEIG, two V and F controllers with their control schemes (for each winding sets) and connected equal resistive loads across the both 3Φ sets. The detailed of each V and F controller block is illustrated, independently, in Figures 5.2 and 5.3, which are combination of solid-state IGBT switch based CC-VSI, AC filter inductors which act as a bridge between the outputs of inverters and SEIG terminals, DC bus capacitor and chopper, respectively, for filtering voltage ripples and controlling dump powers. Identical control schemes of both V and F controllers for each 3Φ sets is also shown, jointly, in Figure 5.4, for the purpose of voltage regulation, elimination of system harmonics and load balancing. The philosophy of control scheme is based on the mechanism of source current control by virtue of A.C. voltage components i.e. in-phase and quadrature. There are two PI controllers and two PWM generators in each of the control schemes. One PI controller is for A.C. terminal voltage regulation and another is for D.C. bus voltage regulation in each set I, and II. Similarly, first PWM generator produces gating pulses T1, T2 and second generates T3, T4 in each control scheme across set I and II, respectively [32].

5.3 Description for Modelling of V and F controller-SP-SEIG System

Mathematical modelling of whole system is demonstrated for simulation purpose below and mainly divided in to two sub-sections:

5.3.1 Modelling of V and F Control Scheme

Proposed Volts and Hz control scheme is considered in closed loop manner in Figure 5.4. The aim of control strategies are, to regulate A.C. and D.C. bus voltages and to generate triggering pulses at gates of IGBT switches in VSI and DC chopper for both 3Φ sets as shown in Figures 5.2 and 5.3. Reference source currents can be generated by instantaneous values of its in-phase and quadrature components as:

$$i'ra = i'rad + i'raq \; ;$$
$$i'rb = i'rbd + i'rbq \; ;$$
$$i'rc = i'rcd + i'rcq \; ; \qquad\qquad (5.1)$$
$$i'rx = i'rxd + i'rxq \; ;$$
$$i'ry = i'ryd + i'ryq \; ;$$

$$i'rz = i'rzd + i'rzq \; ;$$

Where, i´ra, i´rb, i´rc, i´rx, i´ry and i´rz are reference source currents through each of the 3Φ winding sets and i´rad, i´rbd, i´rcd, i´rxd, i´ryd and i´rzd are instantaneous values of their in-phase components. Similarly, i´raq, i´rbq, i´rcq, i´rxq, i´ryq and i´rzq are instantaneous values of their quadrature components. The magnitude of in-phase reference source current 'i´rd' is constant and equal to rated value of active power component of machine current for maintaining uniform power generation. In-phase reference source current 'i'rd' is calculated in Section 5.5.1.1. and instantaneous values of in-phase reference source current can be written as:

$$i'rad = ha \times i'rd \; ;$$
$$i'rbd = hb \times i'rd \; ;$$
$$i'rcd = hc \times i'rd \; ;$$
$$i'rxd = hx \times i'rd \; ;$$
$$i'ryd = hy \times i'rd \; ;$$
$$i'rzd = hz \times i'rd \; ;$$

(5.2)

Where, ha, hb, hc, hx, hy, and hz are in-phase unit templates and given below:

$$h_a = V_a / V_{t1} \; ;$$
$$h_b = V_b / V_{t1} \; ;$$
$$h_c = V_c / V_{t1} \; ;$$
$$h_x = V_x / V_{t2} \; ;$$
$$h_y = V_y / V_{t2} \; ;$$
$$h_z = V_z / V_{t2} \; ;$$

(5.3)

$$V_{t1} = \mathrm{sqrt}\left\{(2/3) \times \left(v_a^2 + v_b^2 + v_c^2\right)\right\} \; ;$$

(5.4)

$$V_{t2} = \mathrm{sqrt}\left\{(2/3) \times \left(v_x^2 + v_y^2 + v_z^2\right)\right\} \; ;$$

(5.5)

The magnitude of quadrature reference source current 'i´rq' is the output of A.C. terminal voltage PI controller for maintaining constant terminal voltage and it is equal to the final simplified values of following derived equations. The output of A.C. voltage PI controller :

$$i'_{rq1(i)} = i'_{rq1(i-1)} + K_{pa1}\left\{V_{er1(i)} - V_{er1(i-1)}\right\} + K_{ia1}V_{er1(i)};$$

(5.6)

$$i'_{rq2(i)} = i'_{rq2(i-1)} + K_{pa2}\left\{V_{er2(i)} - V_{er2(i-1)}\right\} + K_{ia2}V_{er2(i)};$$

(5.7)

Where, $V_{er1\,(i)} = V_{tref(i)} - V_{t1(i)}$; and $V_{er2\,(i)} = V_{tref(i)} - V_{t2(i)}$;

$V_{tref(i)}$ is reference AC terminal voltage and $V_{t1(i)}$ and $V_{t2(i)}$ are realized magnitude of 3Φ AC terminal voltage at ith instant of time. $V_{t1(i)}$ and $V_{t2(i)}$ can be given by the Equations 5.4 and 5.5, Kpa1 and Kpi1 are proportional and integral gain constants for set I, and Kpa2 and Kia2 are proportional and integral gain constants for set II of the (AC terminal voltage) 'PI' controllers. Similarly i'rq1(i) and i'rq2(i) are ith instant compared AC voltage controller outputs, and i'rq1(i-1) and i'rq2(i-1) are (i-1)th instant compared AC voltage controller outputs in set I and II, respectively. In same pattern, $V_{er1(i)}$ and $V_{er2(i)}$ are ith instant AC terminal voltage error on set I and II, respectively, and $V_{er1(i-1)}$ and $V_{er2(i-1)}$ are (i-1)th instant AC terminal voltage error on set I and set II, respectively.

For instantaneous value of quadrature reference source current, following formulation can be written as:

$$
\begin{aligned}
i'raq &= qa \times i'rq1 \; ; \\
i'rbq &= qb \times i'rq1 \; ; \\
i'rcq &= qc \times i'rq1 \; ; \\
i'rxq &= qx \times i'rq2 \; ; \\
i'ryq &= qy \times i'rq2 \; ; \\
i'rzq &= qz \times i'rq2 \; ;
\end{aligned}
\tag{5.8}
$$

Where, qa, qb, qc, qx, qy, and qz are quadrature unit templates and given below:

$$
\begin{aligned}
q_a &= \left\{ (h_c - h_b) \, / \, \sqrt{3} \right\}; \\
q_b &= \left\{ \left((h_b - h_c) \, / \, \left(\sqrt[2]{3} \right) \right) + \sqrt{3} h_a / 2 \right\}; \\
q_c &= \left\{ \left((h_b - h_c) \, / \, \left(\sqrt[2]{3} \right) \right) - \sqrt{3} h_a / 2 \right\}; \\
q_x &= \left\{ (h_z - h_y) \, / \, \sqrt{3} \right\}; \\
q_y &= \left\{ \left((h_y - h_z) \, / \, \left(\sqrt[2]{3} \right) \right) + \sqrt{3} h_x / 2 \right\}; \\
q_z &= \left\{ \left((h_y - h_z) \, / \, \left(\sqrt[2]{3} \right) \right) - \sqrt{3} h_x / 2 \right\};
\end{aligned}
\tag{5.9}
$$

$$\dot{i'}_{rae} = \dot{i'}_{ra} - \dot{i}_{ra};$$
$$\dot{i'}_{rbe} = \dot{i'}_{rb} - \dot{i}_{rb};$$
$$\dot{i'}_{rce} = \dot{i'}_{rc} - \dot{i}_{rc};$$
$$\dot{i'}_{rxe} = \dot{i'}_{rx} - \dot{i}_{rx};$$
$$\dot{i'}_{rye} = \dot{i'}_{ry} - \dot{i}_{ry}; \qquad (5.10)$$
$$\dot{i'}_{rze} = \dot{i'}_{rz} - \dot{i}_{rz};$$

While, ira, irb, irc, irx, iry and irz are source currents in PWM current controllers of both 3Φ sets. Comparision generates error signals which are used for the triggering purpose at the gates of IGBTs (S1-S14) in both the VSI bridges of 3Φ sets and are written in Equation (5.10).

5.3.2 Modelling of V and F Controller

Each V and F controller (similar in logic and operation) across the corresponding set is shown in Figures 5.2 and 5.3. The basic building blocks of V and F controllers are CC-VSI, series connected dump load and DC bus chopper, and their triggering pulses (T1-T4) from PWM current controllers of control schemes. Modelling of CC-VSI followed by DC bus chopper is presented for better understanding of controllers operations during simulation.

5.3.2.1 Model of CC-VSI

There are mainly three sections for modelling purpose as mentioned below:

DC bus voltages:

$$\rho V_{d1} = \{ SW_1 \times i_{ai} + SW_2 \times i_{bi} + SW_3 \times i_{ci} + ((SW_7 \times V_{dc})/R_{d1}) \}/C_{d1}; \qquad (5.11)$$

$$\rho V_{d2} = \{ SW_4 \times i_{xi} + SW_5 \times i_{yi} + SW_6 \times i_{zi} + ((SW_8 \times V_{dc})/R_{d2}) \}/C_{d2};$$

Where, SW1-SW8 are switching functions across IGBTs switches and DC chopper switches for both 3Φ sets in VSI bridges. p is derivative term and remaining symbols (Rd1; Rd2 and Cd1; Cd2) are dump loads and DC bus capacitors, respectively, and their values are calculated in Section 5.5.1.1. Vd1 and Vd2 are reference dc bus voltages.

3Φ AC line voltages:

$$e_{ai} = (V_{d1}/3) \times (2 \times SW_1 - SW_2 - SW_3);$$

$$e_{bi} = (V_{d1}/3) \times (2 \times SW_2 - SW_1 - SW_3);$$

$$e_{ci} = (V_{d1}/3) \times (2 \times SW_3 - SW_1 - SW_2);$$

$$e_{xi} = (V_{d2}/3) \times (2 \times SW_4 - SW_5 - SW_6); \qquad (5.12)$$

$$e_{yi} = (V_{d2}/3) \times (2 \times SW_5 - SW_4 - SW_6);$$

$$e_{zi} = (V_{d2}/3) \times (2 \times SW_6 - SW_4 - SW_5);$$

Where, e_{ai}, e_{bi}, e_{ci}, e_{xi}, e_{yi} and e_{zi} are instantaneous generated inverter AC phase voltages from the output of VSI. Equation (5.12) of CC-VSI can be rearranged after applying kirchoff laws and are used below in Equation (5.13) in the calculation of A.C. inverter currents.

3Φ AC inverter currents:

$$\rho i_{ai} = \left(V_a - e_{ai} - i_{ai} \times R_f\right)/L_f;$$

$$\rho i_{bi} = \left(V_b - e_{bi} - i_{bi} \times R_f\right)/L_f;$$

$$\rho i_{ci} = \left(V_c - e_{ci} - i_{ci} \times R_f\right)/L_f;$$

$$\rho i_{xi} = \left(V_x - e_{xi} - i_{xi} \times R_f\right)/L_f; \qquad (5.13)$$

$$\rho i_{yi} = \left(V_y - e_{yi} - i_{yi} \times R_f\right)/L_f;$$

$$\rho i_{zi} = \left(V_z - e_{zi} - i_{zi} \times R_f\right)/L_f;$$

Where, i_{ai}, i_{bi}, i_{ci}, i_{xi}, i_{yi} and i_{zi} are inverter output controlled current. R_f and L_f are ouput a.c. filter resistance and inductance.

5.3.2.2 Model of DC Chopper

The magnitudes of outputs namely V'_{C1} and V'_{C2} from corresponding D.C. bus voltage PI controllers for maintaining constant D.C. bus voltages from both CC-VSI at i^{th} instant is equal to the simplified values of following derived equations.

Output of D.C. bus PI controller :

$$V'_{c1(i)} = V'_{c1(i-1)} + K_{pd1}\left\{V_{de1(i)} - V_{de1(i-1)}\right\} + K_{id1}V_{de1(i)};$$

$$(5.14)$$

$$V'_{c2(i)} = V'_{c2(i-1)} + K_{pd2}\left\{V_{de2(i)} - V_{de2(i-1)}\right\} + K_{id2}V_{de2(i)};$$

Where, K_{pd1} and K_{id1} are proportional and integral gain constants of DC bus voltage PI controller for set I, and, K_{pd2} and K_{id2} are proportional and integral gain constants of DC bus voltage PI controller for set II. $V'_{c1\,(i)}$ and $V'_{c2\,(i)}$ are i^{th} instant compared output of PI controllers, and $V'_{c1\,(i-1)}$ and $V'_{c2\,(i-1)}$ are $(i-1)^{th}$ instant compared output of PI controllers. Similarly, $V_{de1(i)}$ and $V_{de2(i)}$ are i^{th} instant DC bus voltage error on set I and set II, respectively, and $V_{de1(i-1)}$ and $V_{de2(i-1)}$ are $(i-1)^{th}$ instant DC bus voltage error on set I and set II, respectively. DC bus voltage errors are comparative difference between reference and realized DC bus voltages and can be written by following Equation (5.15).

$$V_{de1\,(i)} = V_{dr(i)} - V_{d1(i)}; \text{ and } V_{de2\,(i)} = V_{dr(i)} - V_{d2(i)}; \qquad (5.15)$$

$V_{dr(i)}$ is reference DC bus voltage. Whereas, $V_{d1(i)}$ and $V_{d2(i)}$ are realized magnitudes of DC bus voltages at i^{th} instant of time. $V_{d1(i)}$ and $V_{d2(i)}$ can be given by the previous Equation (5.11). The difference between compared outputs ($V'_{c1(i)}$ or $V'_{c2(i)}$) and carrier wave (V_{tri}, triangular in nature) in PWM controllers are responsible for generation of gating pulses in determination of triggering patterns at DC chopper switches using switching functions SD1 and SD2 in both VSI of set I and II. When (SD1 or SD2) is high 'value is 1'indicates ($V'_{c1 (i)}$ or $V'_{c2 (i)}$) > V_{tri}) and vice versa.

5.3.3 Modelling of Loaded SP-SEIG

Modelling of SP-SEIG is already demonstrated in Chapter 3 and Reference [4] for analysis and study purpose. Generator is resistively loaded in simple-shunt scheme across both sets. Only one modification took placed during simplification of the controller model for analysis purpose. This is a delta to star conversion at the common coupling points where delta excitation capacitor banks are connected across both 3Φ sets and it is further converted in to star excitation capacitor banks for the simplification in the modelling of controllers. When delta to star conversion took placed at common coupling points of capacitor banks across both 3Φ sets, it transformed like that:

$$\rho V_a = \{(i_a - i_{ai} - i_{al}) - (i_b - i_{bi} - i_{bl})\}/(3 \times C_{p1});$$

$$\rho V_b = \{(i_a - i_{ai} - i_{al}) + 2 \times (i_b - i_{bi} - i_{bl})\}/(3 \times C_{p1});$$

$$V_a + V_b + V_c = 0; \tag{5.16}$$

$$\rho V_x = \{(i_x - i_{xi} - i_{xl}) - (i_y - i_{yi} - i_{yl})\}/(3 \times C_{p2});$$

$$\rho V_y = \{(i_x - i_{xi} - i_{xl}) + 2 \times (i_y - i_{yi} - i_{yl})\}/(3 \times C_{p2});$$

$$V_x + V_y + V_z = 0;$$

and,

$$i_a = (i_{ac} + i_{ai} + i_{al}) ;$$

$$i_b = (i_{bc} + i_{bi} + i_{bl}) ;$$

$$i_c = (i_{cc} + i_{ci} + i_{cl}) ;$$

$$i_x = (i_{xc} + i_{xi} + i_{xl}) ;$$

$$i_y = (i_{yc} + i_{yi} + i_{yl}) ;$$

$$i_z = (i_{zc} + i_{zi} + i_{zl}) ;$$

Where i_{al}, i_{bl}, i_{cl} are 3Φ load currents through set I and i_{xl}, i_{yl}, i_{zl} are 3Φ load currents through set II. Where as, i_a, i_b, i_c are 3Φ line currents through set I and i_x, i_y, i_z are 3Φ line currents through set II. C_{p1} and C_{p2} are no load per phase excitation capacitances which are connected in

parallel across both 3Φ sets I and II. Similarly, i_{ac}, i_{bc}, i_{cc}, i_{xc}, i_{yc} and i_{zc} are capacitor currents through set I and set II. Remaining symbols denote their earlier meanings.

5.4 Design of V and F controller-SP-SEIG using Simulink Model

The Simulink model of SP-SEIG alongwith its V and F controllers is constructed using Simulink Matlab software according to logics of given Figures 5.2 through 5.4.

5.5 Results and Discussion

Whole Simulink model has been computed and results are shown in Figure 5.5, when SP-SEIG is feeding symmetrical resistive load at t=1 sec. Similar response of both sets under symmetrical resistive loads are shown in Figure 5.5. Only one phase of single set response is display out in Figure 5.5. Transients response of 3Φ line voltages (V_a, V_b, V_c /V_x, V_y, V_z), 3Φ line currents (i_a, i_b, i_c / i_x, i_y, i_z), 3Φ load currents (i_{al}, i_{bl}, i_{cl} / i_{xl}, i_{yl}, i_{zl}), 3Φ CC-VSI currents (i_{ai}, i_{bi}, i_{ci} / i_{xi}, i_{yi}, i_{zi}), Magnitude of SP-SEIG terminal voltage along with A.C. reference voltage (V_{t1} /V_{t2}, V_{tr}), Magnitude of SP-SEIG DC bus voltage along with D.C. reference voltage (V_{d1} /V_{d2}, V_{dr}) and generator rotor shaft speed (N_r) are in similar pattern along both 3Φ sets. As generator is loaded with a symmetrical resistive load across both sets at 1 sec, power transformation has started from both controller units towards connected loads across both sets. Result of this, controller current decreases and load current increases. As generator speed (Nr) is also remain constant with applying load, it gives indication of a constant V and F during whole operation of machine in simulation. In this way, controller acts like voltage and frequency regulator and also sometimes can be used as load stabilizer.

5.5.1 Appropriate Values of Different Parameters

5.5.1.1 Controller Parameters

DC bus voltages of CC-VSI inverters: The DC bus voltages ' V_{d1} and V_{d2} ' are instantaneous values and can be defined as:

$$V_{d1} = V_{d2} = \sqrt{\frac{2}{3}} \times \left(\frac{2 \times V_{rated}}{m_i} \right);$$

Where, V_{rated} = rated AC line voltage (415).

m_i = modulation index = 1;

Then, V_{d1} = V_{d2} = 677.69 volt, but after safety consideration V_{d1} = V_{d2} = 750 volt;
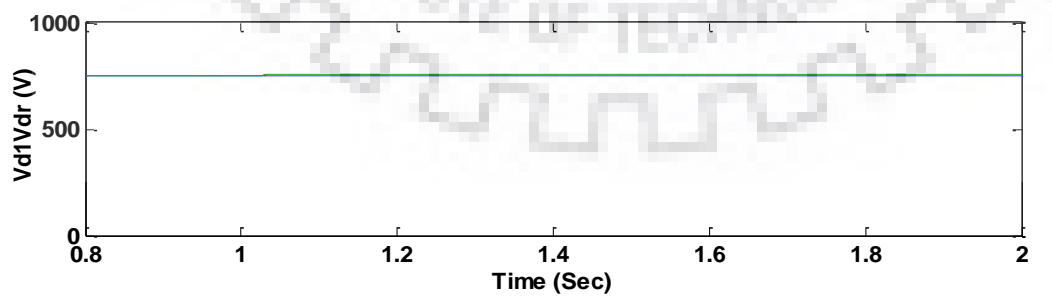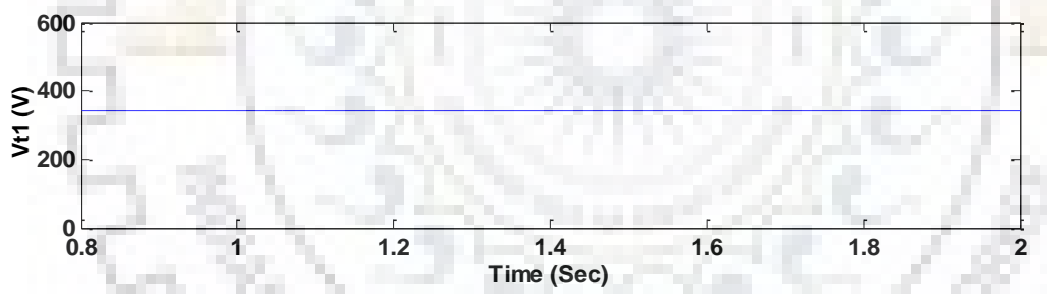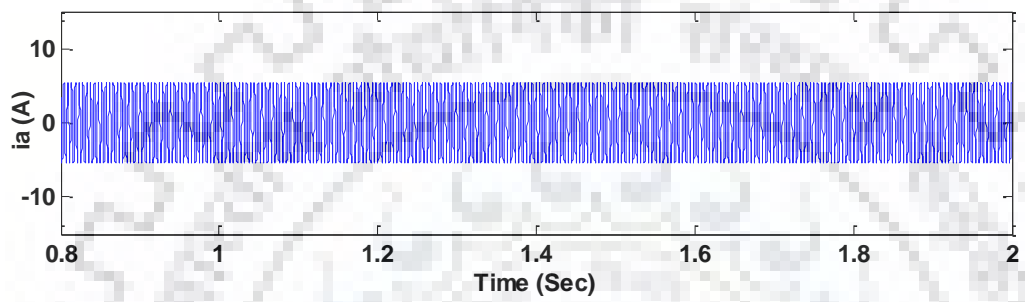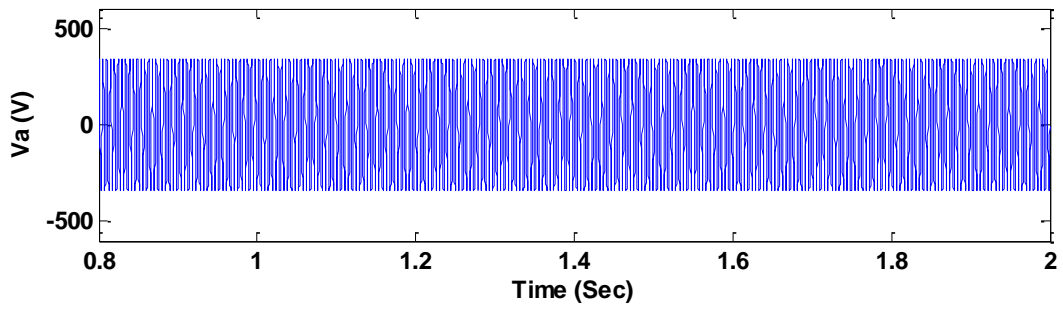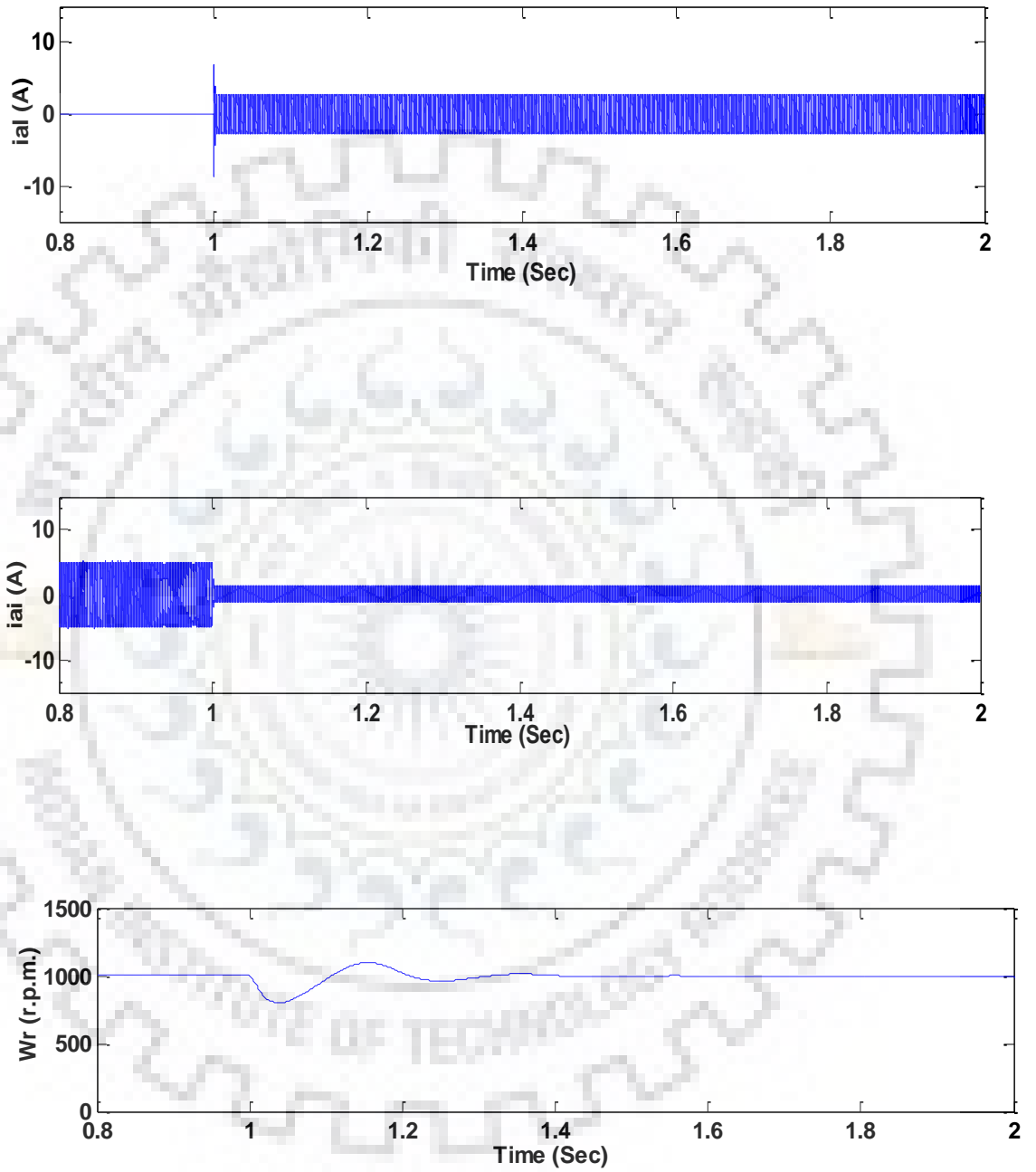
Figure 5.5: Similar transient response of 6Φ SEIG controller under symmetrical resistive loads across both 3Φ sets.

117

DC bus capacitors of CC-VSI inverters: The choice of DC bus capacitances ' C_{d1} and C_{d2} ' are depends upon values of voltage drops in DC bus voltages ' V_{d1} and V_{d2} ' during application and removal of loads across both 3Φ winding sets.

By energy conservation principle,

$$\frac{1}{2} \times C_{d2} \times \left\{ V_{d2}^{2} - V_{d2}^{*2} \right\} = 3 \times V_{rated} \times I_{rated} \times Tc;$$

$$\frac{1}{2} \times C_{d1} \times \left\{ V_{d1}^{2} - V_{d1}^{*2} \right\} = 3 \times V_{rated} \times I_{rated} \times Tc;$$

So, the values of C_{d1} and C_{d2} are calculated as 120μF.
Where,

$\quad$ V_{rated} = rated AC line voltage (415 volts).

$\quad$ I_{rated} = rated AC line current (2.9 amps).

$\quad$ Tc = assume conservation time (848 μs).

V_{d1}^{*} = V_{d2}^{*} = percentage drop in DC bus voltages V_{d1} and V_{d2} (e.g. 1 % drop in 750 volt)= about 742 volt;

Chopper dump resistances (R_{d1} and R_{d2}): The values of DC dump resistances depend upon rated power P_{rated} of SP-SEIG and DC bus voltages 'V_{d1} and V_{d2}' of CC-VSI.
So,

$$R_{d1} = V_{d1}^{2} \big/ P_{rated};$$

$$R_{d2} = V_{d2}^{2} \big/ P_{rated};$$

The calculated values of dump resistances 'R_{d1} and R_{d2}' in similar controllers across both sets are 511 Ω. Where, P_{rated} = 1100 Watt.

A.C. filter resistance (R_f) and inductance (L_f) :

The output A.C. filters of CC-VSI inverters are comprised of R_f and L_f. The detail selection on filter choke resistance and inductance are mentioned in published book. The selected values of R_f and L_f are 1.45 Ω and 2.2 mH.

In-phase reference source currents (i'rd):

The magnitude of in-phase reference source current 'I'rd' is constant and equal to rated value of active power component of machine current:

$$I'_{rd1} = \sqrt{\frac{2}{3}} \times \left(\frac{P_{rated}}{V_{rated}} \right);$$

$$I'_{rd2} = \sqrt{\frac{2}{3}} \times \left(\frac{P_{rated}}{V_{rated}} \right);$$

So, for rated power (P_{rated} =1100 Watt) , the in-phase reference source currents in similar controllers across both sets are i'_{rd1} = i'_{rd2} =2.16 A.

5.5.1.2 SEIG and Load Parameters

For illustration purposes, a 1.1-kW squirrel cage induction machine whose data were taken from Appendix A is used in whole analysis of computer-based simulation of V and F controller-SP-SEIG. The balanced per phase equal static resistive loads are considered for the validity of analytical approach in simulation work.

5.5.2 Analytical Evaluation of Machine Variables

- First of all, i_a, i_b, i_c and i_x, i_y, i_z through both sets are calculated from d-and q-axis currents of machine [4]. From calculated per phase line currents, 3Φ line voltages V_a, V_b, V_c and V_x, V_y, V_z are also calculated from Equation (5.16) in Section 5.3.3.

- Then, proportional and integral gain constants i.e. K_{pa1} and K_{ia1}, and, K_{pa2} and K_{ia2} of both similar controllers on set I and II, respectively, has been selected by using the in-built auto tuned genetic algorithm (in Matlab /Simulink) during analysis. Final tuned values of K_{pa1}, K_{ia1}, K_{pa2} and K_{ia2} are mentioned in Appendix A.

- After tuning of V and F controllers, simulation of whole simulink model of SP-SEIG along with both controllers on each 3Φ set is performed using Matlab platform for simulation period of 2 Sec.

- Finally, simulated (analytical) values of generator performance variables with time are find out and illustrated in Figure 5.5.

5.6 Concluding Remarks

The aim of this research work was to present a short description on modelling, controller design and simulation work for a V and F controller-SP-SEIG at varying resistive loads. In any isolated induction generator, voltage and frequency (V and F) regulation at varying speed and load is necessary to maintain the output power remains constant. The self-excitation phenomenon is incorporated in proposed scheme for generation purpose of rated terminal voltage at no-load condition. The behaviour of V and F controller is mark able in its operation during variations in consumer loads. The DC chopper keeps generated power remains

constant in controller circuits of SP-SEIG. So, SP-SEIG generates constant voltage and frequency by keeping constant generated output power during operation of machine. So, one can say, V and F controller unit of SP-SEIG can behave like multi-purpose controller i.e. as voltage regulator, frequency regulator and also as consumer power regulator /load stabilizer from prediction of transient behaviour of resistively loaded SP-SEIG unit as depicted in Figure 5.5.

Besides the outstanding and beneficial features of SEIG, however, it also has two prominent and handicap millstone. First is need of reactive power during short circuits and second is poor voltage regulation during isolated mode /capacitor excitation of IGs. On faults, IG's dynamic behaviour deserves special attention. Due to abrupt reduction in torque during short circuits, IG's speed may accelerate to higher extent which leads to terminal voltage collapses due to increase in reactive power of IGs. Simplified and cheap volt and hertz controller keeps the value of terminal voltage to generated frequency remain constant so that (machine out power is also almost constant). It avoids variations in machine power by keeping constant terminal voltage and system frequency in adjustable speed application of induction generators like pumps & fans, heat pumps & air conditioner, machine tools & robotics, wind generation system etc. Both balanced and /or unbalanced per phase equal and /or unequal static and dynamic loads can be considered for the analysis purpose.

CHAPTER 6   CONCLUSIONS AND SUGGESTIONS FOR FUTURE WORK OF SP-SEIG

6.1 General

In many developing countries, the cost of delivering power has become quite large, while the establishment and maintenance of the electrification to the remote rural areas have become difficult. For these reasons, distributed power generation has received attention in recent years for far-flung rural electrification and has given rise to suitable stand–alone systems using locally available energy sources. These systems have become a preferred option with increased emphasis on eco-friendly technologies, and use of renewable energy sources such as small hydro, wind and biomass, etc. With this growing demand of isolated power units, self-excited induction generator (SEIG) is rapidly establishing itself in portable and non-conventional energy plants due to its low cost, less maintenance and operational simplicity. In recent years, the excessive use of conventional energy resources such as hydro, nuclear and fossil fuels has resulted in increased energy cost, environmental pollution, global warming and greenhouse gas emission. Due to this, there is need of fuel savings which are responsible for an increase interest in the use of alternative sources of energy and emphasized the use of isolated power units driven by renewable energy sources like wind, hydro, sunlight, bio gas and geothermal power etc. It indicates tendancy towards necessity of adopting an inexpensive generating system, capable of operating in remote areas with different types of prime mover. The stand-alone units are ideally suited to supply far-flung areas where the grid's extension is not feasible due to the economical point of views. The stand-alone SEIG can feed remote single family, village, community, etc., thus these units will quicken the electrification of rural and remote locations. Research is going on for the last several decades to explore the utilization of induction generator as a potential alternatives compared to synchronous generators in the field of alternative resources of energy.

High phase order /multi-phase (in excess of three) machine construction and power transmission are in consideration for the last several years, but their usage is still to be implemented in the society as compared to 3Φ arrangement. With the increased importance of economical growth, environmental concerns, and several other factors, multi-phase systems (sophisticated design methods) are being considered as one of the potential alternatives to conventional 3Φ systems. The investigations spread over a multi-phase machine is not stepping up rapidly as compared to multi-phase drive area in the electric energy generation. The literature regarding multi-phase IG is nearly not available before 20th centuary, only very few findings were drawing attention. The investigations spread since twentieth century reveals

the all technical and economical bottom lines of mult-phase AC machines for the application in marine ships, thermal power plant to drive induced draft fans, electric vehicles and circulation pumps in nuclear power plants etc. However, developments are still in its early stage, and very few important findings have been published in the literatures specifying the utility of multi-phase systems. Multi-phase (in excess of 3Φ) drives hold several advantages over the conventional 3Φ drives, like low magnitude with high frequency of torque pulsations, reduced rotor harmonic current, low space and time harmonic, low current per phase without voltage rise per phase, reduction in D.C. link current harmonic, greater power to mass ratio and higher reliability since loss of one of the many stator phases does not prevent the machine from starting and running [3].

Research in this field is going on and numerous interesting developments have been reported in this thesis and previous literatures. The main contributions are-

6.2 Summary

In Chapter-1, A short description about whole research work is delivered across whole chapter to give a focus on every aspects of novelty in research gap against staleness. It has to be shown the contribution towards proposed researched work. It also comprised basic introduction of every proposed novel research work.

In Chapter-2, It has been drawn attention towards a simplified mathematical model using loop impedance method based on the graph theory and solved by the analytical technique Newton-Raphson method to determine the unknown variables X_m and F of SP-SEIG for performance determination.

In Chapter-3, mixed stator current and magnetizing flux as a state-space variables have been used for modelling and dynamic analysis of simple and compensated six-phase self-excited induction generator.

In Chapter-4, The stability is investigated under perturbation of any one variable from the placement of the eigenvalues of the machine. In this linearized model, the effects of common mutual leakage inductance (L_{lm}) between two 3Φ winding sets and cross-saturation coupling (L_{ldq}) between d- and q-axis of individual stator have not been considered to avoid the complexity of the solution. This analysis also presents the effect of magnetizing inductance during the process of self-excitation and also finds that the speed too plays an important role which is necessary to initiate, and to sustain the self-excitation process in an isolated SP-SEIG

for a given value of capacitance, and load. Magnetizing inductance (L_m) also has an important role in the dynamics of voltage build up and stabilization of SP-SEIG.

In Chapter-5, The voltage and frequency regulation is implemented by using a simplified Simulink matlab model. Simulink model is simple and popular being constructed using new closed loop volts and Hz control strategy. As V and F controller of SP-SEIG was no more in research field before, so, incorporating this type of study could also be beneficial for multi-phase variable speed induction generator controls in future applications where renewable energy sources are naturally attracted as its rotor shaft driver.

6.3 Future Scope

The end of an engineering research gives birth to new trends of technology in the coming future in various interesting fields. In many developing countries, the cost of delivering power has become quite large, while establishment and maintenance of the electrification to remote rural areas have become difficult. For these reasons, distributed power generation has received cognizance in recent years to hook up with the upgraded suitable stand–alone systems using locally available non–conventional energy sources for global rural electrification and copping out with the depletion of conventional energy sources. With this growing demand of isolated power units, SEIG is rapidly establishing itself in portable and non-conventional power plants due to its simplicity, cheapness, little weight and maintenance.

Similarly, to prevent power loss on provincial grid, multi-phase induction generator must be used to serve fault tolerance in stand-alone systems and embedded systems. This is fault analysis during design of protection schemes in drive systems. The concept of parallel redundancy in multi-phase induction generator implements a phase-redundant drive system. Based on promising benefits of H.P.O as mentioned in Section 6.1, multi-phase generators also have applications in high power electric drive system. Applications of H.P.O. drives are specific in high reliability demands like aerospace, ship propulsion, electric vehicles and hybrid vehicles. The promising benefits of H.P.O. /multi-phase induction machines, once took placed in practical applications, will yield improvement in overall performance keeping reduced iron losses; increase of power rating in same frame of connections; lower current without increase in voltage for phases and being high reliable will be used in process industries.

The investigation is carried out on detailed mathematical dynamic modelling of balanced SP-SEIG includes mixed variables (stator currents and magnetizing fluxes) across two axis d-q model and a conventional method using RK4 subroutine is used for the dynamic analysis purpose during balanced and unbalanced conditions in the system; Identification of steady-

state behaviour of simple and compensated SP-SEIG feeding resistive loads based on equivalent circuit of it using network graph theory and conventional NR method for the purpose of formulation and analysis, respectively; The development of linearized state-space model about an operating point related to stability behavior of self-excited induction generator using Taylor's expansion and by incorporating presence of excitation capacitances which are connected across both the winding sets in its system matrix has been displayed dependency of stability phenomenon on the shunt-excitation capacitances; Linearized model of SP-SEIG is applied in establishing transfer functions for the analysis purpose of design and control of the system going through variations of machine variables. A new control strategy is also used for voltage and frequency control purpose in SP-SEIG. In same way, mentioned investigations can be extended for further research in unbalanced SP-SEIG with different winding configuration using AC-DC conversion scheme.

The basic objectives have been considered successfully during research work and different aspects may be use for further research purposes in the same field which includes:

- The computational analysis for the suitable values of capacitances required in self-excitation phenomenon, and during compensation scheme has been done for a successful operation of the machine up to its rated capacity without using any extra voltage regulator devices for escaping from erratic behavior of the system. Extra voltage regulating devices could participate particularly in increase of system cost. The capacitor compensated voltage regulation technique is simple and cheap in comparison to other voltage regulators include power switching devices. It leads towards improved reactive power /voltage control techniques.

- Generalized formulation of equivalent circuits in simple and compensated configuration of SP-SEIG. Under balanced and unbalanced resistive loads. All generalized formulation under different configuration has been developed for steady state behavior of SP-SEIG. Generalized model can further be formalized for investigating the behavior of machine under different types of load. Optimization of model is performed by simple and an easy algorithm used in steady state analysis. The computational procedure may be allowed for different other values of capacitances under simple, short-shunt and long-shunt configurations during investigation of machine performance for comparative study to give an overall view on the suitable choices of the capacitance for self-excitation and compensation scheme of the system up to its rated capacity. Moreover, conventional

124

optimizing methods have provided an idea about better selection of suitable capacitors for self-excitation and compensation purposes during balanced and unbalanced conditions.

- This mixed variable model also includes main-flux saturation due to the variable nature of flux levels under variable machine speed. Model is one of the more complex-type during computation. Exclusive of complexity by virtue of solely non-zero elements of system matrix, it upholds the knowledge of various parameters belongs to stator and rotor equivalent circuit. On the contrary, only four saturation vulnerable matrix elements seize its simplicity in relation to other single variable model. Mixed variable modelling in multi-phase AC generator could commence as a feasible remedy in synthesis of control system. The computational RK algorithm technique can be used for the dynamic /transient analysis of simple and compensated SP-SEIG feeding resistive and resistive-inductive loads. The modification can also be take place during processing of algorithm under variable speed operating conditions (less /more than base speed as per flux level variations) due to mixed nature of state space variables i.e. stator current and magnetizing flux in the cultivate system model matrix. This transient analysis can also apply for different operating conditions.

- A linearized model based on eigenvalue of system is obtained with simple SP-SEIG feeding resistive load for stability study. Eigenvalue stability model with presence of excitation capacitances can be extended to a compensated version of SP-SEIG for assessing the detail stability behavior under different operating conditions. Various other graphical tools can be devised in implementation of various system transfer function for design and control purposes. As stability behaviour of SEIG is intricated by keeping unknown terminal voltage and frequency initially, and nonlinear magnetizing reactance. So, small signal linearized model will play very significant role during its stability analysis. It can provide very insightful survey in stability of wind (or hydro) turbine driven SEIG during island operation. It will provide stable operation; which depends on many design factors of machine; during small disturbances. Stability factor is considered by the design engineers during machine steady state operation.

- To explore the use of an induction generator as variable speed drive system, a simplified Simulink model is prepared using voltage-fed inverter control scheme. Basically a V and F (Volts-and-Hz) control is a popular and simple scheme of speed control in induction machine usually used in industries for several decades. Simulink model is little bit of complex being constructed in closed loop using two PI controllers in control scheme.

Controller tuning nature has simultaneous requirement of two control variables magnitude in feedback loops and also inattention the internal coupling effects in multivariable, non-linear induction generators. Further, a SP-SEIG has been used in adjustable speed applications along with its new control strategy in frequency and voltage control keeping generated power remains constant. Followed by this work, new V and F controller can be act as voltage and frequency regulator, and also as a load balancer during unbalanced load conditions. So, new proposed control strategy enhances the dynamic performances of proposed system against system speed and consumer load variations.

All algorithm and models can be modified for different operating conditions under different loads i.e. statics and dynamics. Dynamic loads i.e. induction motor could be used in past research work with 3Φ self-excited induction generators. Static loads i.e. R-C, R-L and R-L-C can also be used further in research work besides keeping attention during past several years. Thesis research work introduces the unified and simplified mathematical treatment using Stanley's transformation during machine mathematical modelling for steady-state, dynamic, stability and control analysis of six-phase self-excited induction generator (SP-SEIG), for applications in renewable energy generation. Presented work may also be suggested in developing of hybrid systems.

BIBLIOGRAPHY

[1] G. K. Singh, "Multi-phase induction machine drive research—a survey," Electric Power Systems Research, vol. 61, pp. 139-147, 2002.

[2] G. K. Singh, "Modeling and analysis of six-phase synchronous generator for stand-alone renewable energy generation," Energy, vol. 36, pp. 5621-5631, 2011.

[3] A. S. Kumar, J. L. Munda, and G. K. Singh, "Wind-driven stand-alone six-phase self-excited induction generator transients under different loading conditions," Electrical Engineering, vol. 97, pp. 87-100, 2014.

[4] G. K. Singh, "Modeling and experimental analysis of a self-excited six-phase induction generator for stand-alone renewable energy generation," Renewable energy, vol. 33, pp. 1605-1621, 2008.

[5] G. K. Singh, "Self-excited induction generator research—a survey," Electric Power Systems Research, vol. 69, pp. 107-114, 2004.

[6] G. K. Singh, A. S. Kumar, and R. P. Saini, "Steady-state modeling and analysis of six-phase self-excited induction generator for renewable energy generation," Electric Power Components and Systems, vol. 38, pp. 137-151, 2009.

[7] G. K. Singh, A. S. Kumar, and R. P. Saini, "A self-excited six-phase induction generator for stand-alone renewable energy generation: experimental analysis," European Transactions on Electrical Power, vol. 20, pp. 884-900, 2010.

[8] G. K. Singh, A. S. Kumar, and R. P. Saini, "Performance evaluation of series compensated self-excited six-phase induction generator for stand-alone renewable energy generation," Energy, vol. 35, pp. 288-297, 2010.

[9] G. K. Singh, A. S. Kumar, and R. P. Saini, "Performance analysis of a simple shunt and series compensated six-phase self-excited induction generator for stand-alone renewable energy generation," Energy Conversion and Management, vol. 52, pp. 1688-1699, 2011.

[10] Ion Boldea. Variable speed generator CRC Press 2006.

[11] V. T. Somasekhar, K. Gopakumar, M. R. Baiju, K. K. Mohapatra, and L. Umanand, "A multilevel inverter system for an induction motor with open-end windings," IEEE Transactions on Industrial Electronics, vol. 52, pp. 824-836, 2005.

[12] K. Marouani, L. Baghli, D. Hadiouche, A. Kheloui, and A. Rezzoug, "A new PWM strategy based on a 24-sector vector space decomposition for a six-phase VSI-fed dual stator induction motor," IEEE Transactions on Industrial Electronics, vol. 55, pp. 1910-1920, 2008.

[13] M. A. Abbas, R. Christen, and T. M. Jahns, "Six-phase voltage source inverter driven induction motor," IEEE Transactions on Industry Applications, pp. 1251-1259, 1984.

[14] K. H. Youssef, M. A. Wahba, H. A. Yousef, and O. A. Sebakhy, "A new method for voltage and frequency control of stand-alone self-excited induction generator using pulse width modulation converter with variable DC-link voltage," Electric Power Components and Systems, vol. 38, pp. 491-513, 2010.

[15] R. R. Chilipi, B. Singh, and S. S. Murthy, "Performance of a Self-Excited Induction Generator With DSTATCOM-DTC Drive-Based Voltage and Frequency Controller," IEEE Transactions on Energy Conversion, vol. 29, pp. 545-557, 2014.

[16] E. Muljadi, T. B. Nguyen, and M. A. Pai, "Transient stability of the grid with a wind power plant," in Power Systems Conference and Exposition, 2009. PSCE'09. IEEE/PES, 2009, pp. 1-7.

[17] E. Muljadi, T. B. Nguyen, and M. A. Pai, "Impact of wind power plants on voltage and transient stability of power systems," in Energy 2030 Conference, 2008. ENERGY 2008. IEEE, 2008, pp. 1-7.

[18] M. A. Pai, "Small signal stability in power system analysis," Electrical Engineering, pp. 51-57, 1997.

[19] M. Touma-Holmberg and K. Srivastava, "Double winding, high-voltage cable wound generator: steady-state and fault analysis," Energy Conversion, IEEE Transactions on, vol. 19, pp. 245-250, 2004.

[20] G. K. Singh and D. Singh, "Small Signal Stability Analysis of Six-phase Synchronous Generator," Przegląd Elektrotechniczny, vol. 89, 2013.

[21] E. E. Ward and H. Härer, "Preliminary investigation of an invertor-fed 5-phase induction motor." Proceedings of the Institution of Electrical Engineers. Vol. 116. No. 6. IET, 1969.

[22] R. H. Nelson and P. C. Krause, "Induction machine analysis for arbitrary displacement between multiple winding sets." IEEE Transactions on Power Apparatus and Systems 3 (1974): 841-848.

[23] E. Levi, "Multiphase electric machines for variable-speed applications." IEEE Transactions on industrial electronics 55, no. 5 (2008): 1893-1909.

[24] M. Ouhrouche, X. D. Do, Q. M. Lê, and R. Chaîné, "EMTP based simulation of a self-excited induction generator after its disconnection from the grid," IEEE Transactions on Energy Conversion, vol. 13, pp. 7-14, 1998.

[25] B. Singh, M. Singh, and A.K. Tandon, "Transient performance of series-compensated three-phase self-excited induction generator feeding dynamic loads," IEEE Transactions on industry Applications, vol. 46, pp. 1271-1280, 2010.

[26] Y. W.Liao and E. Levi, "Modelling and simulation of a stand-alone induction generator with rotor flux oriented control," Electric power systems research, vol. 46, pp. 141-153, 1998.

[27] R. H. Park, "Two-reaction theory of synchronous machines generalized method of analysis-part I," Transactions of the American Institute of Electrical Engineers, vol. 48, pp. 716-727, 1929.

[28] P.C. Krause "Analysis of electric machinery, New-York; Mc Graw Hill Book Company;1986.

[29] A. P. Grilo, A. D. A. Mota, L. T. M. Mota, and W. Freitas, "An analytical method for analysis of large-disturbance stability of induction generators," IEEE Transactions on Power Systems, vol. 22, pp. 1861-1869, 2007.

[30] S. Gupta, "Analysis and development of load controller and static compensator for self-excited induction generator based autonomous generating system," PH.D. thesis. Indian Institute of technology, Delhi, 2004.

[31] S. P. Singh, S. K. Jain, and J. Sharma, "Voltage regulation optimization of compensated self-excited induction generator with dynamic load," IEEE Transaction on Energy Conversion, vol. 19, pp. 724 – 732, Dec. 2004.

[32] B. Singh and S. Sharma, "Voltage and frequency controllers for standalone wind energy conversion systems," IET Renewable Power Generation, vol. 8, pp. 707-721, 2014.

[33] P. K. S. Khan and J. K. Chatterjee, "Three-phase induction generators: a discussion on performance," Electric Machines & Power Systems, vol. 27, pp. 813-832, 1999.

[34] A. IQBAL, G. K. Singh, and V. PANT, "Stability analysis of an asymmetrical six-phase synchronous motor," Turkish Journal of Electrical Engineering & Computer Sciences, vol. 24, pp. 1674-1692, 2016.

[35] G.K. Singh, V. Pant, and Y.P. Singh, "Stability analysis of a multiphase (six-phase) induction machine", Computers and Electrical Engineering, vol. 29, pp. 727-756, 2003.
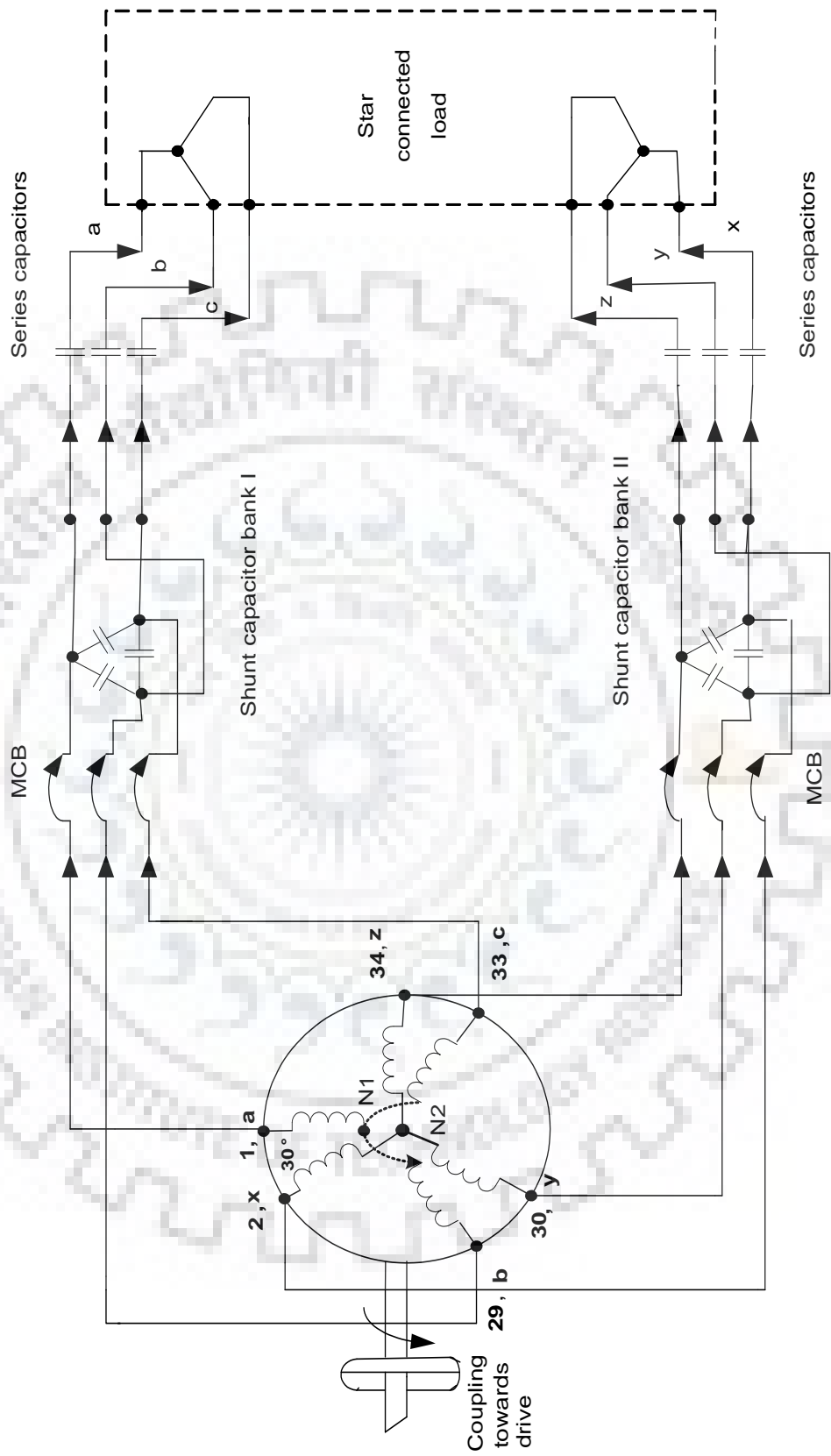
Figure A1. Block diagram of generalized SP-SEIG setup.

MACHINE SPECIFICATIONS

Block diagram of generalized six-phase machine setup is shown in Figure A1.

Six-phase squirrel cage induction machine:

6-pole, 36 slots, 1.1 kW, 415 V, 2.9 A, 50 Hz, 960 RPM.

D.C. series motor drive along with control pannel:

5 kW, 20 V, 17 A, 50 Hz, 3000 RPM.

MACHINE PARAMETERS

"**Synchronous speed test**" was also performed to achieve the magnetizing current and terminal voltage of the machine in order to find a corresponding magnetization curve (airgap voltage versus magnetizing reactance) and test data are arranged in Table A 1. The magnetization-characteristic of SP-SEIG is given in Figure A 2. For the analysis of 6 poles, SP-SEIG, "**No-load and blocked rotor test**" were also performed to achieve the parameters of test machine. The machine parameters are given below for the six-phase connection. For star-connection of stator:

In Actual form,

Stator resistance $r_1 = r_2 = 4.12\ \Omega$.
Stator leakage inductance $L_{l1} = L_{l2} = 21.6$ mH.
Rotor resistance $r_r = 8.79\ \Omega$.
Rotor leakage inductance $L_{lr} = 43.3$ mH.
Magnetizing inductance $L_m = 233.8$ mH.
Capacitance /phase required for self-excitation $C_1 = C_2 = 38.5\mu F$.

Magnetizing inductance L_m is non-linear function of magnetizing current i_m can be obtained from the no-load magnetization curve of the machine. The value of L_m is determined by the curve-fitting tool and expressed as

$$L_m = d_1 + d_2 i_m + d_3 i_m^2 + d_4 4 i_m^3 \quad,$$

132

where,

d_1, d_2, d_3, d_4 are constant and their values are $d_1=0.1031$, $d_2=0.019$, $d_3=-0.004$, $d_4=0.0002$.

Variations of the air gap voltage V_g /F with X_m can be approximated by the following order of polynomials known as the magnetization curve of the test machine.

$$V_g/F = -0.00001 \, X_m{}^3 - 0.0033 \, X_m{}^2 - 1.067 \, X_m + 598.63$$
$$V_g/F = -0.0097 \, X_m{}^2 - 0.0879 X_m + 550.18.$$
$$V_g/F = -3.2101 \, X_m + 786.93.$$

In P.U. form,

Vbase = 230 V.

Ibase = 2.9 A.

Zbase = 230V / 2.9A = 80Ω.

The measured parameters of the test machine in p. u . were:

Stator resistance $R_1 = R_2 = 0.05385$,

Stator leakage reactance $X_1 = X_2 = 0.0885$,

Rotor resistance $r_r = 0.11475$,

Rotor leakage reactance $X_r = 0.1775$, $X_{lm} = 0.00973$,

Magnetizing reactance $X_m = 2.93$,

Per-unit variations of the air gap voltage V_g /F with X_m can be approximated by the following order of polynomials known as the magnetization curve of the test machine.

$$V_g/F = 0.0333 \, X_m{}^3 - 0.3533 \, X_m{}^2 + 0.3661 \, X_m + 1.3748;$$
$$V_g/F = -0.1346 \, X_m{}^2 - 0.0967 \, X_m + 1.6882;$$
$$V_g/F = -0.6907 \, X_m + 2.304;$$

SP-SEIG - V and F CONTROLLERS PARAMETERS

PI CONTROLLER (set I) and (set II):

AC voltage PI gain: Kpa1 / Kpa2 = 325; Kia1 / Kia2 = 40;

DC voltage PI gain: Kpd1 / Kpd2 = 0.01; Kid1 / Kid2 = 0.001;

Table A 1: Synchronous speed test data

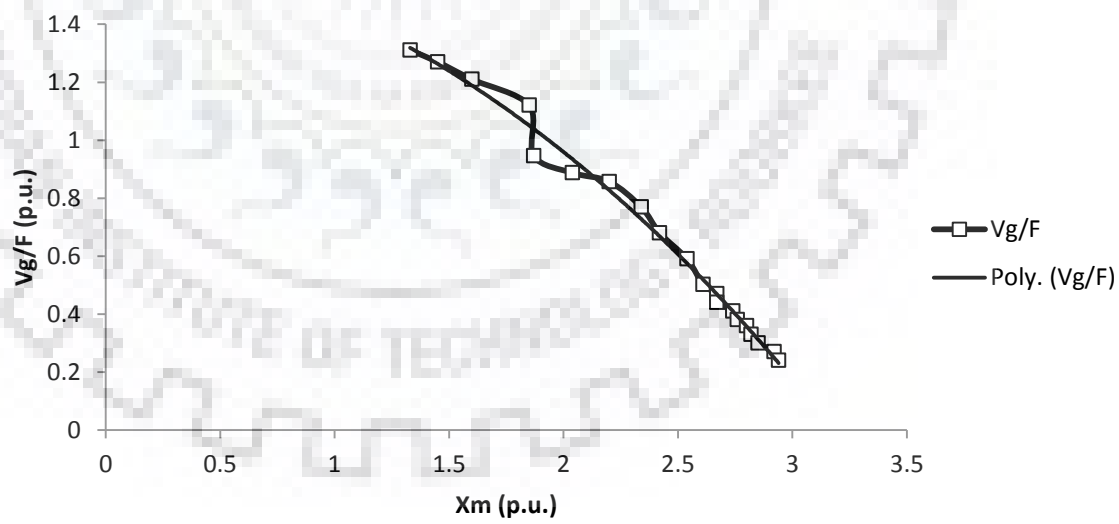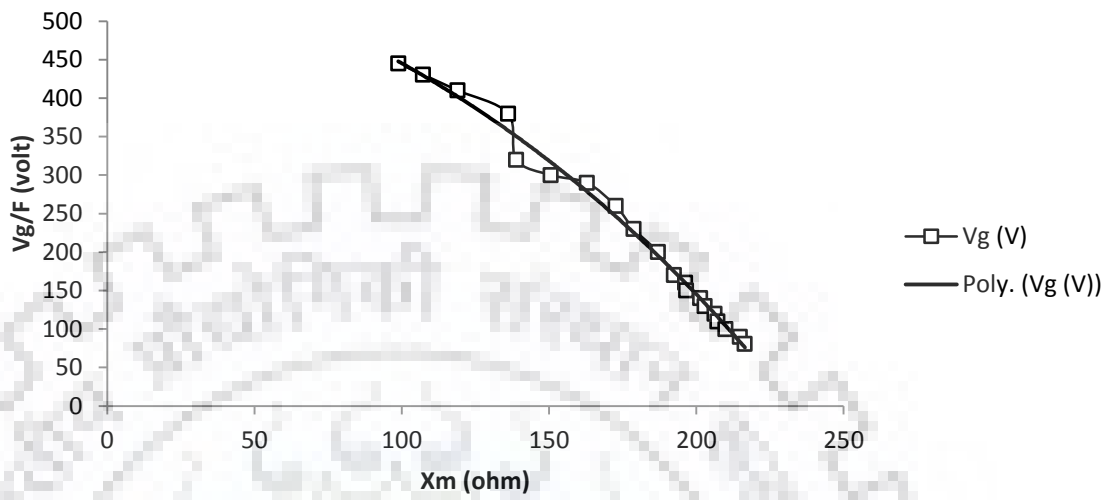| S.No.	I/P Voltage (V)	I/P Power (Kw)	I/P Current (A)
1	70.7	0.01	0.19
2	80.6	0.02	0.21
3	90.0	0.02	0.24
4	100	0.03	0.28
5	110	0.03	0.33
6	120	0.04	0.37
7	130	0.05	0.38
8	140	0.06	0.39
9	150	0.06	0.43
10	160	0.07	0.47
11	170	0.08	0.50
12	200	0.12	0.60
13	230	0.15	0.71
14	260	0.22	0.84
15	290	0.28	0.97
16	320	0.37	1.15
17	350	0.47	1.35
18	380	0.61	1.60
19	410	0.79	1.99
20	430.7	0.90	2.32
21	445	1.09	2.60

Figure A 2. Magnetization curve of SP-SEIG

135

DEVELOPMENT OF 6Φ WINDING FROM 3Φ WINDING

Today, 3Φ induction motors are replacing others existing prime movers in home, offices and industry being cheap, reliable, robust and having maintenance free operation. Design of 6Φ windings enlargement includes how to assign 3Φ windings in to in-built stator slots by keeping in mind basic aims of polyphase AC windings. 6Φ winding has been distributed and expanded in a double-layer manner as seems from Figure B1. Windings are a collection of coils in which starting coil side takes one slot (one side in to first layer) and returns into another separate slot (another side in to second layer) from left to right in full-pitched double-layer windings. In double-layer configuration, top-layer (first-layer) is near to air-gap and bottom-layer (second-layer) is away from air-gap as per standard consideration. Winding should have symmetrical distribution across every phase being displaced by same electrical angle. Allocations of slots are as follows across phases and poles:

Coils per phase can be connected in series or series-parallel manner and written as:

Coils per phase = Ns /q;

where,

Ns= number of slots;

q=number of phases in the stator winding;

Slots /pole /phase from one layer to another layer is called as a phase belt of coil sides displaced with arbitrary electrical radians from original phase belt to return phase belt. It is given by following relation:

Slots/pole/phase (Nsq) = Ns / (P*q);

where,

P = given number of poles;

Now, the **number of phase belt per pole** is Nsq =180º / ζ;

where,

ζ = phase belt angle;

Here, for six-phase machine ζ = 60º and an asymmetrical displacement is 30º between the both winding sets in SP-SEIG. Phase belt angle equal to 60º has been divided into two equal portions each equal to 30º. This phase belt splitting increases Kω value from 0.965 (3Φ) to 1.0 (6Φ) connection. The number of minimum stator terminals / leads are equal to the number of phases for a given machine. Neutral is excluded from this discussion and has a unique identification separate from phase distribution.

Slot pitch angle = (360°/ Ns) mechanical degree;

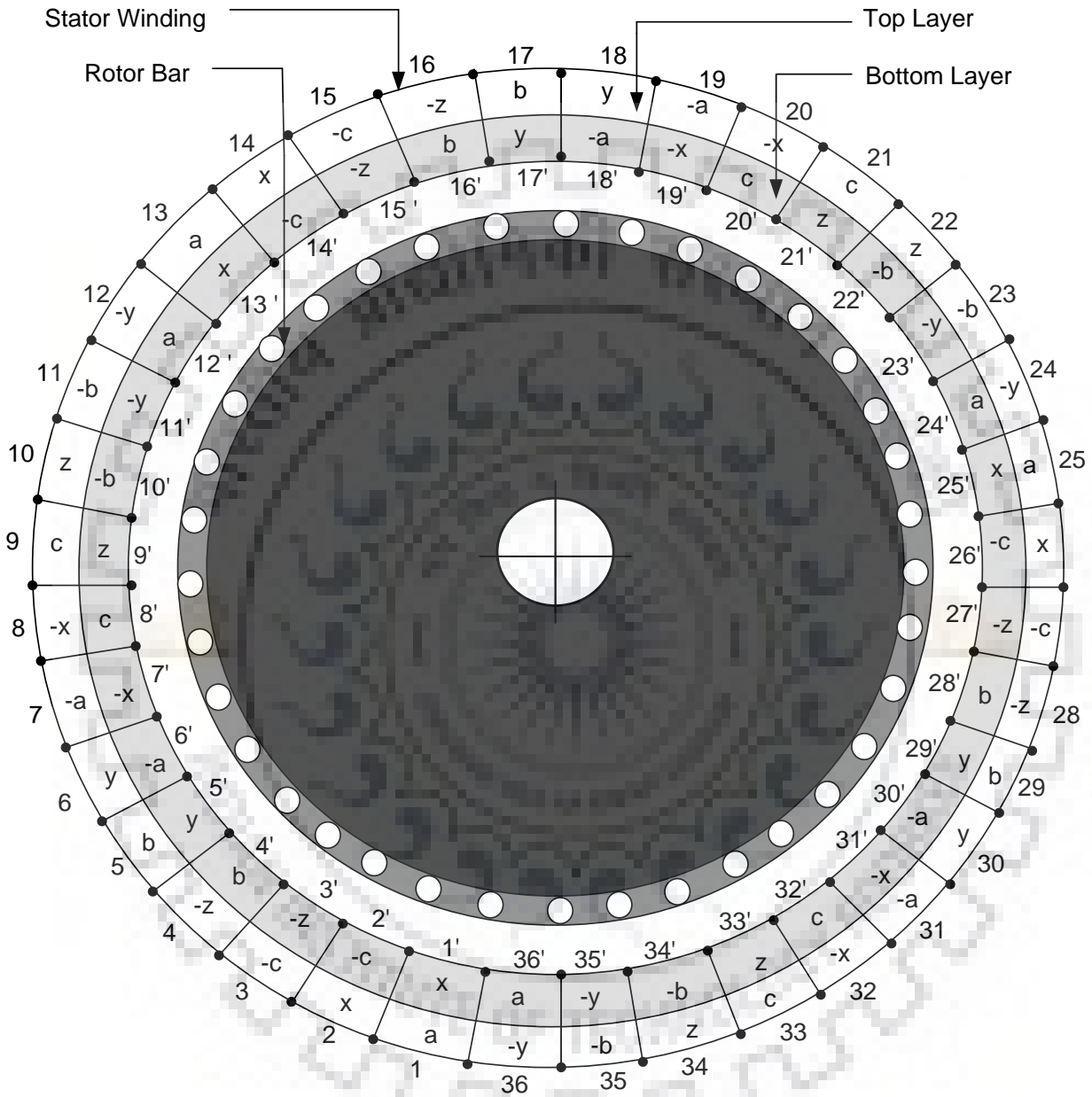or,   = ((360°/ Ns)*P/2) electrical degree;

Figure B1. A 6-phase, 6-pole, 36-slot, full-pitched, double-layer windings of squirrel-cage induction machine with split-phase belts.
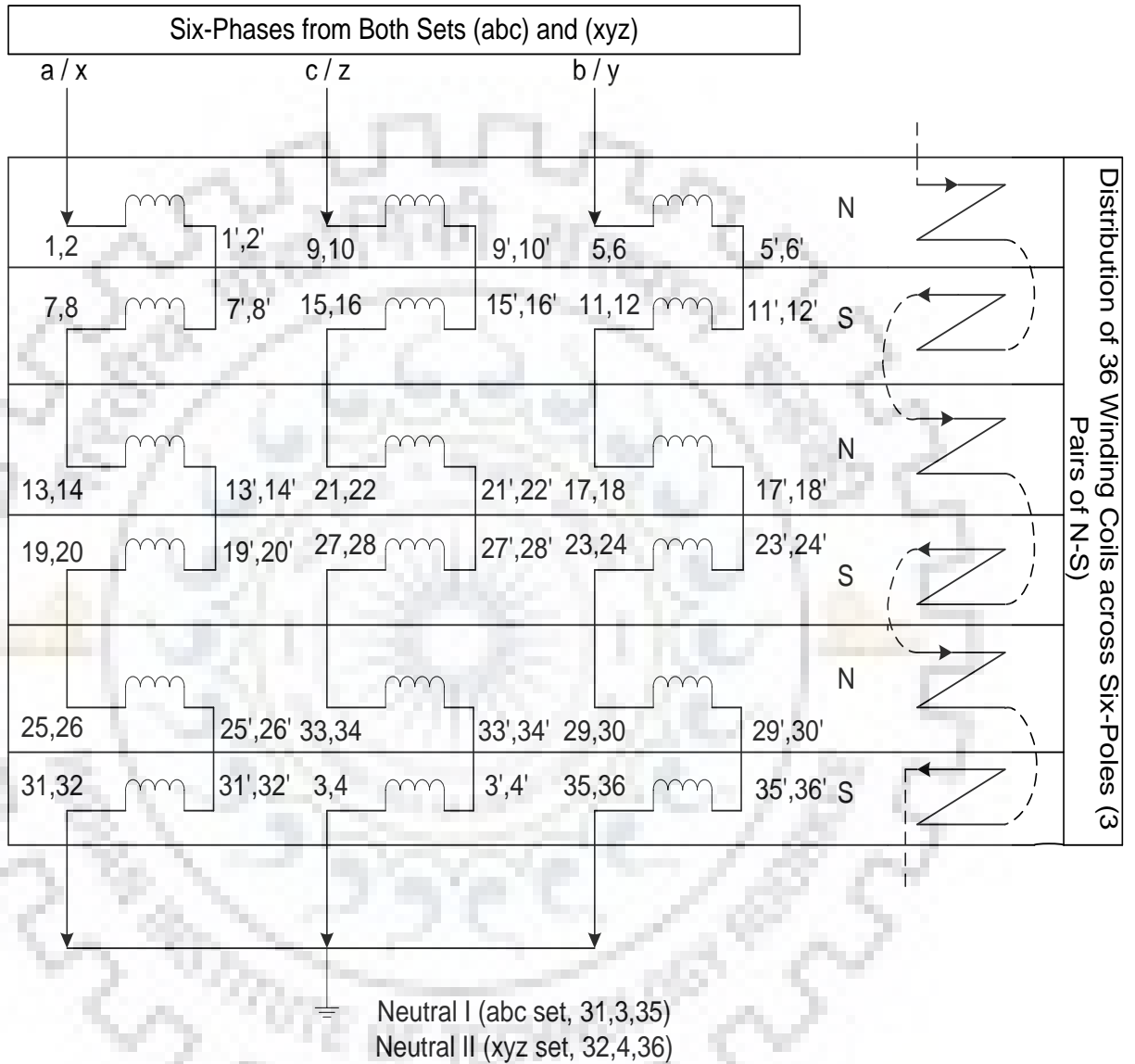
Figure B2. Arrangements of doubled-layered, distributed, lap-connected, full-pitched coils in 36 slots of 6 pole 6-phase induction machine.

RECONFIGURATION OF 3Φ IN TO 6Φ MACHINE

In reconfiguaration process, consider P-pole machine with Ns stator slots. In a six-phase winding configuaration, there are twelve coils per phase. These colis are connected into six groups per phase. Each group consist of two coils. Each two colis in every group are connected in series as shown in Figure B2. Practically, all the twelve coils are not connected in series. The 6 stator phases are combined into the two separate groups of star–connected 3Φ winding sets (*abc* and *xyz*) by having isolated neutral points from each other to prevent the triplen harmonics and propagation of faults. For the best performance of multi-phase machines, angular displacement between the every multiple 3Φ sets must be in given order. For even number of sets,

$$\text{Displacement} = \pi / n ;$$

For odd number of sets,

$$\text{Displacement} = 2\pi / n;$$

where,

$$n = \text{Number of phases};$$

From Figure B2. and above discussions,

- Six coils per phase (a/x, b/y, c/z)
- Two coils per pole (N or S)
- Four coils per pole-pair (N-S)
- Twelve slots per pole-pair (N-S) of stator
- Phases (a and x), (b and y) and (c and z) are in same slots of stator periphery.
- Start and finish end of each phase creates a six-phase winding
- Netural I (N1) and II (N2) are respectively correspond to (abc) and (xyz) winding sets shown in the block diagram of Figure A1 in APPENDIX- A.
- Direction of current flow is decided by N and S poles has been arranged in standard continuous alternate order.

STATOR WINDING DESIGN PARAMETERS

For six-poles,

$$\text{Slots/pole/phase (Nsq)} = 36 / (6*6);$$
$$= 1 \text{slots/pole/phase};$$
$$\text{Slot pitch angle} = 360°/ 36;$$

140

= 10° mechanical;

=10° mechanical*6/2;

=30° electrical;

For double-layered layout,

Number of coils / phase= 6;

Number of turns / coil = (½) of number of turns / coil in

3Φ machine;

For full-pitched winding,

Angle between the start and end of each coils = 180° electrical.

Coil-span = 6 slot pitches